# μ(I) rheology for granular flows with applications for avalanches and column collapse

Pierre-Yves Lagrée*,

Lydie Staron*, Stéphane Popinet *o, Daniel Lhuillier *, Christophe Josserand *

*Institut Jean le Rond d'Alembert, CNRS, Université Pierre & Marie Curie, 4 place Jussieu, Paris, France

o National Institute of Water and Atmospheric Research, PO Box 14-901 Kilbirnie, Wellington, New Zealand

NumHyp Roscoff 20/09/11

# outline

- what is a granular fluid? some images
- the μ(I) friction law obtained from experiments and discrete simulation
- the viscosity associated to the μ(I) friction law
- the Saint Venant Savage Hutter Hyperbolic model
- implementing the μ(I) friction law in Navier Stokes
- Examples of flows: focusing on the granular column collapse (limits of Saint Venant Savage Hutter Hyperbolic model)


- What is a granular media?
- size > 100µm
- grains of sand, small rocks, glass beads, animal feed pellet, medicines, cereals, wheat, sugar, rice...
- 50 % of the traded products

spoil tip (boney pile, gob pile, bing or pit heap), «terril» in french

Fig. 20. Frank slide.

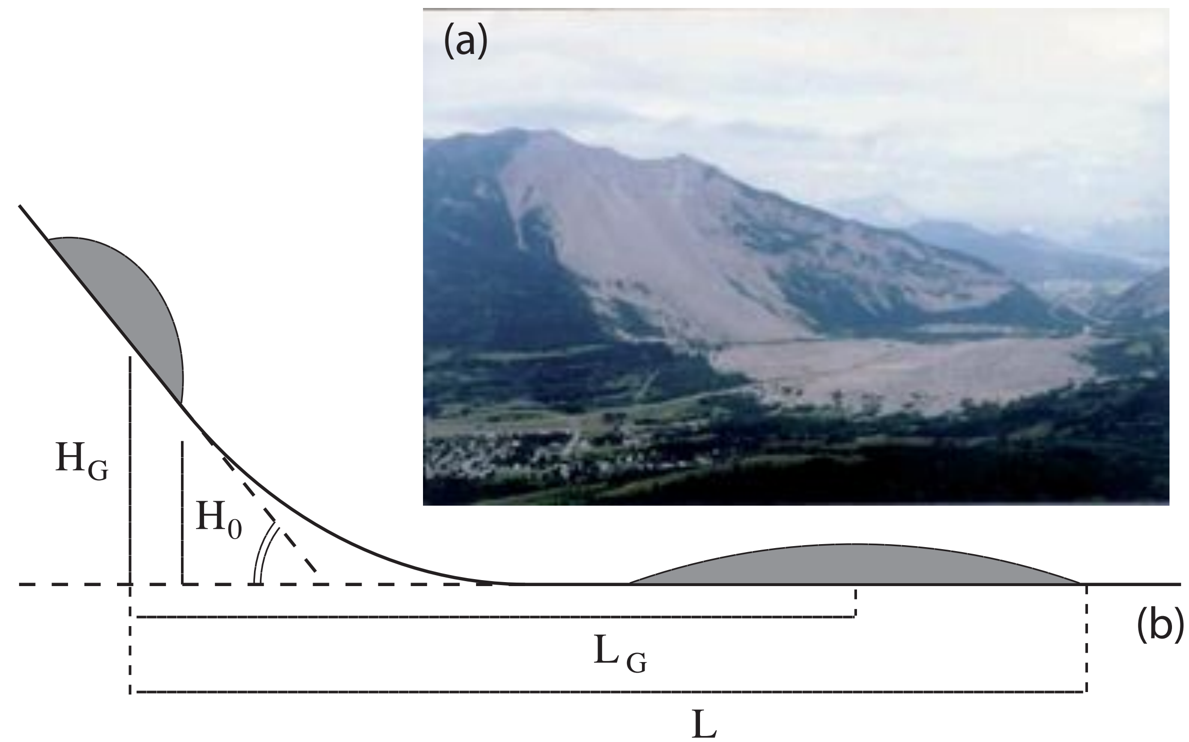


Staron


Environmental Modelling & Software xx (2006) 1e18
www.elsevier.com/locate/envsoft


The effect of the earth pressure coefficients on the runout of granular material


Marina Pirulli [a,*], Marie-Odile Bristeau [b], Anne Mangeney [c], Claudio Scavia

http://www.pbase.com/image/63044602 2006 Gary Hebert

# Lofoten Norway



photo PYL

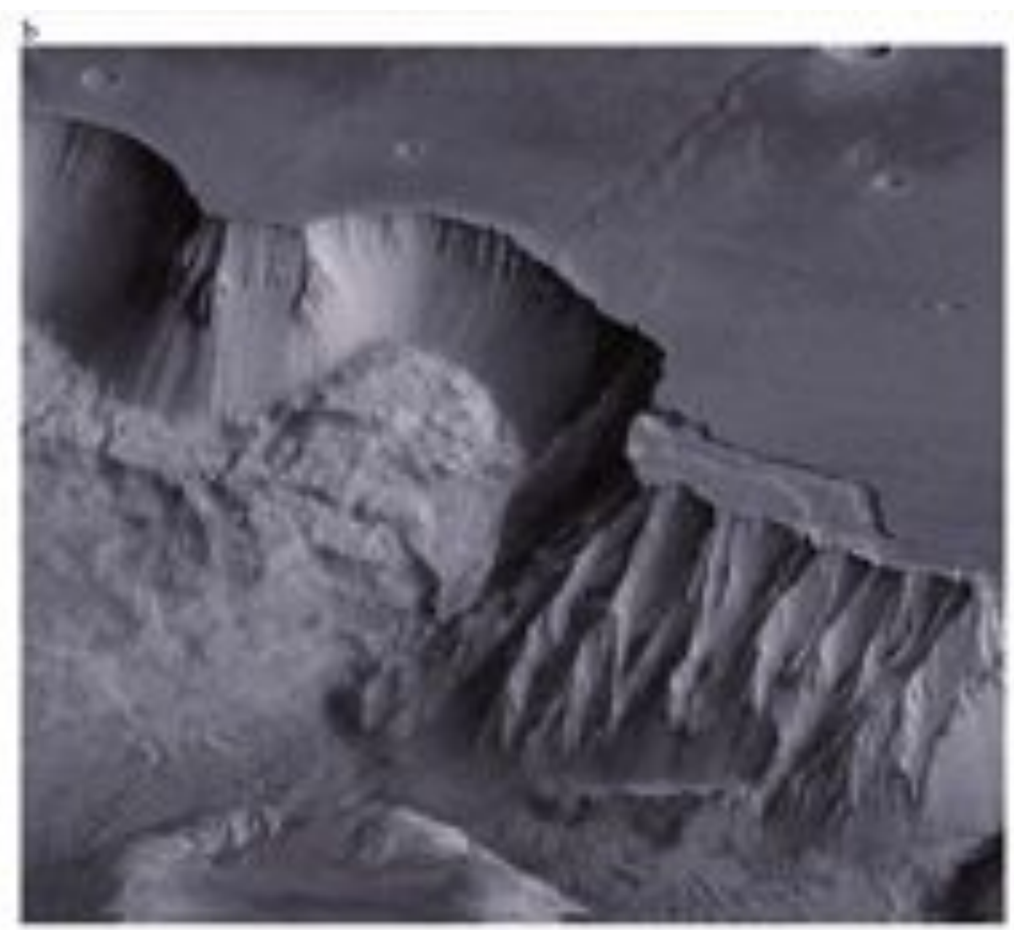

http://books.google.fr/books?id=HY6Z5od4-E4C&pg=PA49&dq=granular+flow&hl=fr&ei=lamtTaa_NYyVOoToIdcL&sa=X&oi=book_result&ct=result&resnum=10&ved=0CFkQ6AEwCTgK#v=onepage&q&f=true

http://www.cieletespace.fr/image-du-jour/5126_la-saison-des-avalanches-sur-mars

# Granular Column Collapse

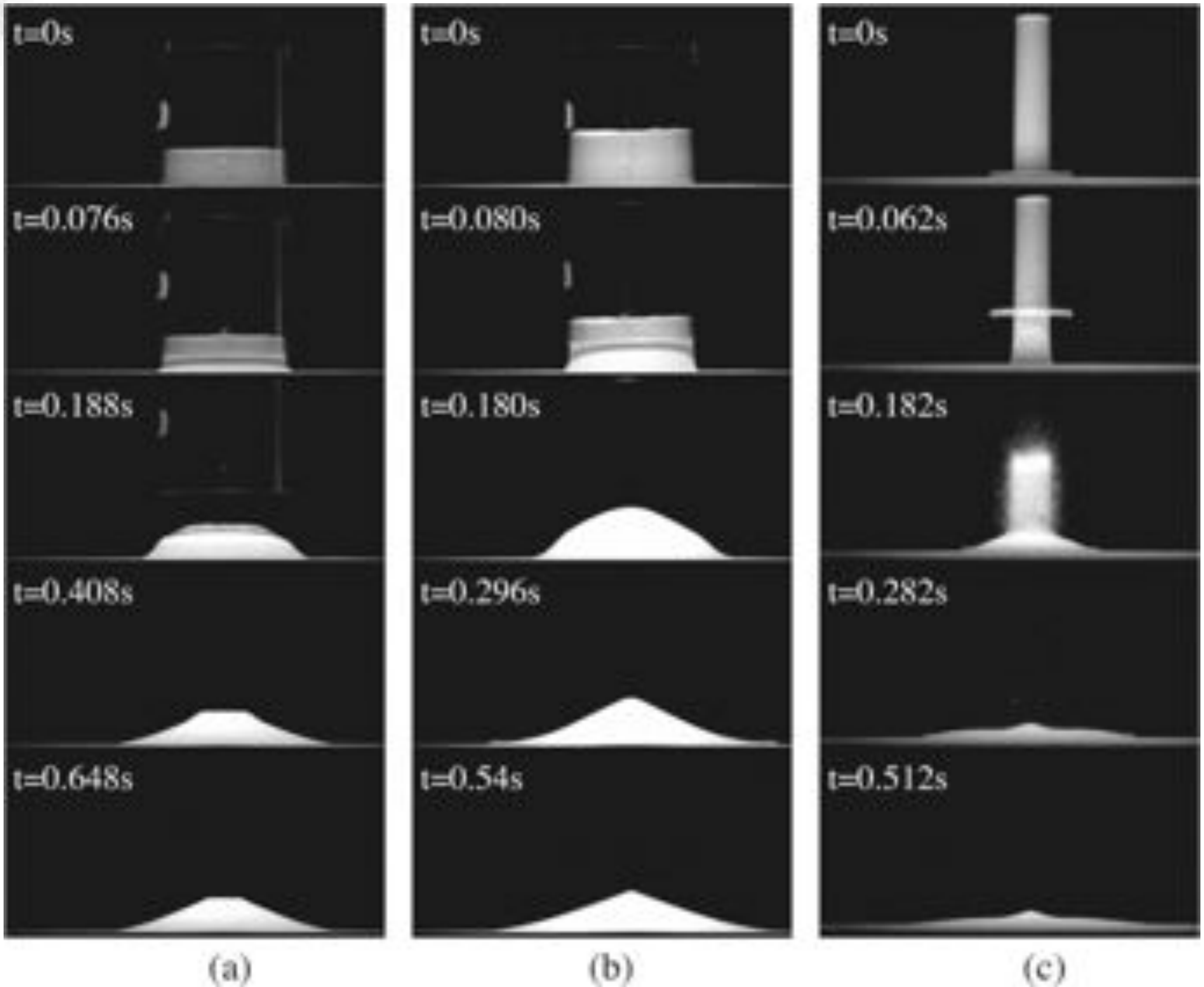


The sand pit problem: quickly remove the bucket of sand

http://www.mylot.com/w/photokeywords/pail.asp

# Granular Column Collapse

aspect ratio $a = H_0/R_0 = H_0/L_0$

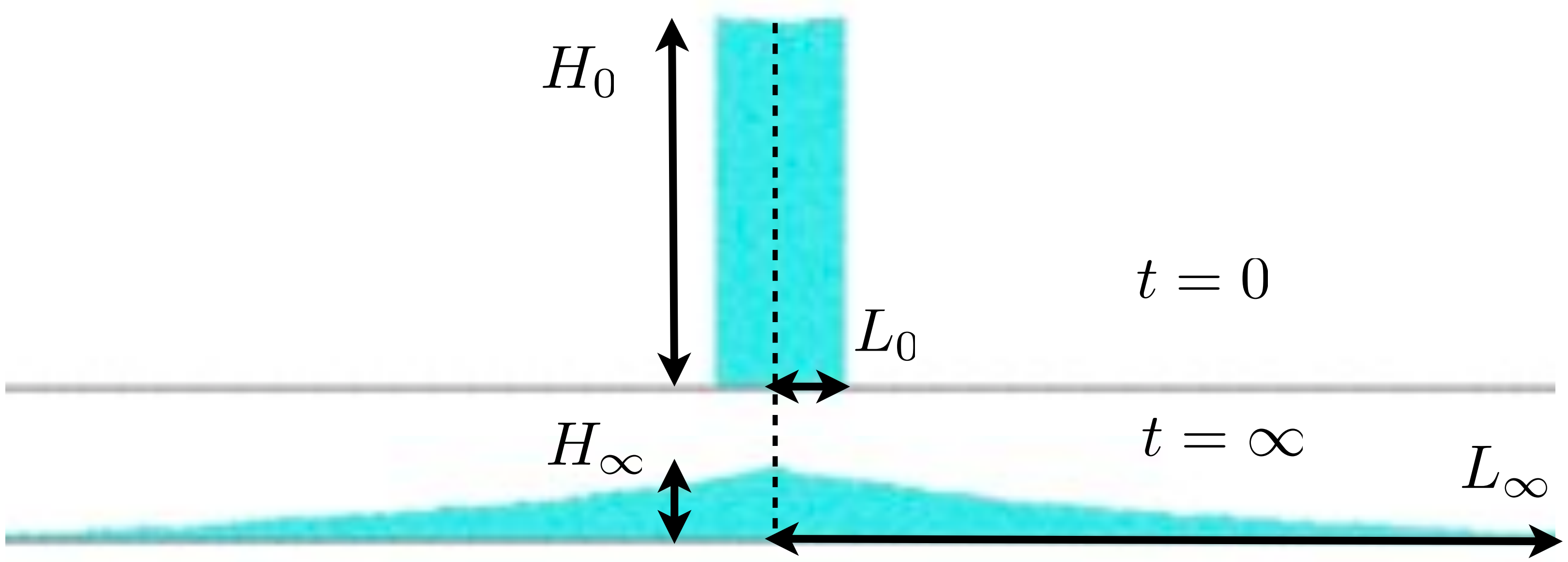


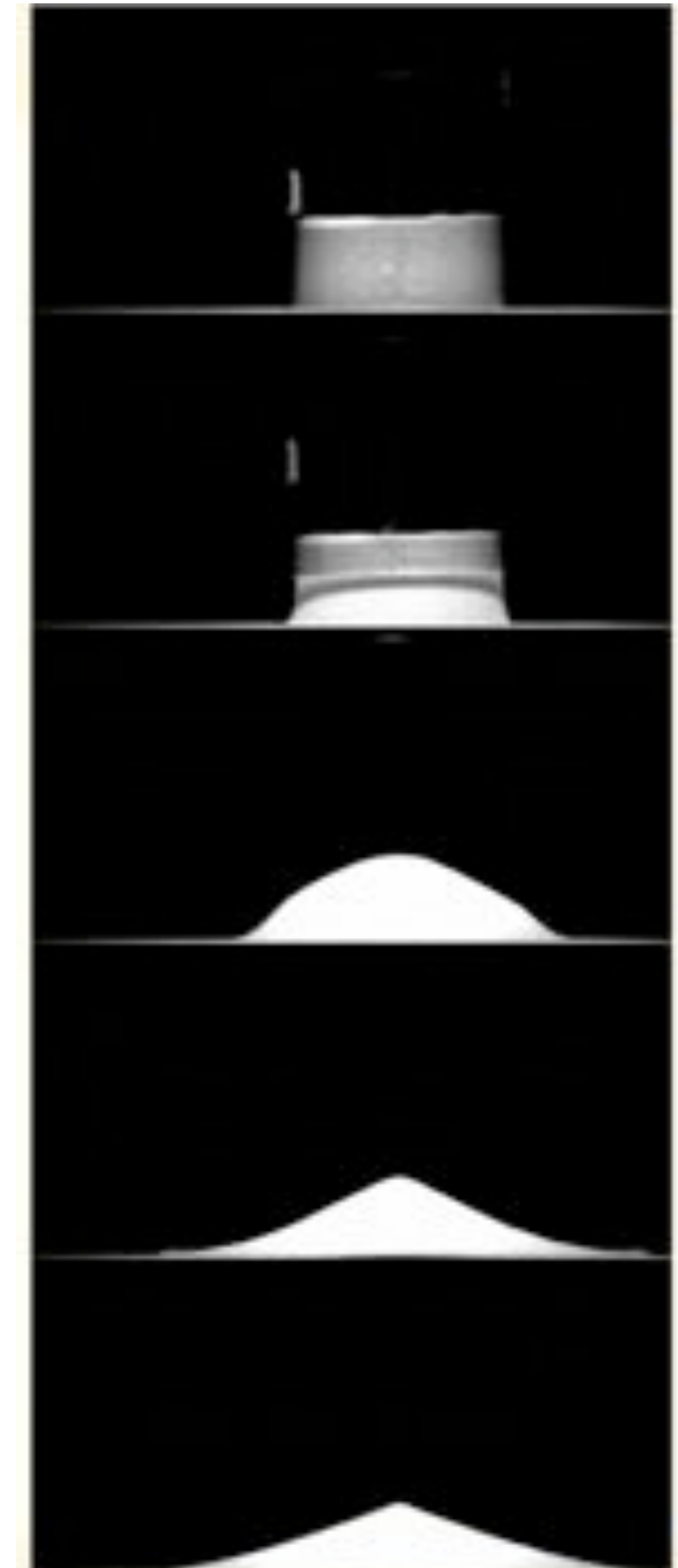

Lajeunesse et al., 2004

The sand pit problem: quickly remove the bucket of sand

# Granular Column Collapse

A possible experimental set up is a container filled by sand (left), the aspect ratio (height/length) is *a*. At initial time, the gate is opened quickly. After the avalanche, the grains stop, the final configuration is at rest (right). We compare results from Discrete Contact Method Simulations (simulation of the displacement of each grain) to a continuum Navier Stokes simulation with the μ(I) rheology *Gerris*.

The sand pit problem: quickly remove the bucket of sand

# outline

- what is a granular fluid? some images
- the μ(I) friction law obtained from experiments and discrete simulation
- the viscosity associated to the μ(I) friction law
- the Saint Venant Savage Hutter Hyperbolic model
- implementing the μ(I) friction law in Navier Stokes
- Examples of flows: focusing on the granular column collapse (limits of Saint Venant Savage Hutter Hyperbolic model)

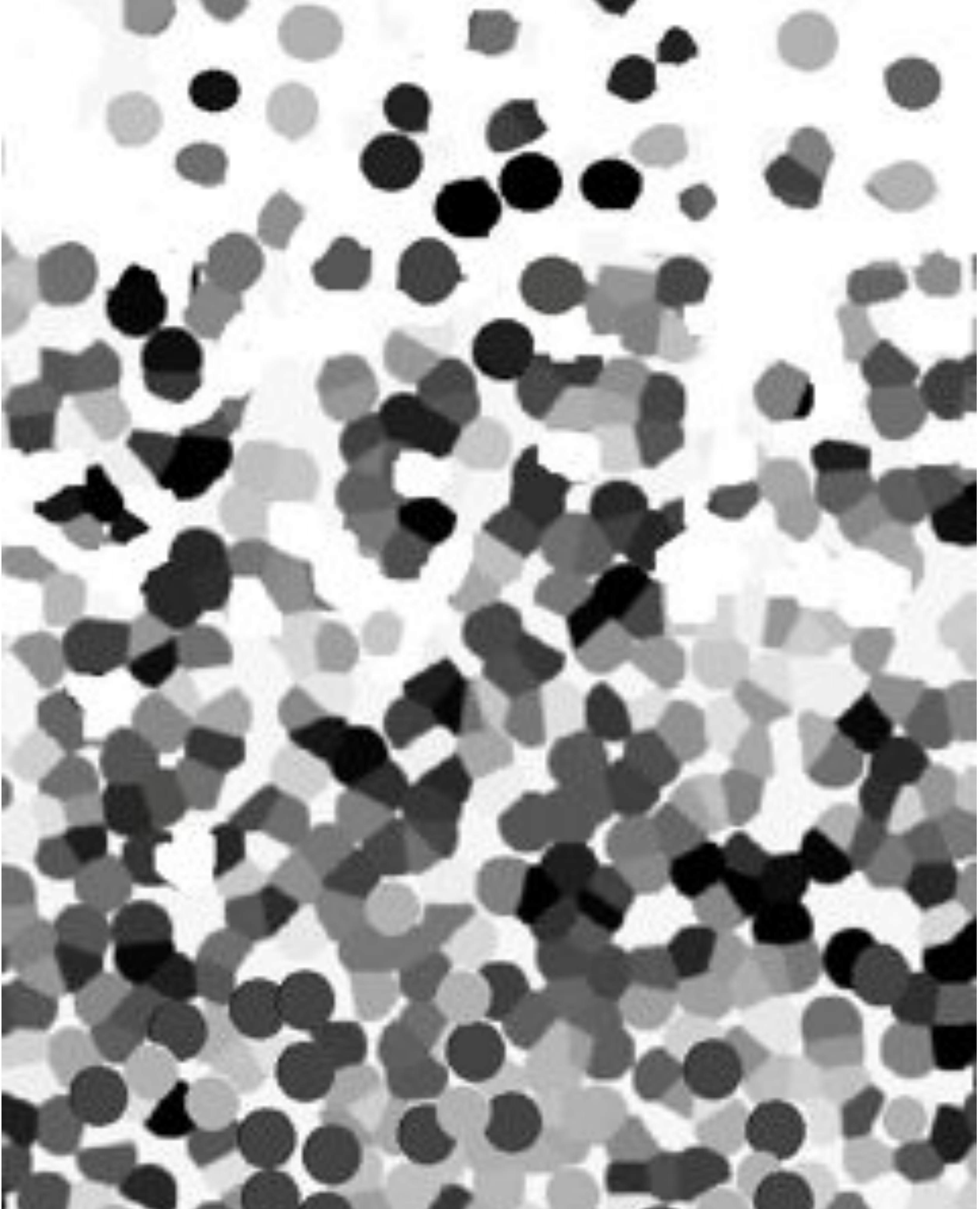

grains

impacts:
suspension

granular media
contacts

like a solid:

from the grains to the fluid

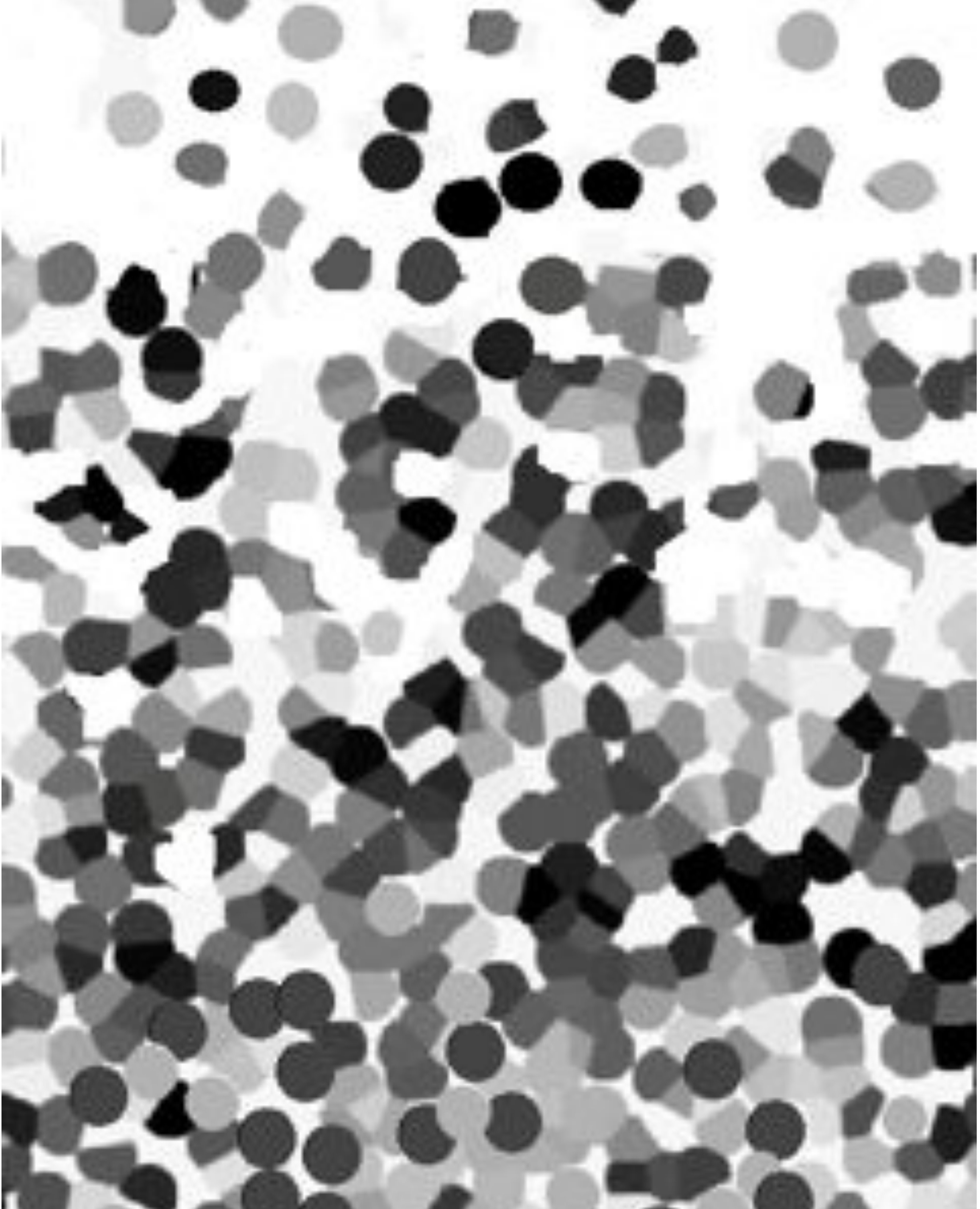

grains

$\phi_{min}$ 0.5 (2D) 0.55 (3D)

$\phi_{min} < \phi < \phi_{Max}$

$\phi_{max}$ 0.8 (2D) 0.65 (3D)

from the grains to the fluid

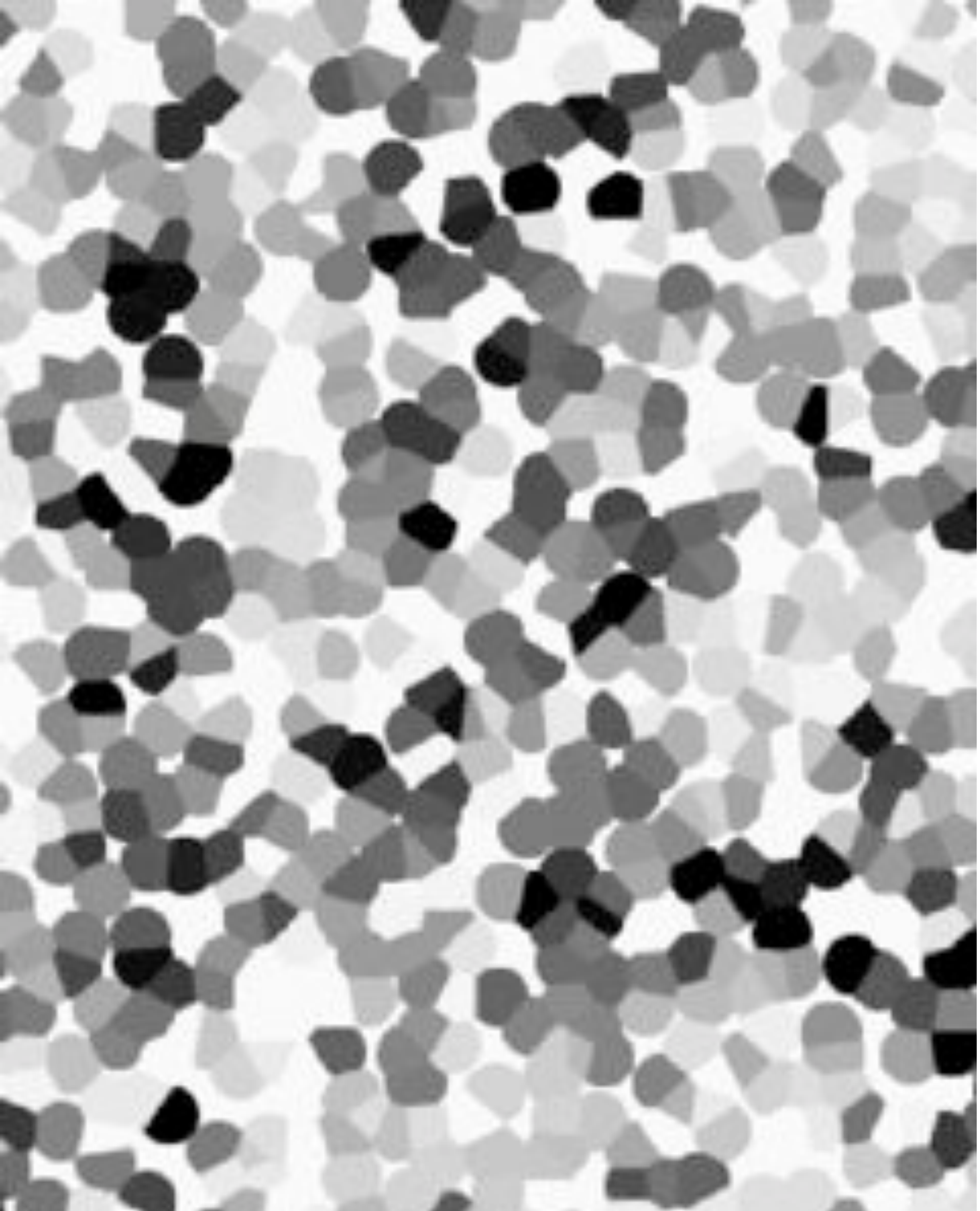

~~grains~~

continuum media hypothesis

from the grains to the fluid

- experiments on model material (glass bead, sand), rheology, images
- numerical experiments of contact dynamics (disks, polygona, spheres)

- Simple configuration: shear/ inclined plane

# Molecular Dynamics:

$$m\frac{d}{dt}\overrightarrow{U} = \overrightarrow{F} + \overrightarrow{F}_n + \overrightarrow{F}_t$$ Newton's equations

branch a spring -dashpot

$$F_n = -k\delta - \gamma\frac{d\delta}{dt}$$

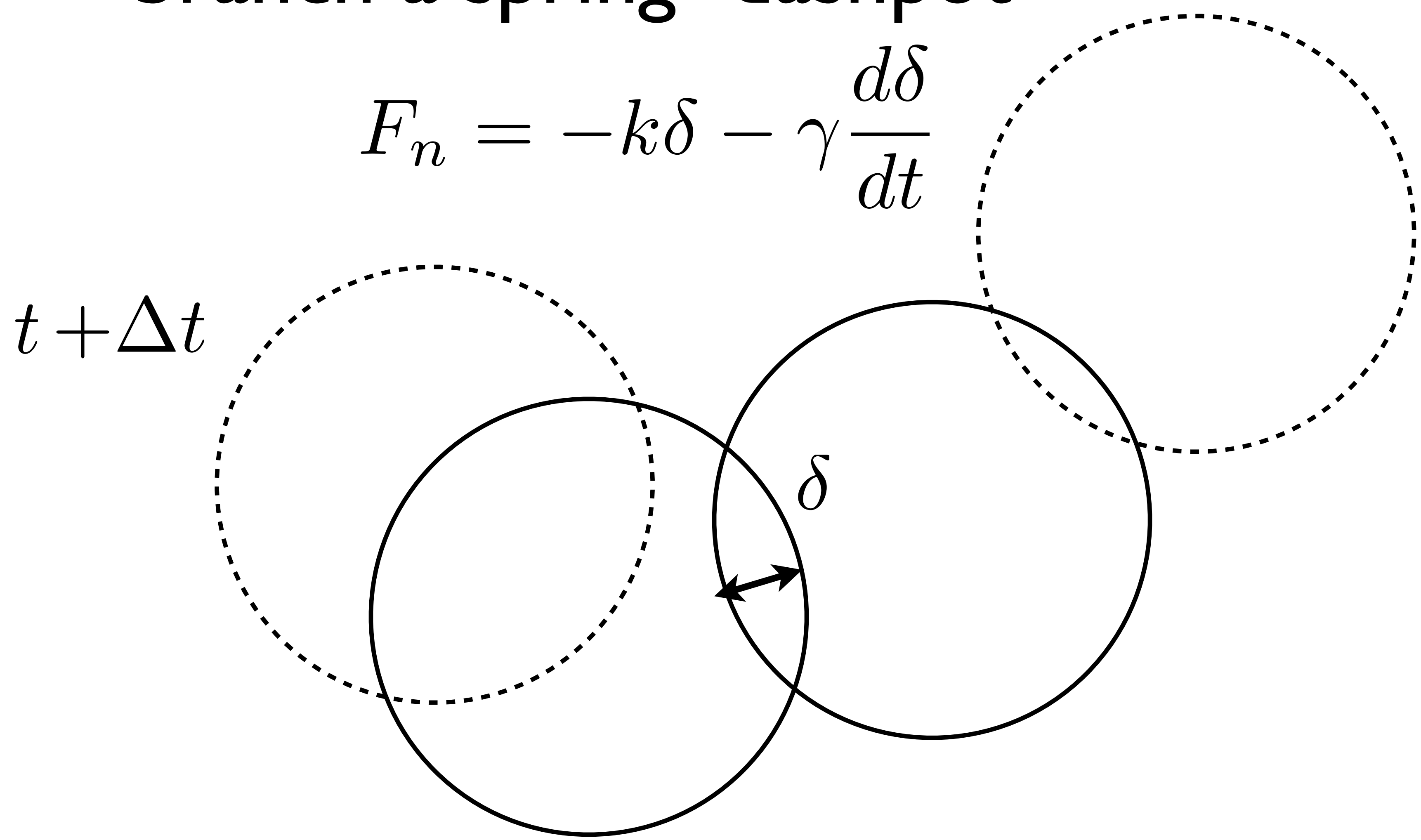


tangential Coulombic Friction $F_t < \mu F_n$

# Contact Dynamics de (Moreau 1988)

rigid grains
coefficient of friction μ

$$m \frac{d}{dt} \overrightarrow{U} = \overrightarrow{F}$$

Newton's equations

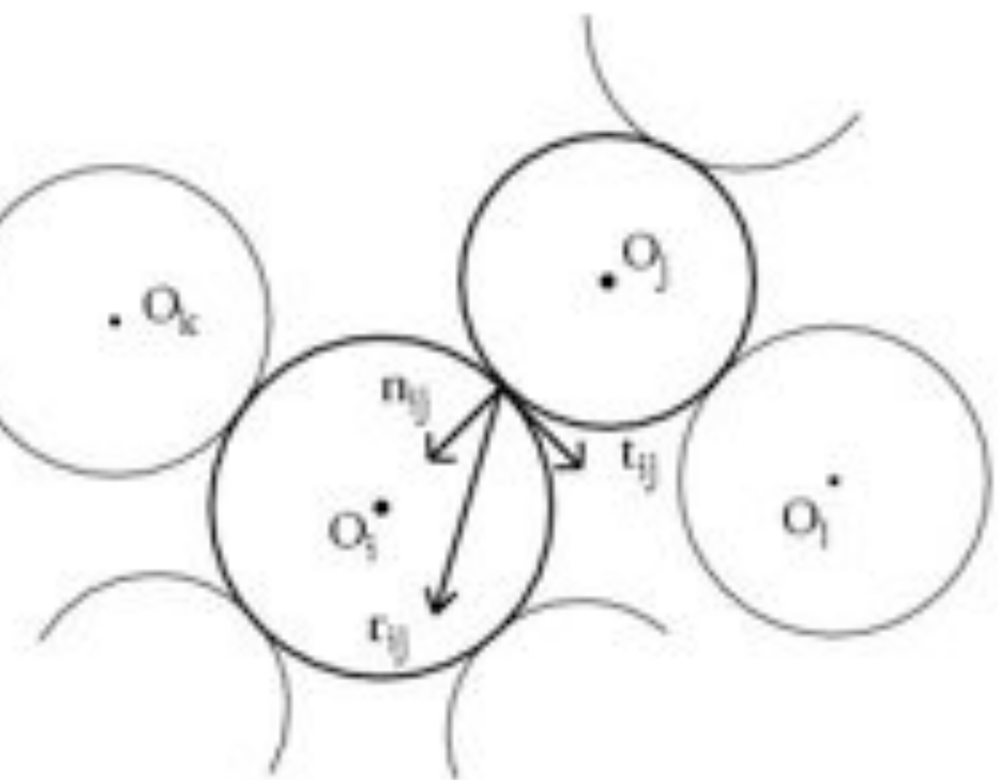

# Contact Dynamics de (Moreau 1988)

rigid grains
coefficient of friction μ

$$m(\overrightarrow{U}^+ - \overrightarrow{U}^-) = \overrightarrow{F}\delta t$$ Newton's equations

take the form of an equality between the change of momenta and the average impulse during δt.

written for each grain at the contact

$u_n, u_t$

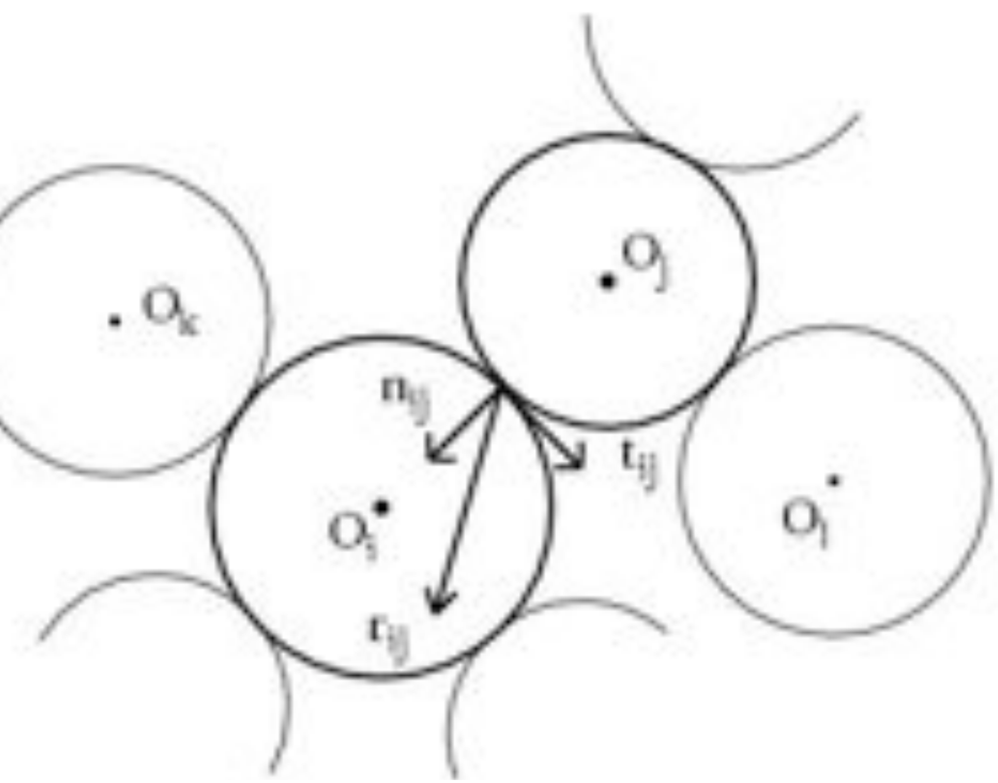


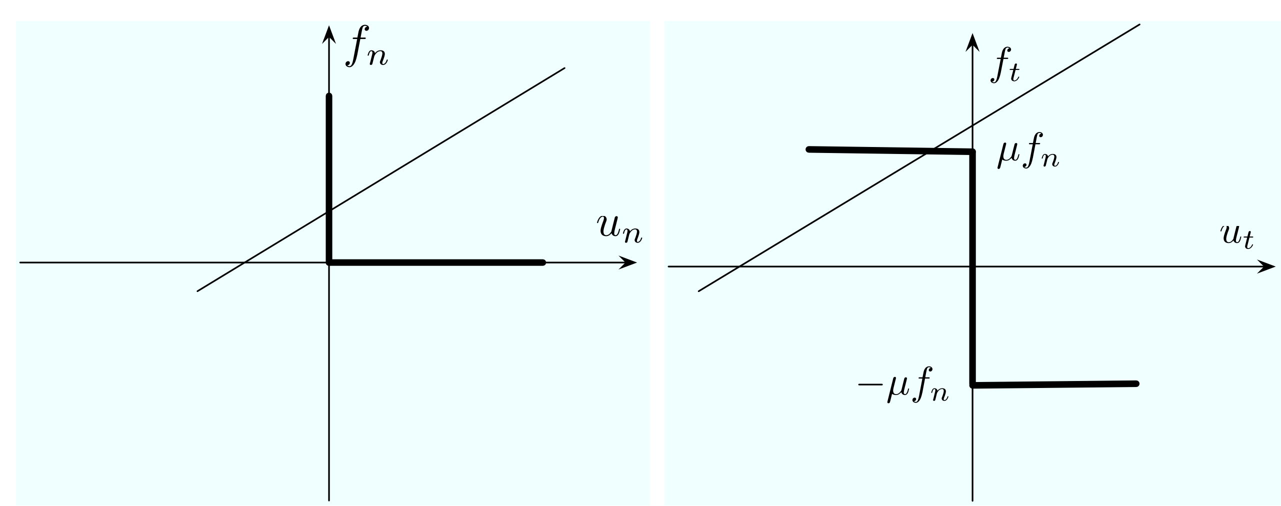

- Looking for a continuum description
- Lot of recent experiments
- Simulations with Contact Dynamics

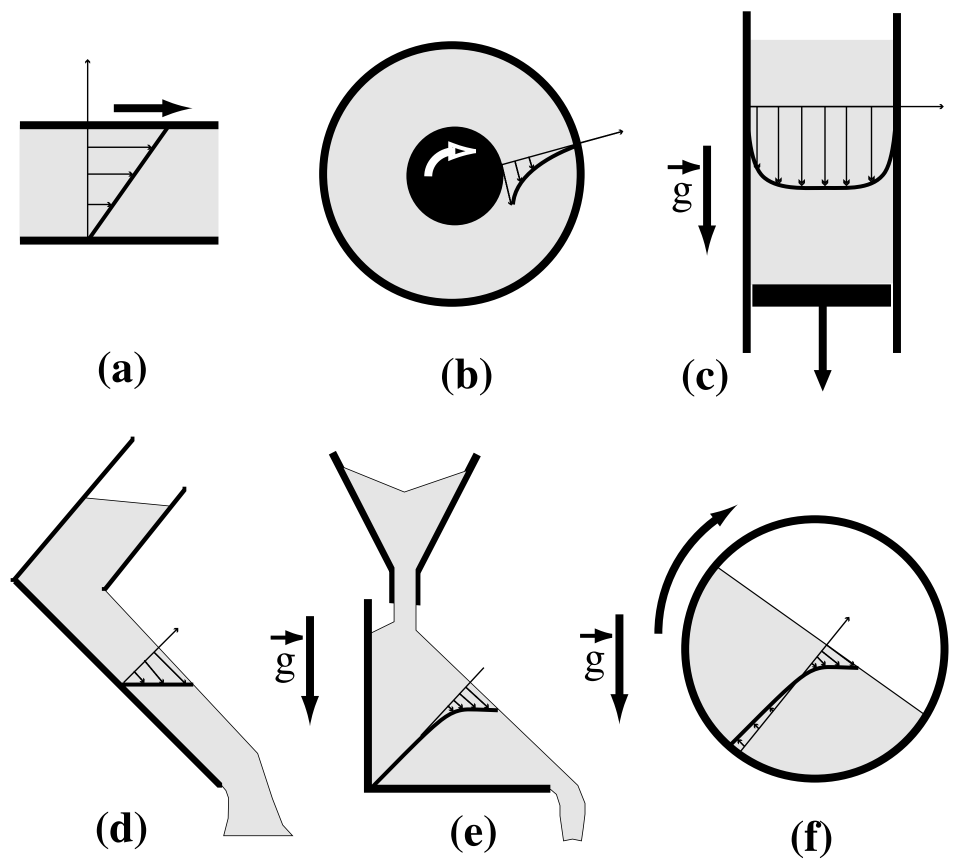


**Fig. 1.** The six configurations of granular flows: (a) plane shear, (b) annular shear, (c) vertical-chute flows, (d) inclined plane, (e) heap flow, (f) rotating drum.

GDR MiDi EPJ E 04

- Looking for a continuum description
- Lot of recent experiments
- Simulations with Contact Dynamics

- Defining a «viscosity»
- Implement it in the Navier Stokes solver *Gerris*
- Test on exact  «Bagnold» avalanche solution
- Test on granular collapse

$V(z)$

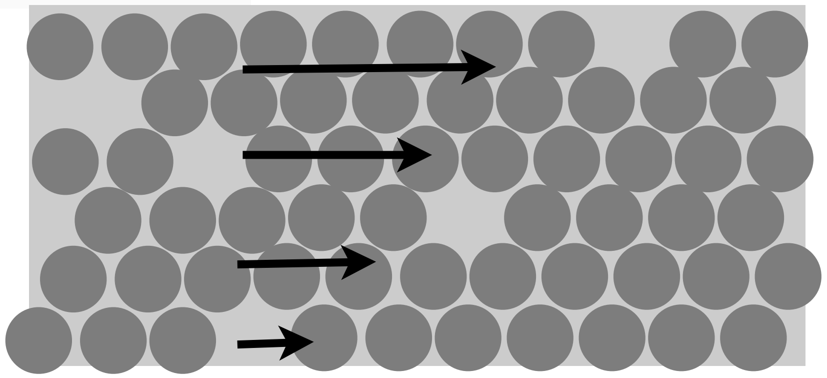

constitutive law?

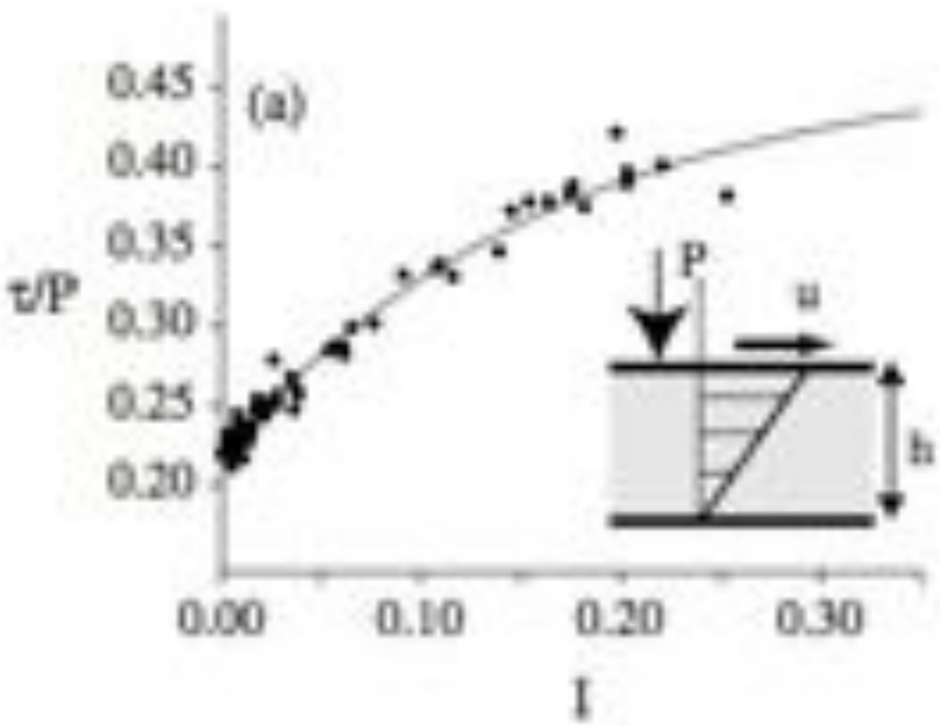


$V(z)$

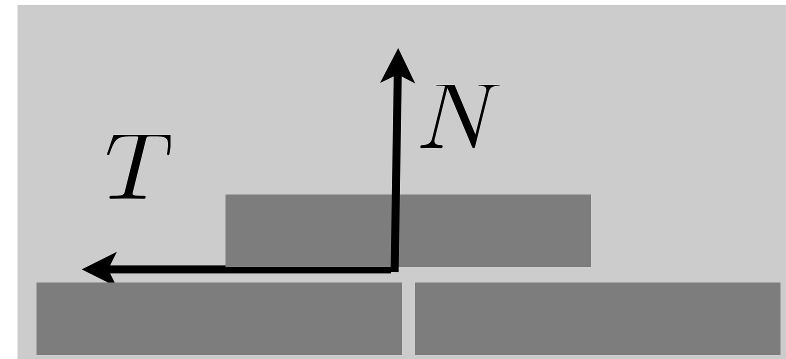


$$T = \mu N$$

Coulomb dry friction

Coulomb friction law

$$\boxed{\tau = \mu P}$$

$V(z)$

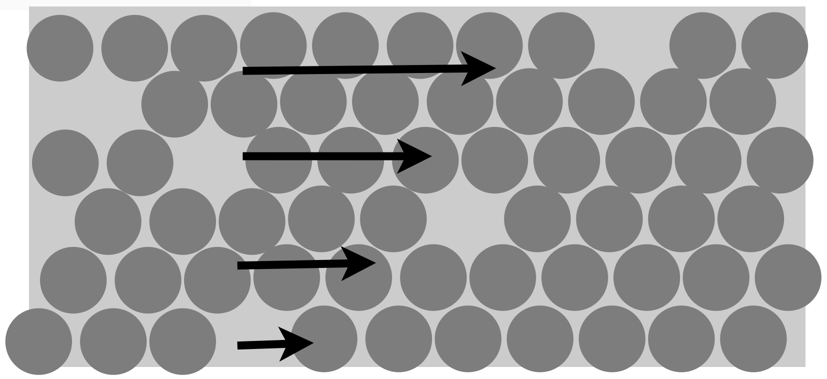

$V(z)$

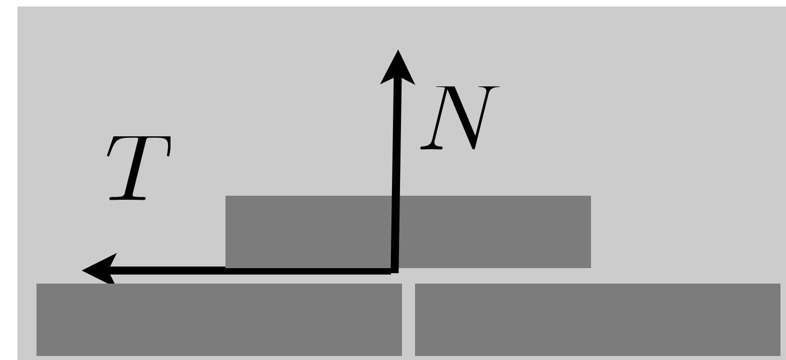


$$T = \mu N$$

Coulomb friction law

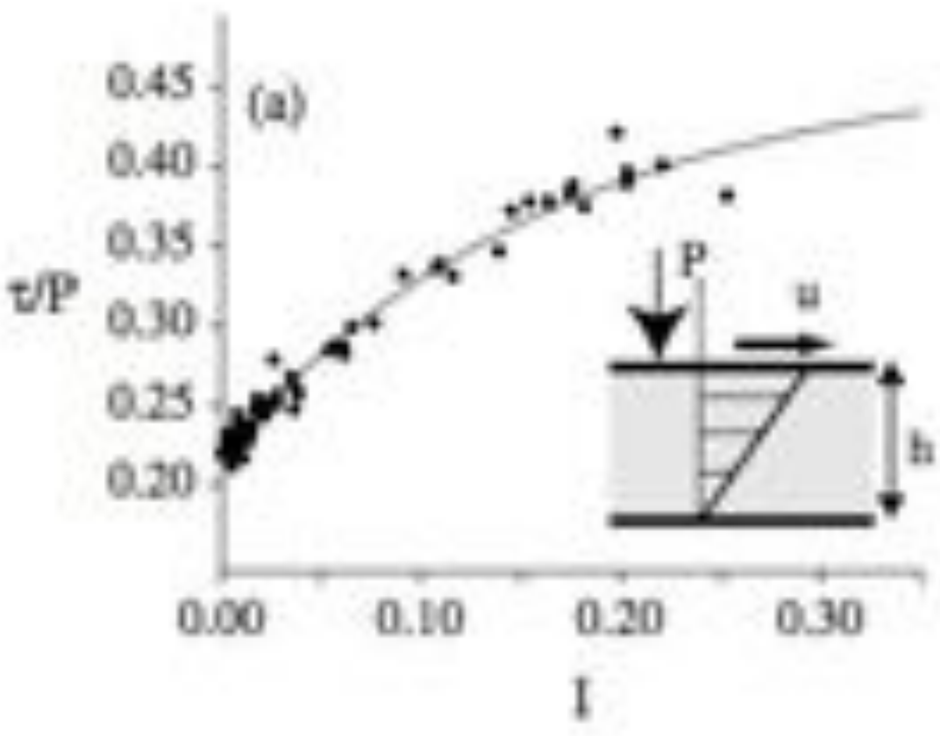


$$I = \frac{d\frac{\partial u}{\partial y}}{\sqrt{P/\rho}}$$

$$\boxed{\tau = \mu(I)P}$$

non dimensional number: «Froude»

local «Inertial Number» (Da Cruz 04-05)

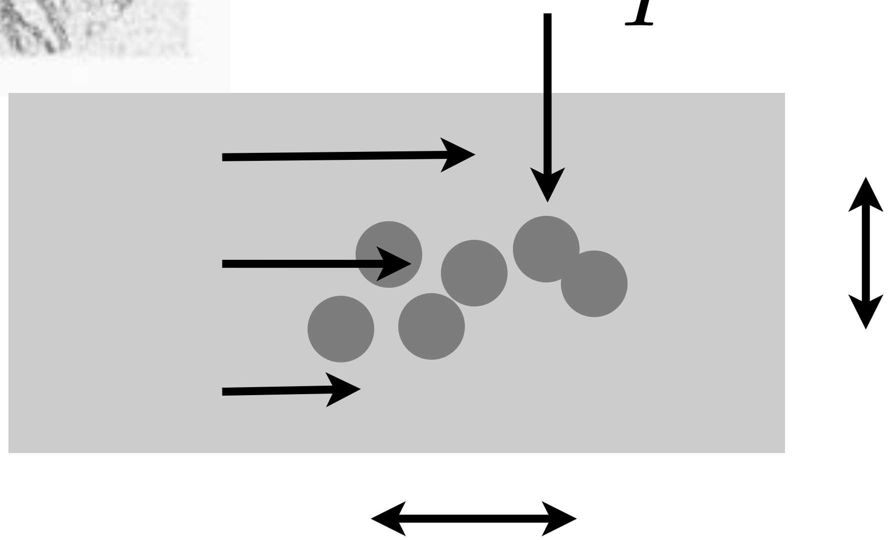


$$md^2y/dt^2 = Pd^2$$

$$t^2 = \rho d^2/(P)$$

$$\frac{dx}{dt} = d\frac{\partial u}{\partial y} \qquad t = 1/\frac{\partial u}{\partial y}$$

$$\frac{\text{falling time}}{\text{displacement time}} \qquad I = \frac{d\frac{\partial u}{\partial y}}{\sqrt{P/\rho}}$$

$u(y)$

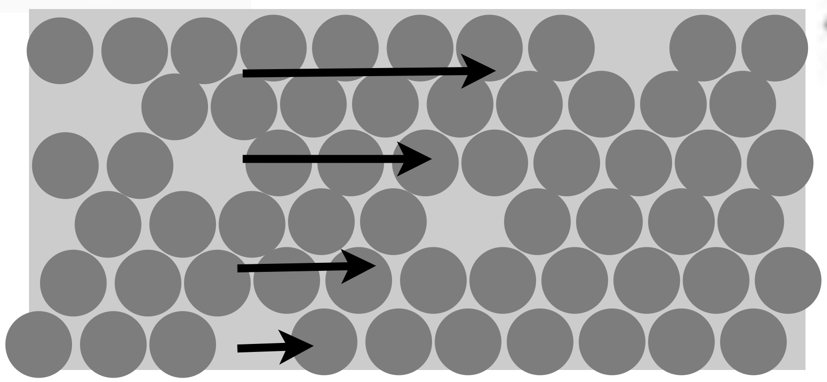

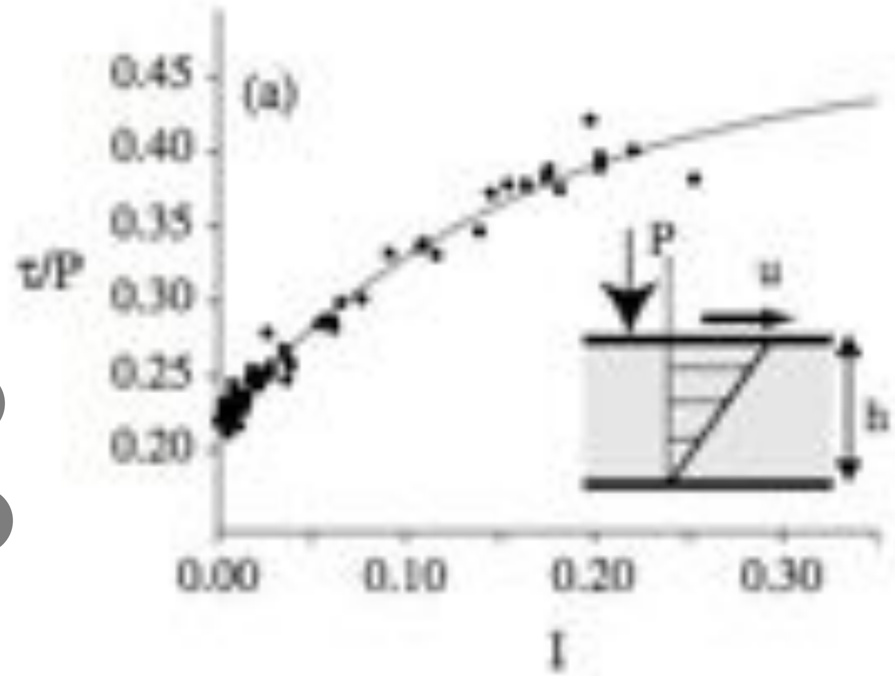


by grain dynamics

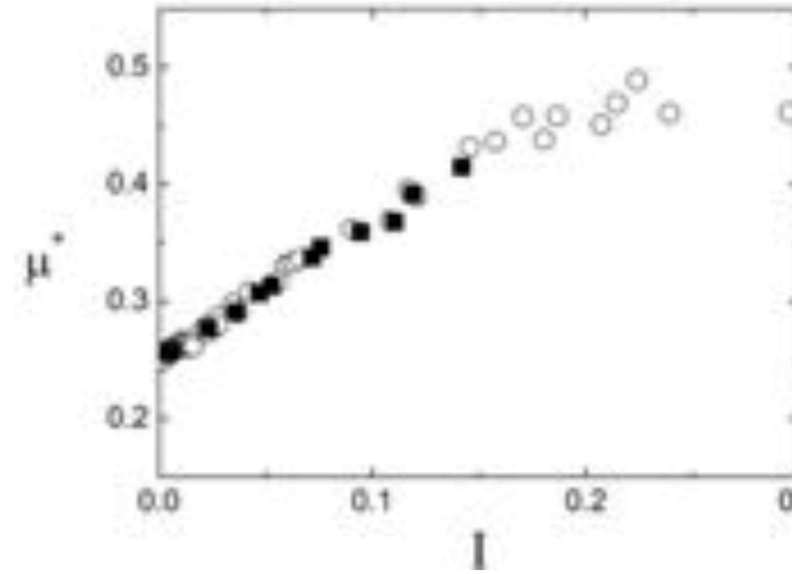


Da Cruz PRE 05

Coulomb friction law

$$\tau = \mu(I)P$$

$$\frac{\text{falling time}}{\text{displacement time}} \qquad I = \frac{d\frac{\partial u}{\partial y}}{\sqrt{P/\rho}}$$

Pouliquen 99
Pouliquen Forterre JSM 06
Da Cruz 04-05
GDR Midi 04
Josserand Lagrée Lhuillier 04

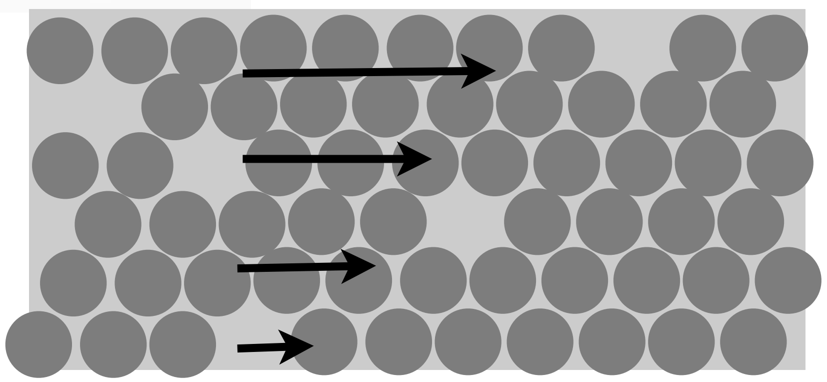


by grain dynamics

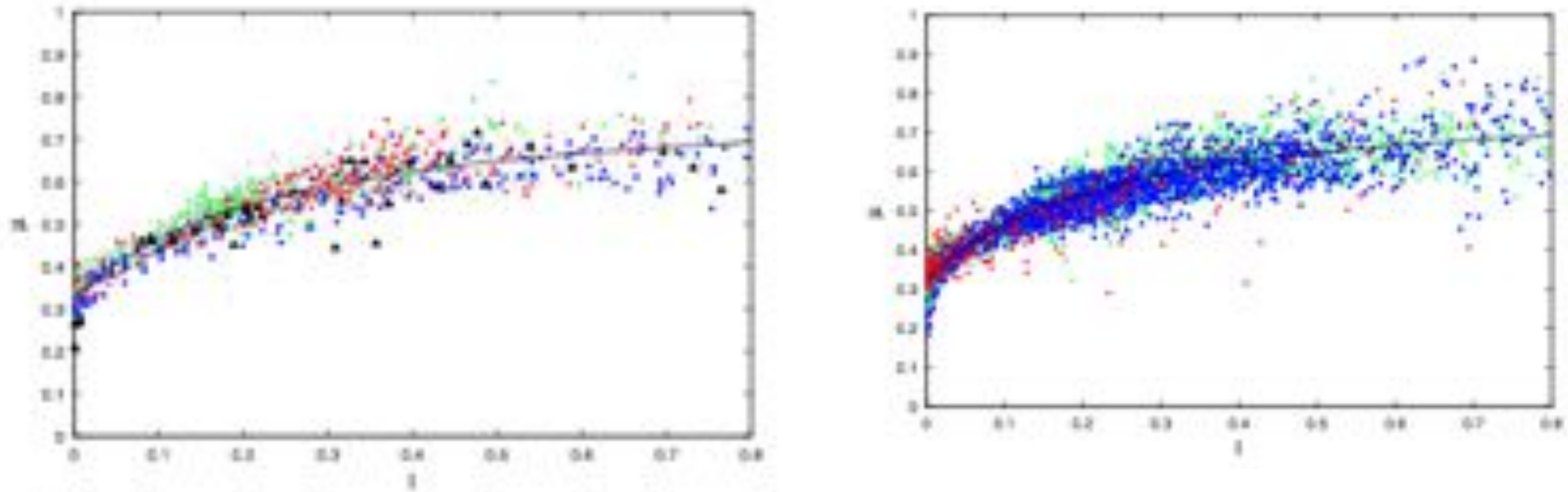

Lacaze Kerswell 09

## Coulomb friction law

$$\tau = \mu(I)P$$

$$I = \frac{d\frac{\partial u}{\partial y}}{\sqrt{P/\rho}}$$

$$\mu(I) = \mu_1 + \frac{\mu_2 - \mu_1}{I_0/I + 1}$$

$$\mu_1 \simeq 0.32 \quad (\mu_2 - \mu_1) \simeq 0.23 \quad I_0 \simeq 0.3$$

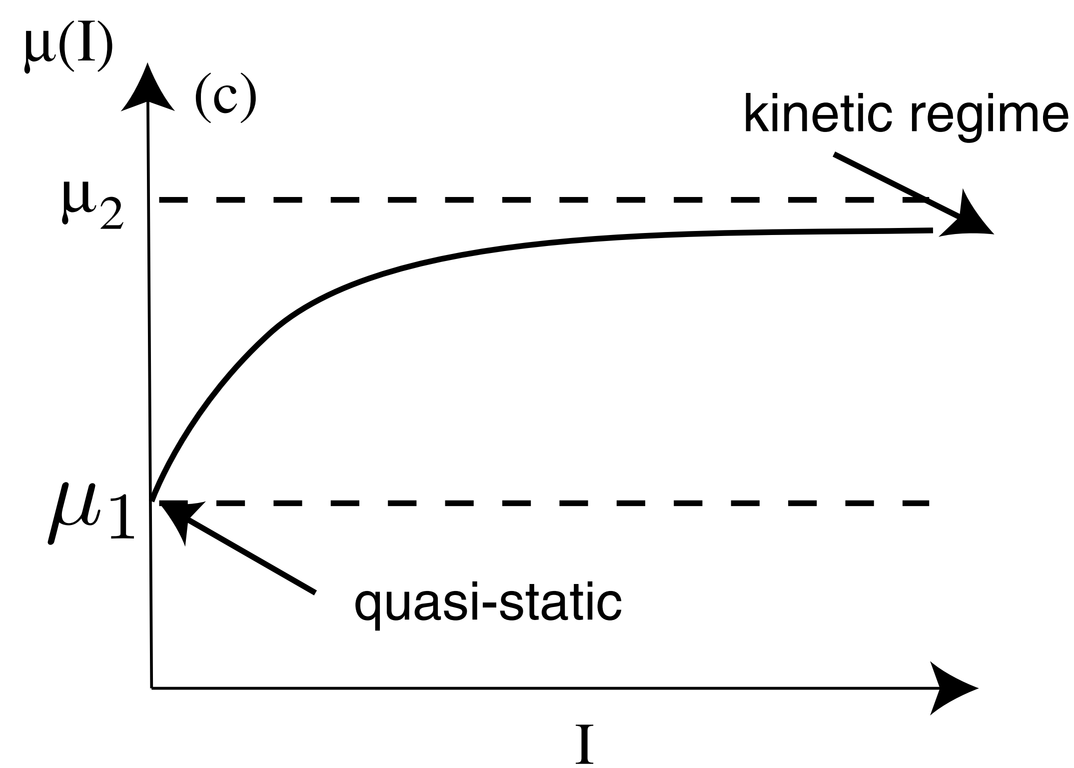

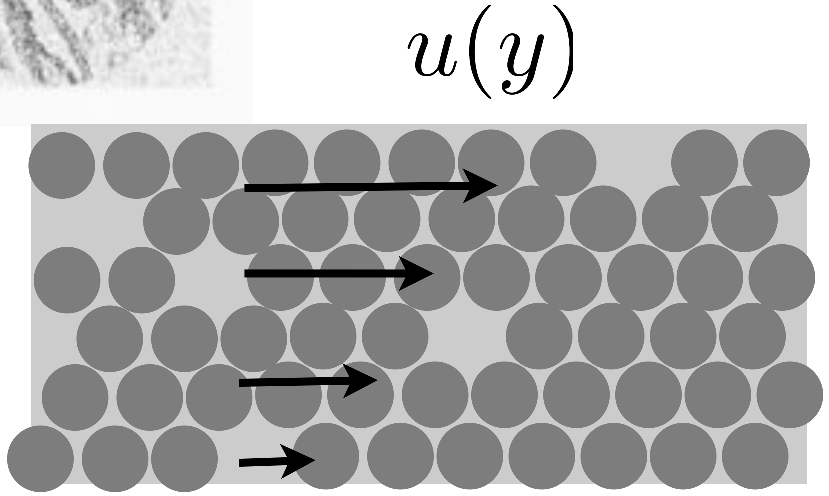


Coulomb friction law

$$\tau = \mu(I)P \qquad\qquad I = \frac{d\frac{\partial u}{\partial y}}{\sqrt{P/\rho}}$$

«Drucker-Prager»
plastic flow

equivalent viscosity

$$\eta \frac{\partial u}{\partial y} = \mu(I)p \quad \rightarrow \quad \eta = \frac{\mu(I)p}{\frac{\partial u}{\partial y}}$$

# implementation in Navier Stokes?

Jop Forterre Pouliquen 2005

$$\mu(I) = \mu_1 + \frac{\mu_2 - \mu_1}{I_0/I + 1}$$

$$D_2 = \sqrt{D_{ij} D_{ij}} \qquad D_{ij} = \frac{u_{i,j} + u_{j,i}}{2}$$

construction of a viscosity based on the *D2* invariant and redefinition of *I*

$$I = d\sqrt{2} D_2 / \sqrt{(|p|/\rho)}.$$

$$\eta = \left( \frac{\mu(I)}{\sqrt{2} D_2} p \right)$$

«Drucker-Prager»

$$\nabla \cdot \mathbf{u} = 0, \quad \rho \left( \frac{\partial \mathbf{u}}{\partial t} + \mathbf{u} \cdot \nabla \mathbf{u} \right) = -\nabla p + \nabla \cdot (2\eta \mathbf{D}) + \rho g,$$

Boundary Conditions: no slip and *P=0* at the interface

# outline

- what is a granular fluid? some images
- the μ(I) friction law obtained from experiments and discrete simulation
- the viscosity associated to the μ(I) friction law
- the Saint Venant Savage Hutter Hyperbolic model
- implementing the μ(I) friction law in Navier Stokes
- Examples of flows: focusing on the granular column collapse (limits of Saint Venant Savage Hutter Hyperbolic model)


ST VENANT

- Couche Mince Saint Venant Shallow Water Savage Hutter

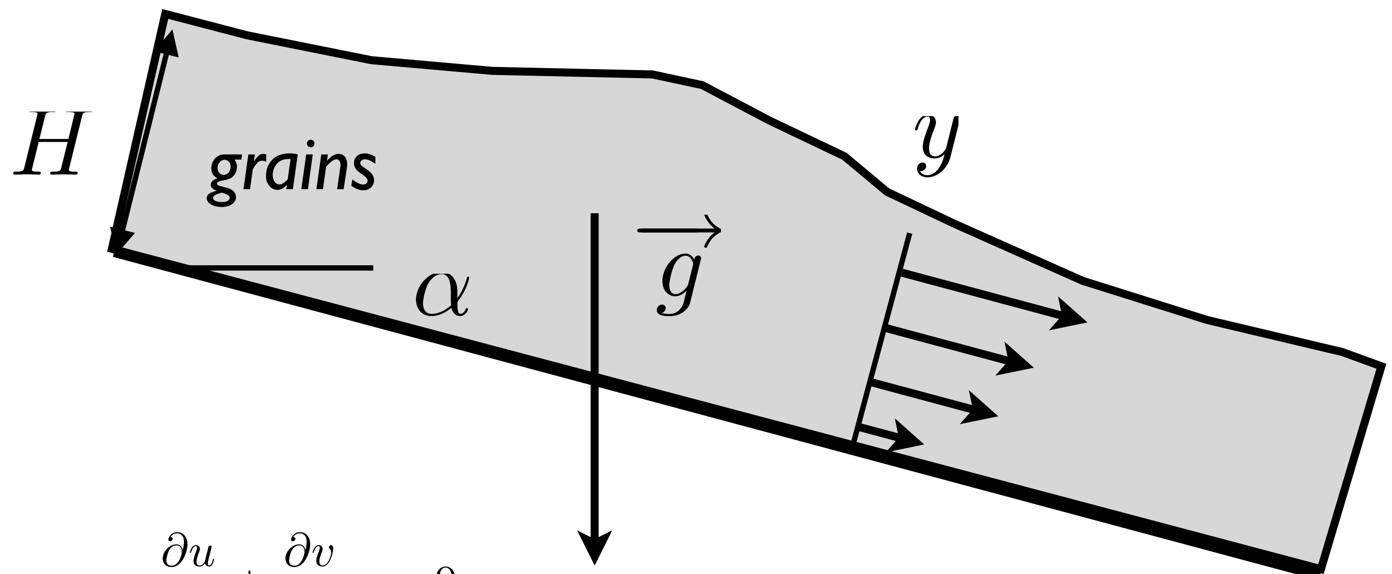


$$\varepsilon = H/L$$

$$\begin{cases} \frac{\partial u}{\partial x} + \frac{\partial v}{\partial y} & = 0 \\ \rho(\frac{\partial u}{\partial t} + \frac{\partial u^2}{\partial x} + \frac{\partial uv}{\partial y}) & = -g\rho \sin\alpha - \frac{\partial p}{\partial x} + \frac{\partial \tau_{xx}}{\partial x} + \frac{\partial \tau_{xy}}{\partial y} \\ \rho(\frac{\partial v}{\partial t} + \frac{\partial uv}{\partial x} + \frac{\partial v^2}{\partial y}) & = -g\rho \cos\alpha - \frac{\partial p}{\partial y} + \frac{\partial \tau_{yx}}{\partial x} + \frac{\partial \tau_{yy}}{\partial y} \end{cases}$$

$$p = -\rho g \cos\alpha(\eta(x,t) - y)$$

$$\tau_{xy} = \rho g H \sin\alpha \bar{\tau}_{xy}$$

$$\rho U_0^2/L \longleftrightarrow -\frac{\partial p}{\partial x} = -\rho g \frac{\partial \eta}{\partial x}$$

$$\rho U_0^2/(H/\varepsilon) = \rho g \varepsilon.$$

$$\boxed{U_0 = \sqrt{gH}.}$$

# Saint-Venant Savage Hutter

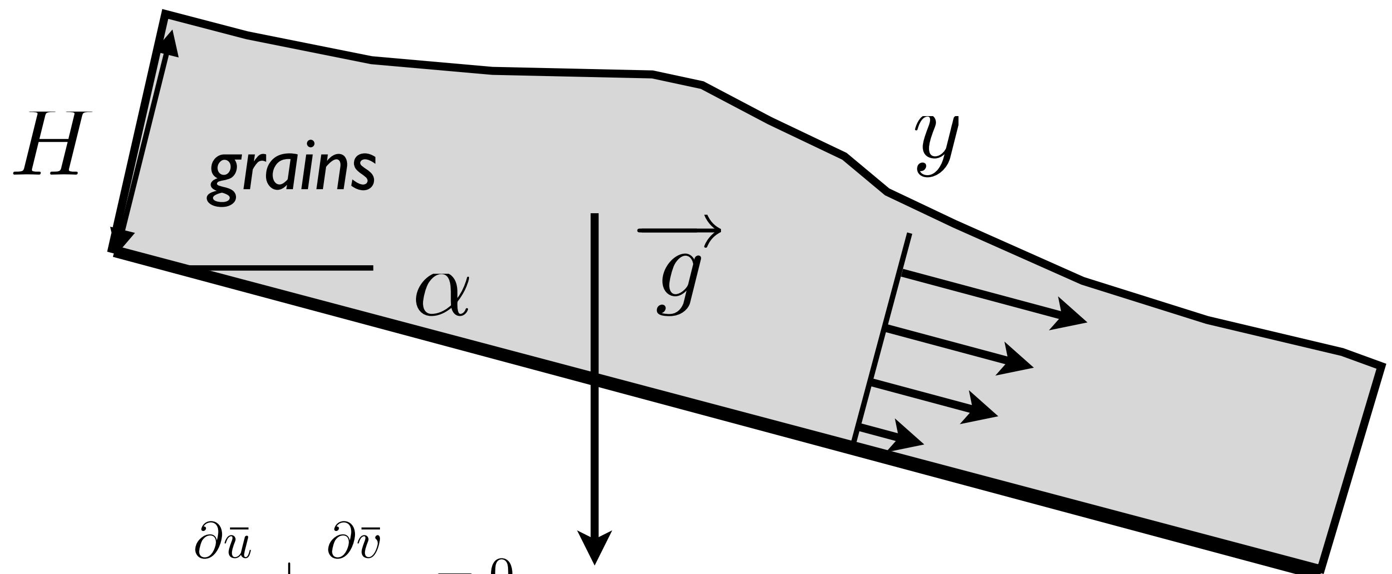


$$\varepsilon = H/L$$

$$\left\{\begin{array}{rl} \dfrac{\partial \bar{u}}{\partial \bar{x}} + \dfrac{\partial \bar{v}}{\partial \bar{y}} & = 0 \\ \varepsilon(\dfrac{\partial \bar{u}}{\partial \bar{t}} + \dfrac{\partial \bar{u}^2}{\partial \bar{x}} + \dfrac{\partial \bar{u}\bar{v}}{\partial \bar{y}}) & = -\sin\alpha - \varepsilon \dfrac{\partial \bar{p}}{\partial \bar{x}} + \sin\alpha\varepsilon \dfrac{\partial \bar{\tau}_{xx}}{\partial \bar{x}} + \sin\alpha \dfrac{\partial \bar{\tau}_{xy}}{\partial \bar{y}} \\ \varepsilon^2(\dfrac{\partial \bar{v}}{\partial \bar{t}} + \dfrac{\partial \bar{u}\bar{v}}{\partial x} + \dfrac{\partial \bar{v}^2}{\partial \bar{y}}) & = -\cos\alpha - \dfrac{\partial \bar{p}}{\partial \bar{y}} + \sin\alpha\varepsilon \dfrac{\partial \bar{\tau}_{yy}}{\partial \bar{x}} + \sin\alpha \dfrac{\partial \bar{\tau}_{yx}}{\partial \bar{y}} \end{array}\right.$$

$$p = -\rho g \cos\alpha(\eta(x,t) - y) \qquad \tau_{xy} = \rho g H \sin\alpha \bar{\tau}_{xy}$$

$$\rho U_0^2/L \longleftrightarrow -\frac{\partial p}{\partial x} = -\rho g \frac{\partial \eta}{\partial x}$$

$$\rho U_0^2/(H/\varepsilon) = \rho g \varepsilon.$$

$$\boxed{U_0 = \sqrt{gH}.}$$

# Saint-Venant Savage Hutter

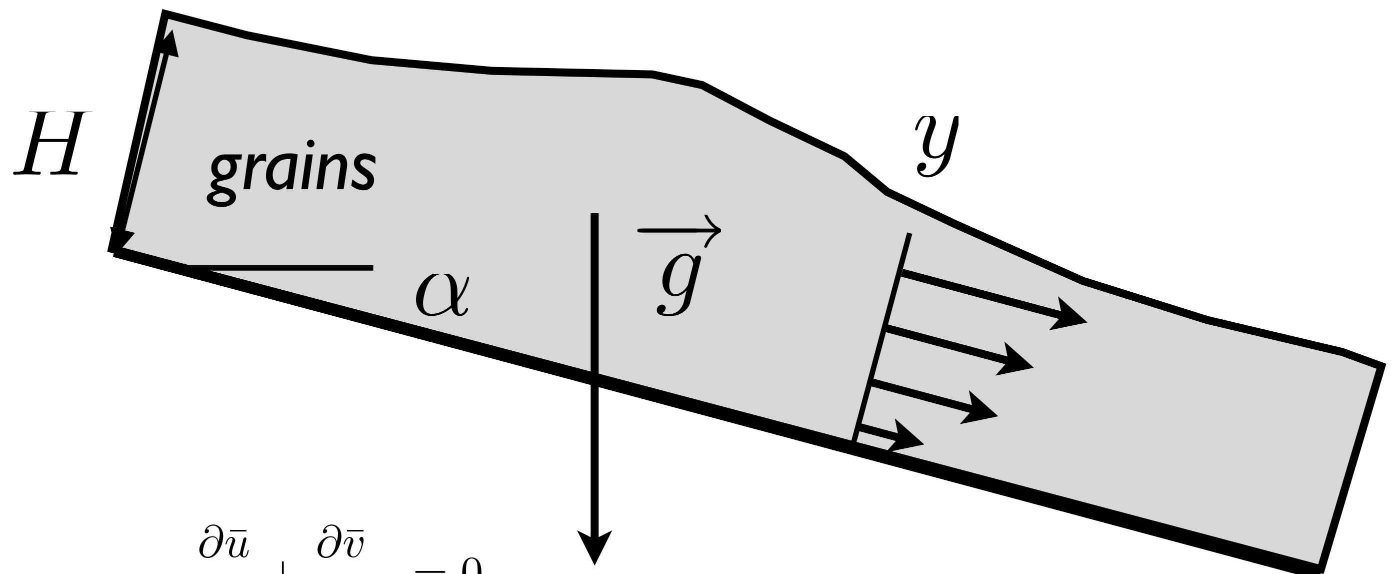


$$
\left\{
\begin{aligned}
\frac{\partial \bar u}{\partial \bar x} + \frac{\partial \bar v}{\partial \bar y} &= 0\\
\varepsilon\left(\frac{\partial \bar u}{\partial \bar t} + \frac{\partial \bar u^2}{\partial \bar x} + \frac{\partial \bar u \bar v}{\partial \bar y}\right) &= -\sin\alpha - \varepsilon\frac{\partial \bar p}{\partial \bar x} + \sin\alpha\frac{\partial \bar\tau_{xy}}{\partial \bar y}\\
0 &= -\cos\alpha - \frac{\partial \bar p}{\partial \bar y}
\end{aligned}
\right.
$$

$$\int dy$$

$$\frac{\partial h}{\partial t} + \frac{\partial}{\partial x}\int_f^\eta u(x,y,t)dy = 0$$

μ(I) at the wall

$$\frac{\partial}{\partial t}\int_f^\eta u(x,y,t)dy + \frac{\partial}{\partial x}\left(\int_f^\eta u(x,y,t)^2 dy + \cos\alpha\frac{g}{2}(h^2)\right) = -gh\sin(\alpha) - \cos\alpha gh\frac{d}{dx}f - \mu(I(0))gh\cos(\alpha).$$

Saint-Venant Savage Hutter

$$\frac{\partial h}{\partial t} + \frac{\partial (Q)}{\partial x} = 0 \quad \frac{\partial Q}{\partial t} + \frac{\partial}{\partial x}\left(\frac{5Q^2}{4h} + \frac{g}{2}(h^2)\right) = -gh\mu(I)\frac{Q}{|Q|}$$

Integral over the layer of grains

Saint-Venant Savage Hutter *Gerris*

$$\frac{\partial h}{\partial t} + \frac{\partial(Q)}{\partial x} = 0 \quad \frac{\partial Q}{\partial t} + \frac{\partial}{\partial x}(\frac{5Q^2}{4h} + \frac{g}{2}(h^2)) = -gh\mu(I)\frac{Q}{|Q|}$$

*Gerris* is a free finite volume code by Stéphane Popinet

one part of the code is a Shallow Water solver

$$\frac{Q^* - Q^n}{\Delta t} + \frac{\partial}{\partial x}(\frac{Q^2}{h} + \frac{g}{2}(h^2)) = 0 \qquad \frac{Q^{n+1} - Q^*}{\Delta t} = -gh^*\mu(I^*)\frac{Q^{n+1}}{|Q^*|}$$

Audusse et al.

# Saint-Venant Savage Hutter *Gerris*

$$\frac{\partial h}{\partial t} + \frac{\partial (Q)}{\partial x} = 0 \quad \frac{\partial Q}{\partial t} + \frac{\partial}{\partial x}\left(\frac{5Q^2}{4h} + \frac{g}{2}(h^2)\right) = -gh\mu(I)\frac{Q}{|Q|}$$

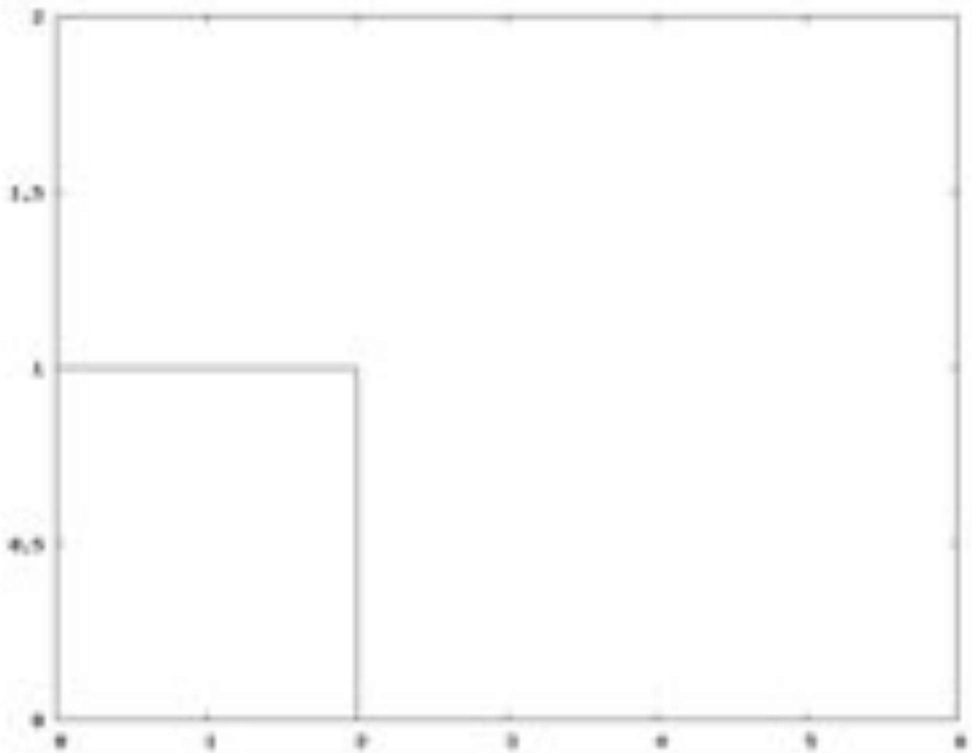


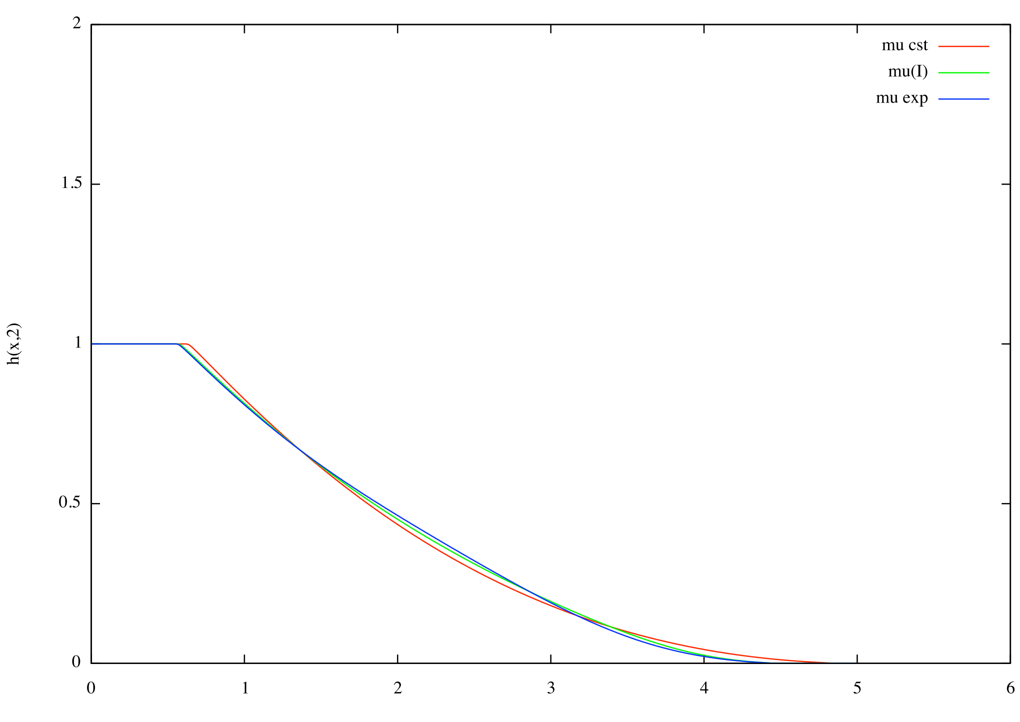


$$\mu(I) = \mu_s$$

$$\mu(I) = \mu_s + \frac{\Delta\mu}{\frac{I_0}{I} + 1}$$

$$\mu(I) = \mu_s + \Delta\mu e^{-\beta/I}$$

mu = 0.45
mu = (0.4 + 0.26/(0.4/In +1))
mu = (0.4 + 0.26*exp(-0.136/In))

Saint-Venant Savage Hutter *Gerris*

$$\frac{\partial h}{\partial t} + \frac{\partial (Q)}{\partial x} = 0 \quad \frac{\partial Q}{\partial t} + \frac{\partial}{\partial x}\left(\frac{5Q^2}{4h} + \frac{g}{2}(h^2)\right) = -gh\mu(I)\frac{Q}{|Q|}$$

valid by hypothesis for small aspect ratio

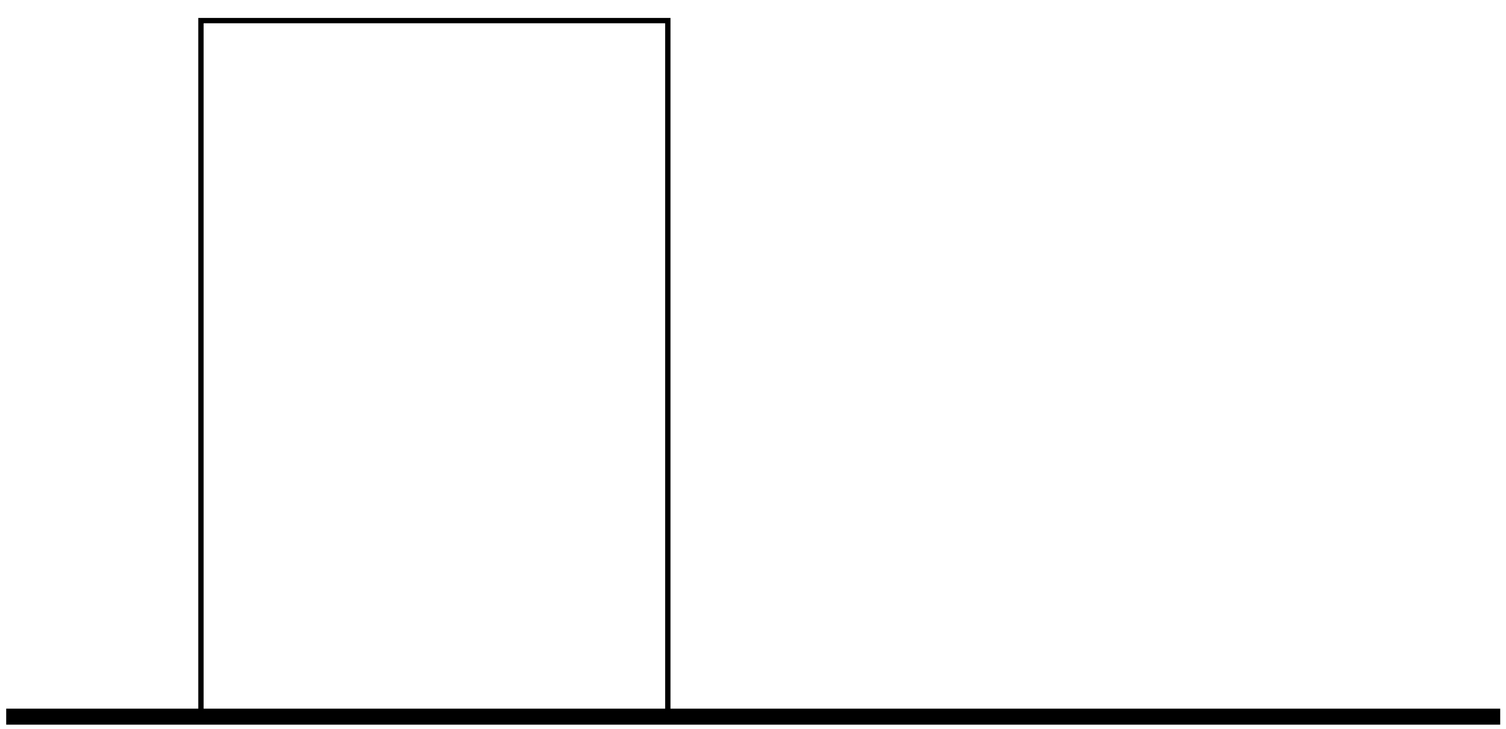

Saint-Venant Savage Hutter *Gerris*

$$\frac{\partial h}{\partial t} + \frac{\partial (Q)}{\partial x} = 0 \quad \frac{\partial Q}{\partial t} + \frac{\partial}{\partial x}\left(\frac{5Q^2}{4h} + \frac{g}{2}(h^2)\right) = -gh\mu(I)\frac{Q}{|Q|}$$

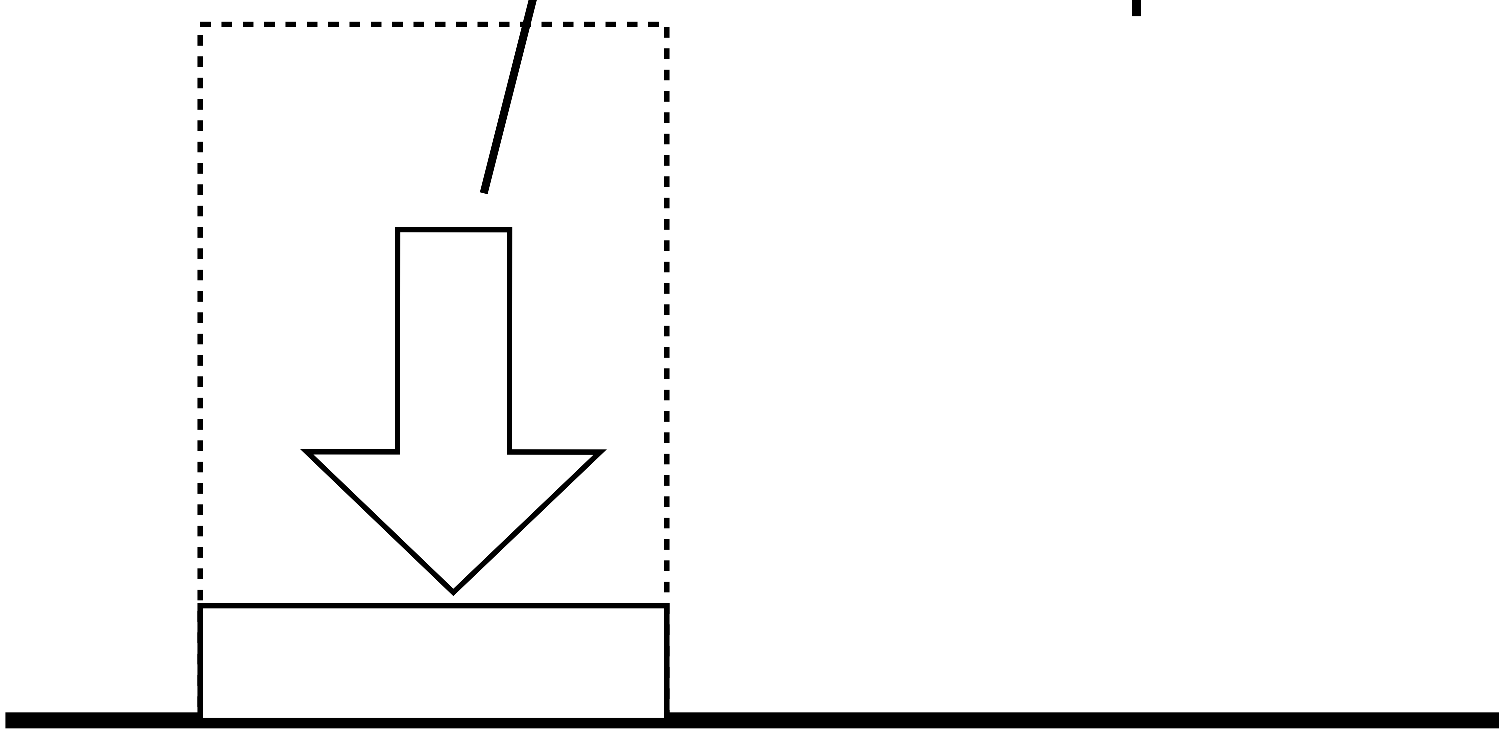

add a source term corresponding to pluviation

# Saint-Venant Savage Hutter *Gerris*

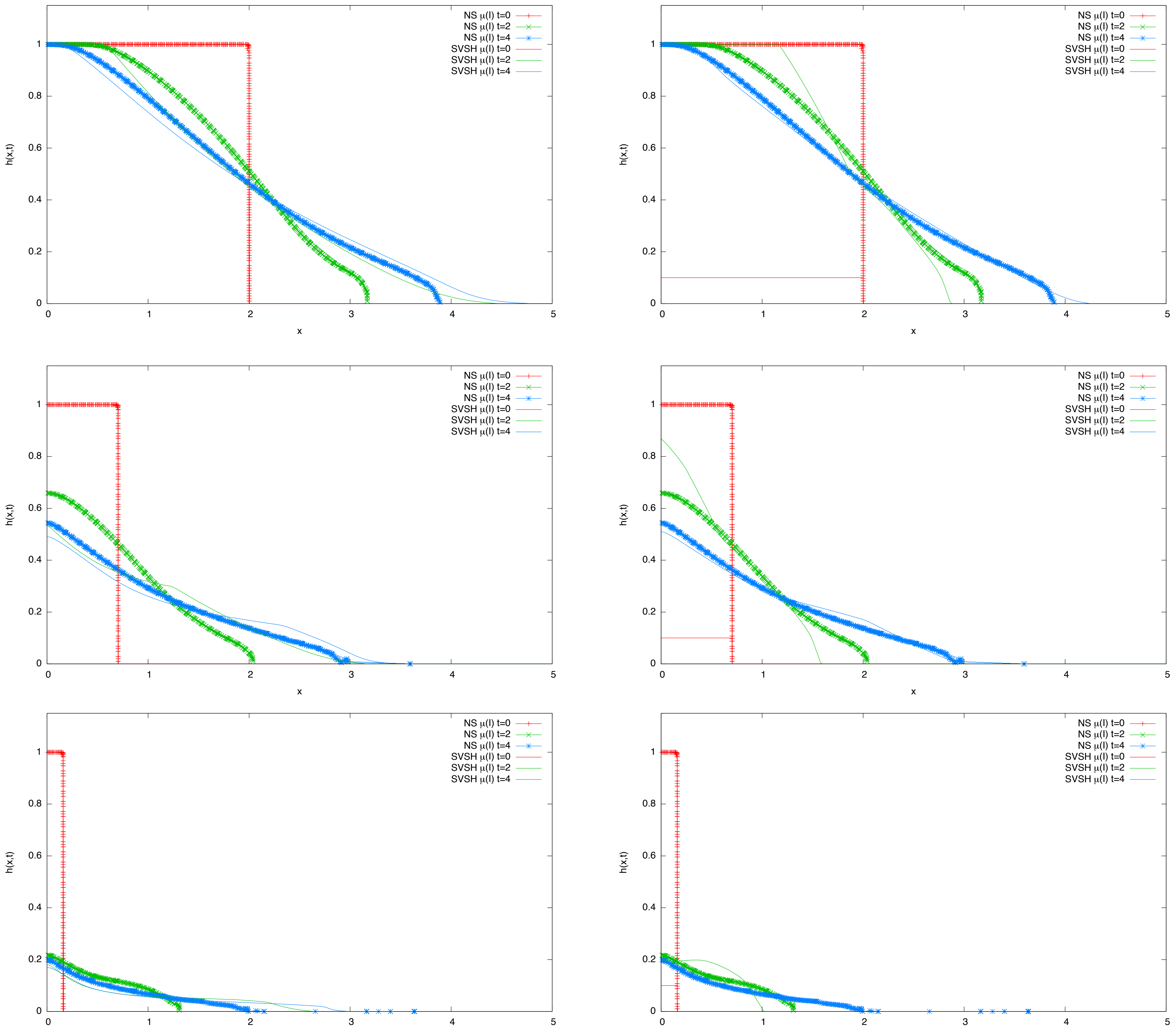


L. Satron, J. Hinch (DAMTP), A. Mangeney (IPGP), E. Larieu (IMFT)

# Saint-Venant Savage Hutter *Gerris*

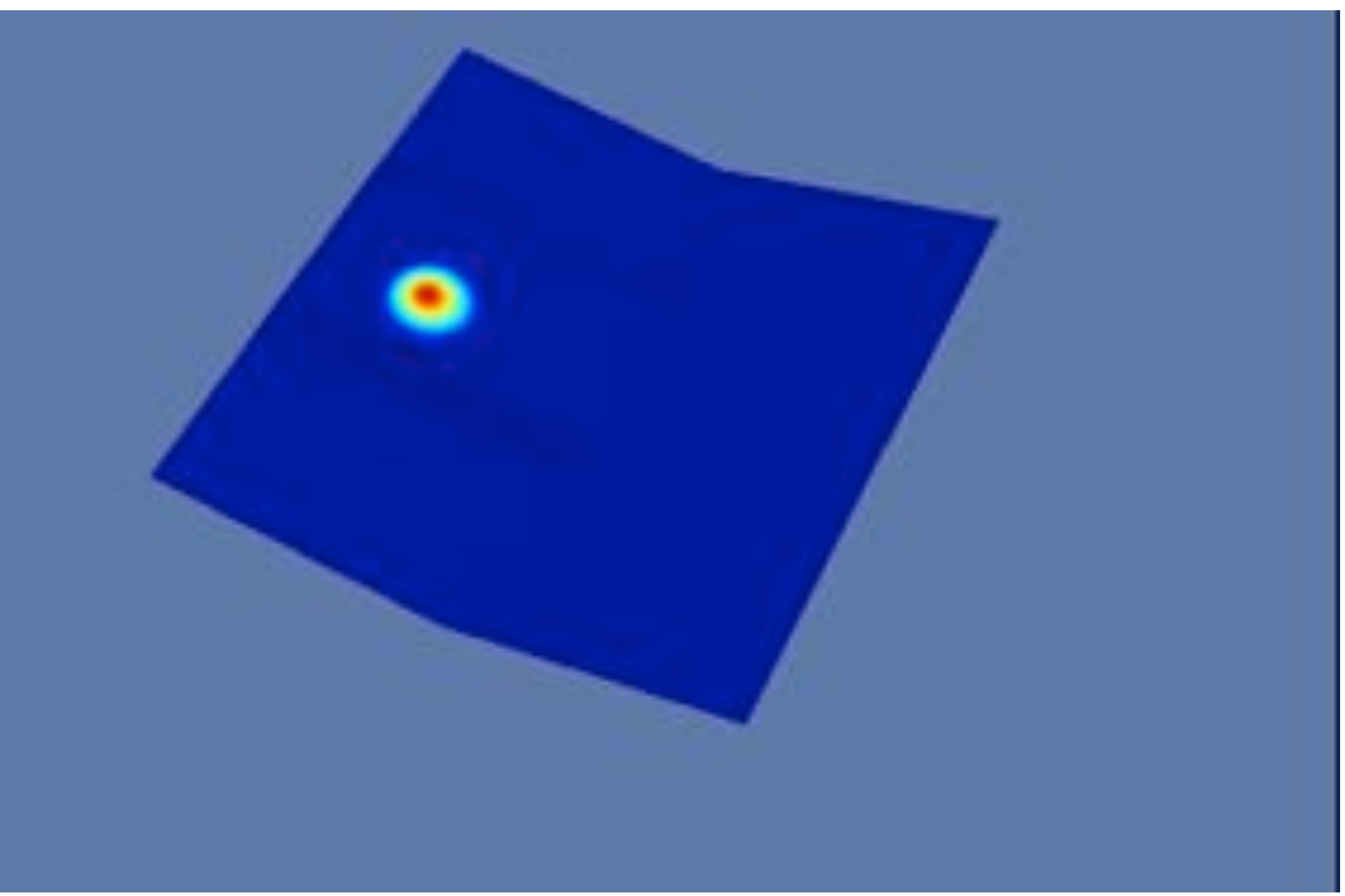

# Saint-Venant Savage Hutter *Gerris*

WIELAND, J. M. N. T. GRAY AND K. HUTTER 1999

Marina Pirulli, Marie-Odile Bristeau Anne Mangeney, Claudio Scavia 2006

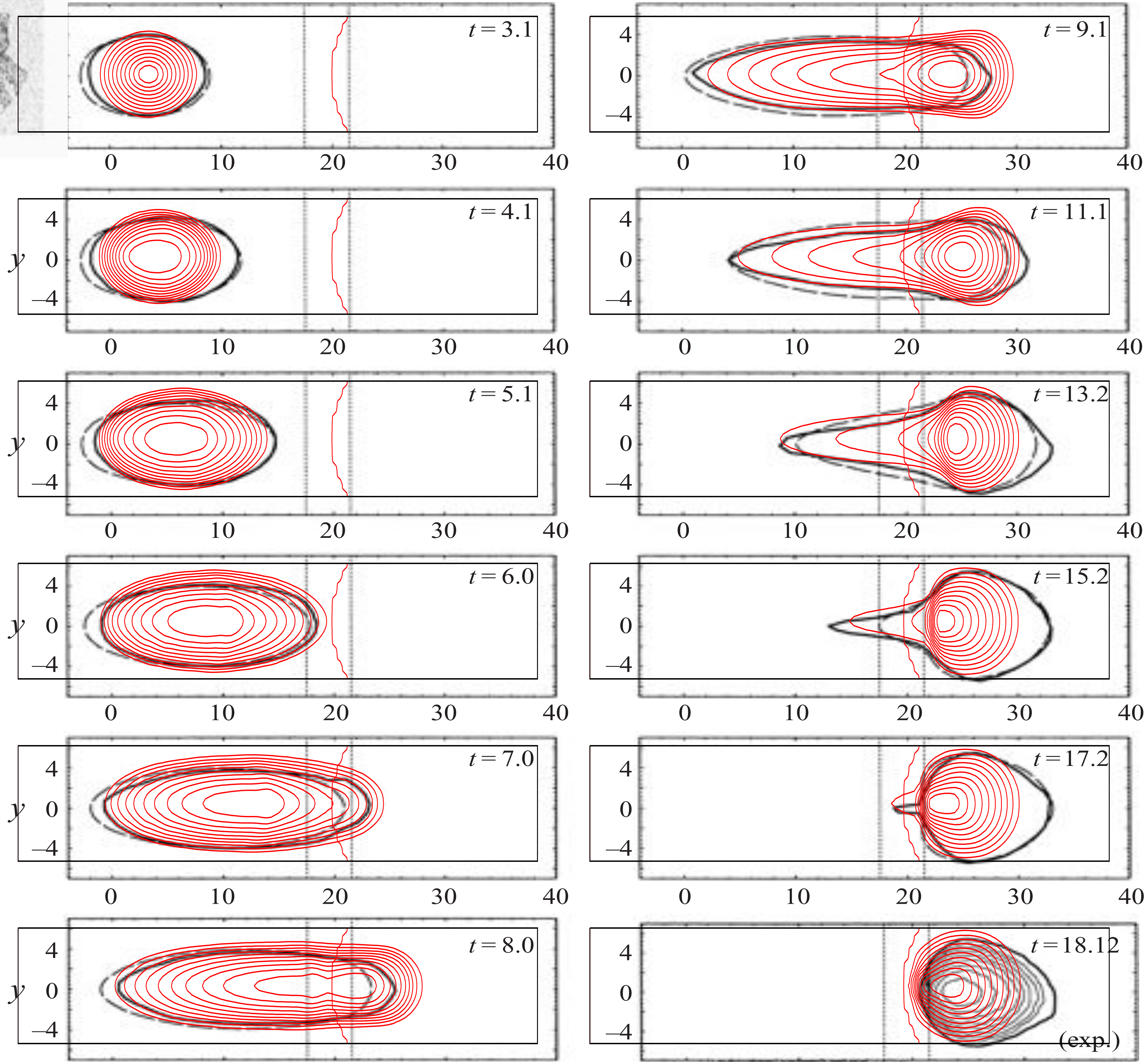

# outline

- what is a granular fluid? some images
- the μ(I) friction law obtained from experiments and discrete simulation
- the viscosity associated to the μ(I) friction law
- the Saint Venant Savage Hutter Hyperbolic model
- implementing the μ(I) friction law in Navier Stokes
- Examples of flows: focusing on the granular column collapse (limits of Saint Venant Savage Hutter Hyperbolic model)

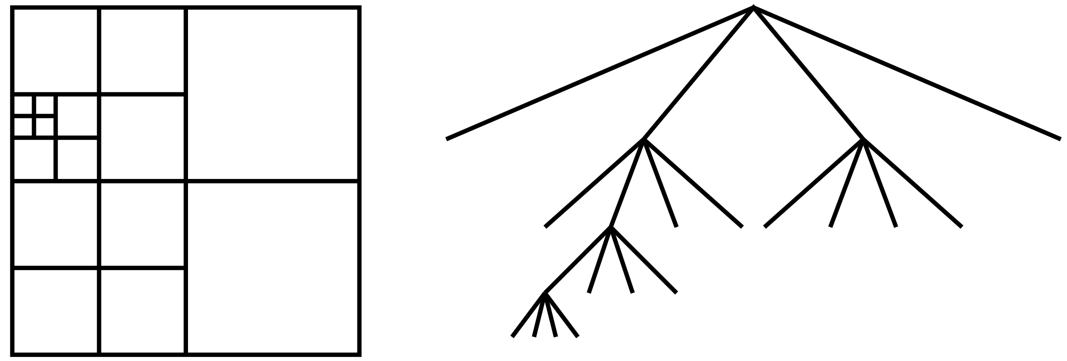


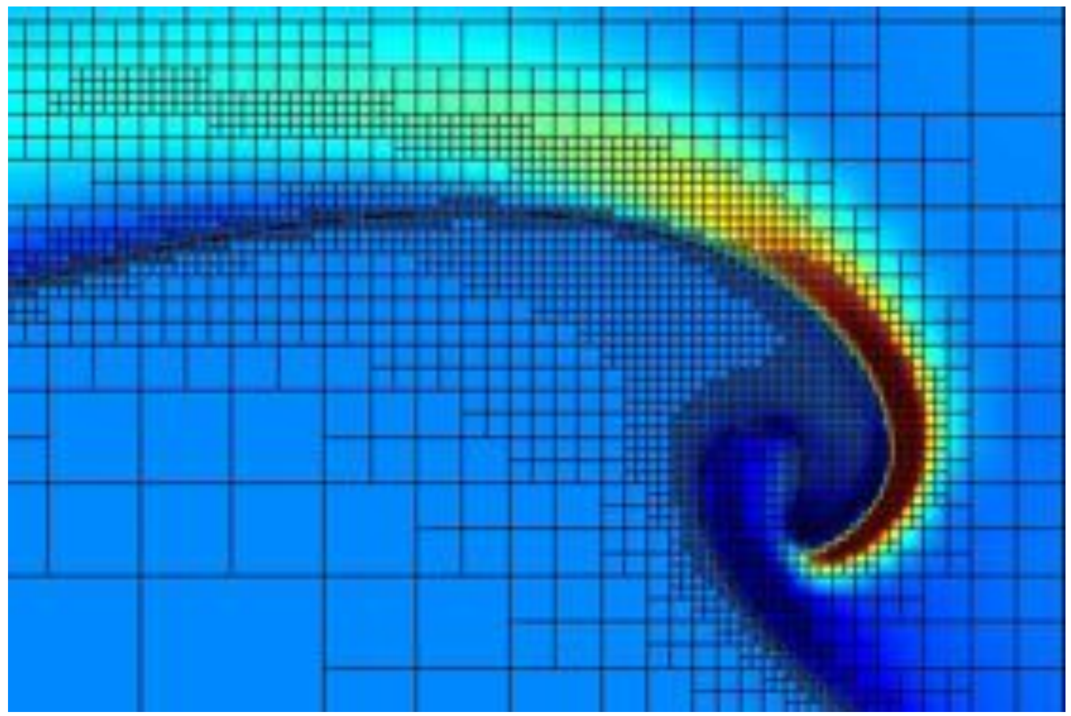

- *Gerris* is a finite volume code by Stéphane Popinet NIWA

one part of the code is a Navier Stokes solver

- automatic mesh adaptation
- Volume Of Fluid method for two phase flows
- free on sourceforge

# rheology; defining a viscosity

$$\mu(I) = \mu_1 + \frac{\mu_2 - \mu_1}{I_0/I + 1}$$

$$\eta \frac{\partial u}{\partial y} = \mu(I) P$$

local equilibrium

$$\eta = \frac{\mu\left(\frac{d\,\frac{\partial u}{\partial y}}{\sqrt{P/\rho}}\right) P}{\frac{\partial u}{\partial y}}$$

construction of a viscosity

P. Jop, Y. Forterre, O. Pouliquen, (2006) "A rheology for dense granular flows", Nature 441, pp. 727-730

# implementation in *Gerris* flow solver?

$$\mu(I) = \mu_1 + \frac{\mu_2 - \mu_1}{I_0/I + 1}$$

$$D_2 = \sqrt{D_{ij} D_{ij}} \qquad D_{ij} = \frac{u_{i,j} + u_{j,i}}{2}$$

construction of a viscosity based on the *D*2 invariant and redefinition of *I*

$$\eta = \min(\eta_{max}, \max\left(\frac{\mu(I)}{\sqrt{2} D_2} p \ , \ 0\right)) \qquad I = d\sqrt{2} D_2 / \sqrt{(|p|/\rho)}.$$

- the «min» limits viscosity to a large value
- always flow, even slow

## Boundary Conditions: no slip and *P=0* at the interface

# implementation in *Gerris* flow solver?

$$\mu(I) = \mu_1 + \frac{\mu_2 - \mu_1}{I_0/I + 1}$$

$$D_2 = \sqrt{D_{ij} D_{ij}} \qquad D_{ij} = \frac{u_{i,j} + u_{j,i}}{2}$$

construction of a viscosity based on the *D2* invariant and redefinition of *I*

$$\eta = \min(\eta_{max}, \max\left(\frac{\mu(I)}{\sqrt{2}D_2} p \ , \ 0\right)) \qquad I = d\sqrt{2}D_2/\sqrt{(|p|/\rho)}.$$

$$\nabla \cdot \mathbf{u} = 0, \quad \rho\left(\frac{\partial \mathbf{u}}{\partial t} + \mathbf{u}\cdot\nabla\mathbf{u}\right) = -\nabla p + \nabla\cdot(2\eta\mathbf{D}) + \rho g,$$

Boundary Conditions: no slip and *P=0* at the interface

# implementation in *Gerris* flow solver?

$$\mu(I) = \mu_1 + \frac{\mu_2 - \mu_1}{I_0/I + 1}$$

$$D_2 = \sqrt{D_{ij}D_{ij}} \qquad D_{ij} = \frac{u_{i,j} + u_{j,i}}{2}$$

construction of a viscosity based on the *D*2 invariant and redefinition of *I*

$$\eta = \min(\eta_{max}, \max\left(\frac{\mu(I)}{\sqrt{2}D_2}p\ ,\ 0\right)) \qquad I = d\sqrt{2}D_2/\sqrt{(|p|/\rho)}.$$

$$\nabla \cdot \mathbf{u} = 0, \ \ \rho\left(\frac{\partial \mathbf{u}}{\partial t} + \mathbf{u}\cdot\nabla\mathbf{u}\right) = -\nabla p + \nabla\cdot(2\eta\mathbf{D}) + \rho g,$$

$$\frac{\partial c}{\partial t} + \nabla\cdot(c\mathbf{u}) = 0, \ \ \rho = c\rho_1 + (1-c)\rho_2, \ \ \eta = c\eta_1 + (1-c)\eta_2$$

The granular fluid is covered by a passive light fluid (it allows for a zero pressure boundary condition at the surface, bypassing an up to now difficulty which was to impose this condition on a unknown moving boundary).

Boundary Conditions: no slip and *P=0* at the top

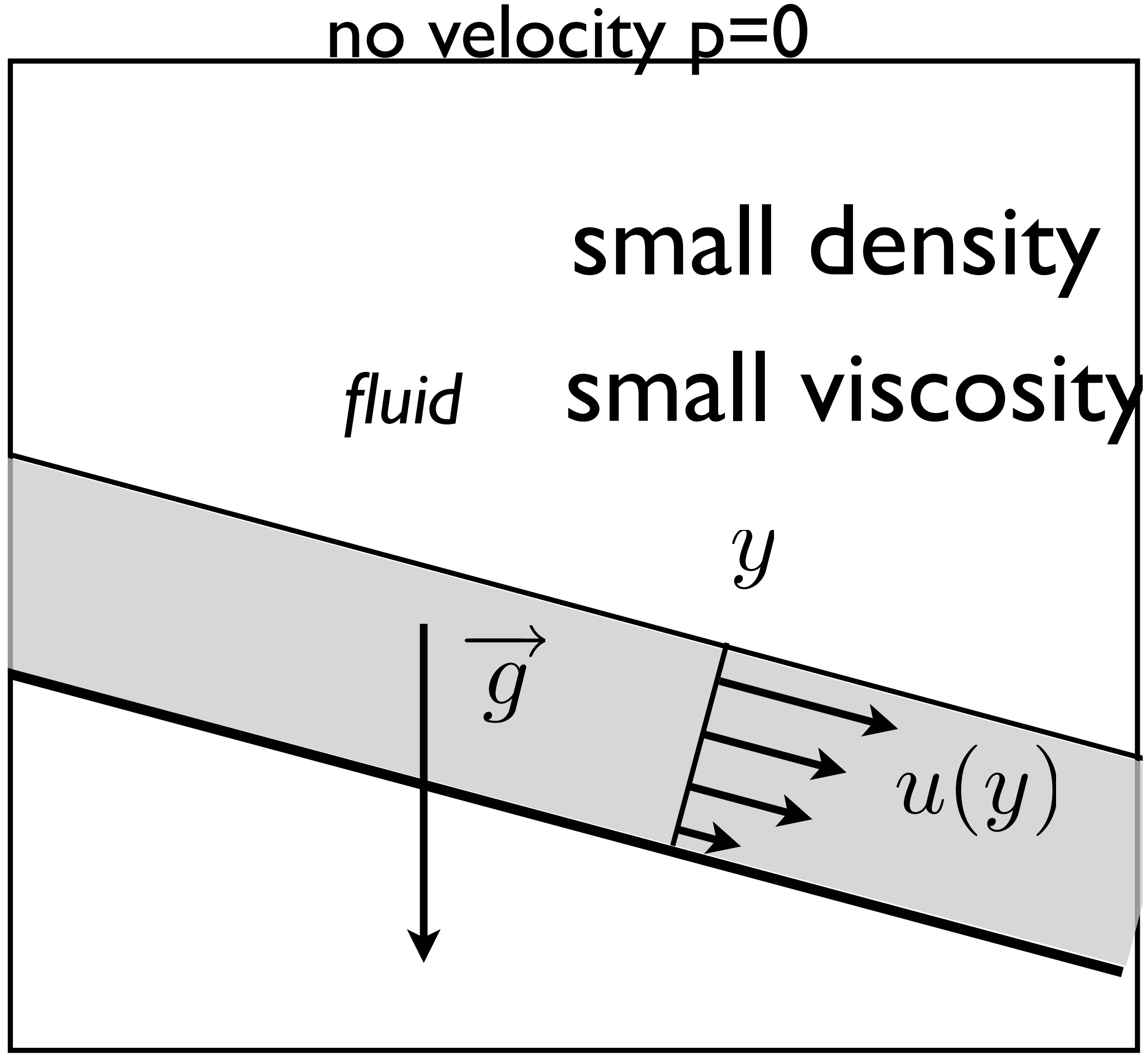


$$\frac{\partial c}{\partial t} + \nabla \cdot (c\mathbf{u}) = 0, \quad \rho = c\rho_1 + (1-c)\rho_2, \quad \eta = c\eta_1 + (1-c)\eta_2$$

The granular fluid is covered by a passive light fluid (it allows for a zero pressure boundary condition at the surface, bypassing an up to now difficulty which was to impose this condition on a unknown moving boundary).

# Boundary Conditions: no slip and *P=0* at the top

# Projection Method


$$\rho_{n+\frac{1}{2}}\left(\frac{\mathbf{u}_*-\mathbf{u}_n}{\Delta t}+\mathbf{u}_{n+\frac{1}{2}}\cdot\boldsymbol{\nabla}\mathbf{u}_{n+\frac{1}{2}}\right)=\boldsymbol{\nabla}\cdot(\eta_{n+\frac{1}{2}}\mathbf{D}_*)-\boldsymbol{\nabla}p_{n-\frac{1}{2}},$$

$$\mathbf{u}_{n+1}=\mathbf{u}_*-\frac{\Delta t}{\rho_{n+\frac{1}{2}}}(\boldsymbol{\nabla}p_{n+\frac{1}{2}}-\boldsymbol{\nabla}p_{n-\frac{1}{2}}),$$

$$\boldsymbol{\nabla}\cdot\mathbf{u}_{n+1}=0.$$

## multigrid solver for Laplacien of pressure

$$\boldsymbol{\nabla}\cdot\left(\frac{\Delta t}{\rho_{n+\frac{1}{2}}}\boldsymbol{\nabla}p_{n+\frac{1}{2}}\right)=\boldsymbol{\nabla}\cdot\left(\mathbf{u}_*+\frac{\Delta t}{\rho_{n+\frac{1}{2}}}\boldsymbol{\nabla}p_{n-\frac{1}{2}}\right)$$

## implicit for u*

$$\frac{\rho_{n+\frac{1}{2}}}{\Delta t}\mathbf{u}_\star-\frac{1}{2}\nabla\cdot(\eta_{n+\frac{1}{2}}\nabla\mathbf{u}_\star) \quad = \quad \rho_{n+\frac{1}{2}}\left[\frac{\mathbf{u}_n}{\Delta t}-\mathbf{u}_{n+\frac{1}{2}}\cdot\nabla\mathbf{u}_{n+\frac{1}{2}}\right]-\nabla p_{n-\frac{1}{2}}+\frac{1}{2}\nabla\mathbf{u}_n^T\nabla\eta_{n+\frac{1}{2}}.$$

# VOF reconstruction

$$\frac{c_{n+\frac{1}{2}}-c_{n-\frac{1}{2}}}{\Delta t}+\nabla\cdot(c_n\mathbf{u}_n)=0$$

# outline

- what is a granular fluid? some images
- the μ(I) friction law obtained from experiments and discrete simulation
- the viscosity associated to the μ(I) friction law
- the Saint Venant Savage Hutter Hyperbolic model
- implementing the μ(I) friction law in Navier Stokes
- Examples of flows: focusing on the granular column collapse (limits of Saint Venant Savage Hutter Hyperbolic model)

# Test of the code: «Bagnold» avalanche

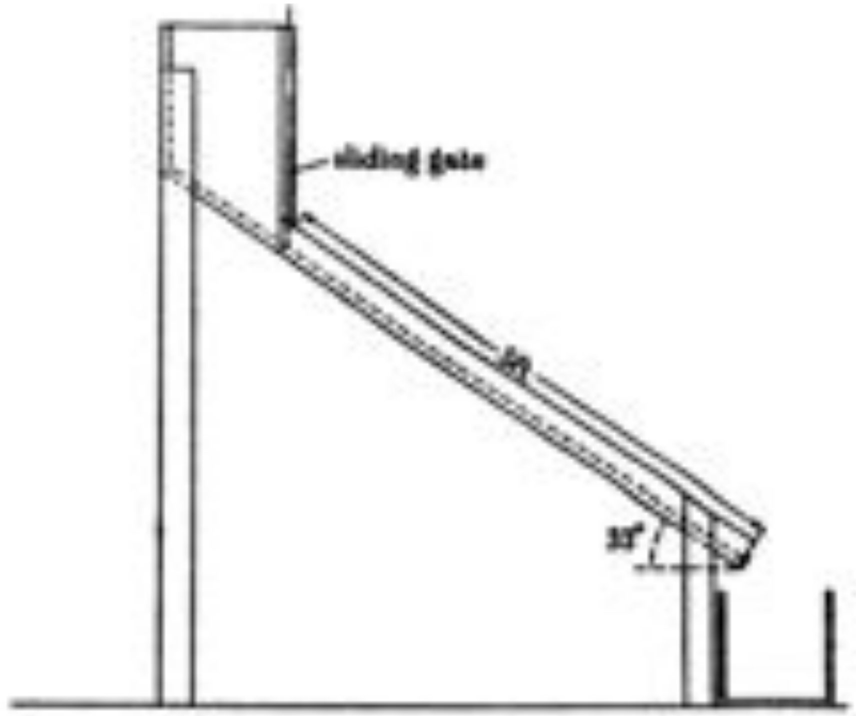


kind of Nuβelt solution

$$T \propto \sigma(\lambda D)^2 \, (dU/dy)^2$$

$$U = \frac{2}{3} \times 0.165 \, (g \sin \beta)^{1/2} \, \frac{y'^{3/2}}{D} \, .$$

TABLE 1.

| flow height Y (cm) | measured speed (cm/sec) | speed, from (9) (cm/sec) | ratio |
|---|---|---|---|
| 0.5 | 17.2 | 26.4 | 1.53 |
| 0.65 | 27.5 | 38.8 | 1.41 |
| 0.75 | 30.0 | 48.0 | 1.6 |
| 0.9 | 39.0 | 63.0 | 1.61 |

Bagnold 1954

# Test of the code: «Bagnold» avalanche

kind of Nuβelt solution

Contact Dynamic simulation Lydie Staron

# Test of the code: «Bagnold» avalanche

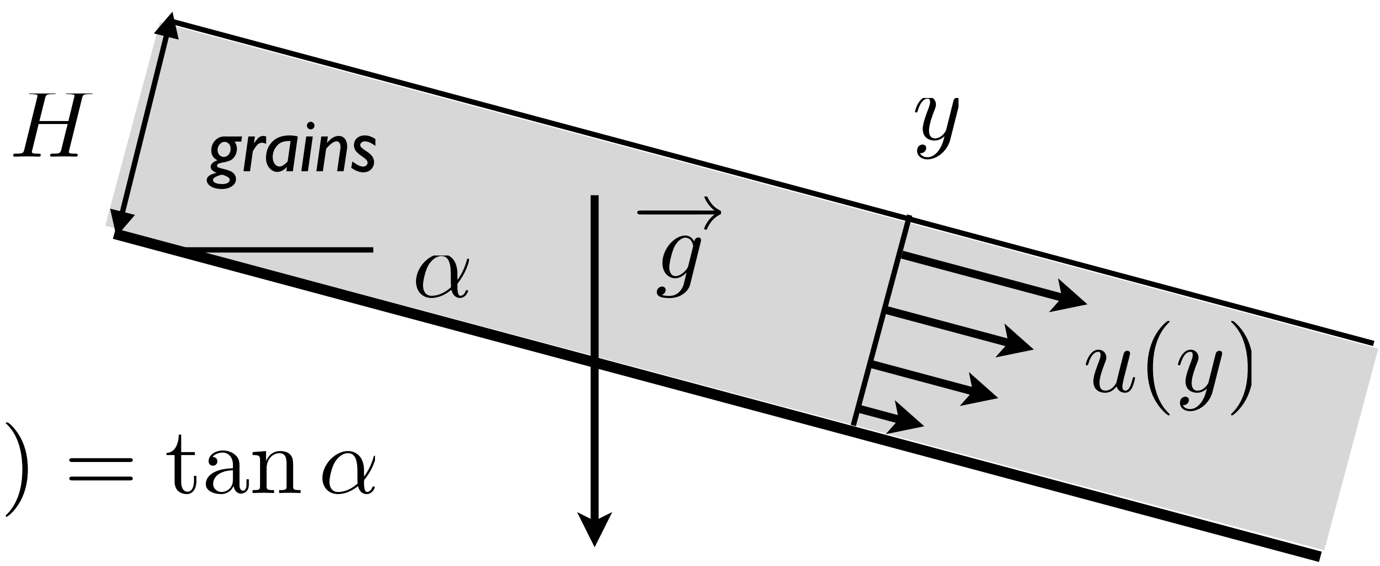


$$\mu(I) = \tan\alpha$$

$$u = \frac{2}{3} I_\alpha \sqrt{gd\cos\alpha \frac{H^3}{d^3}} \left(1 - \left(1 - \frac{y}{H}\right)^{3/2}\right),$$

$$v = 0, \;\; p = \rho g H \left(1 - \frac{y}{H}\right)\cos\alpha.$$

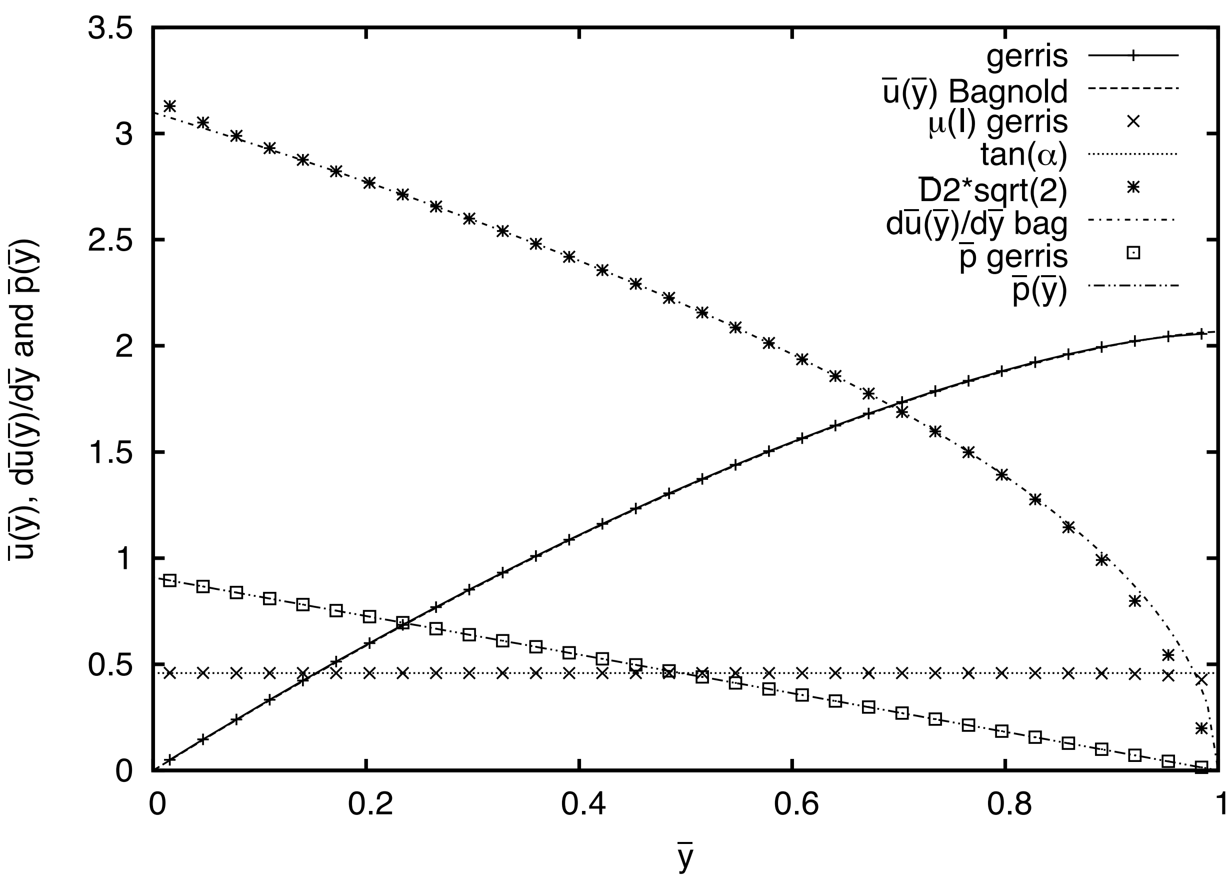

# Test of the code: «Bagnold» avalanche

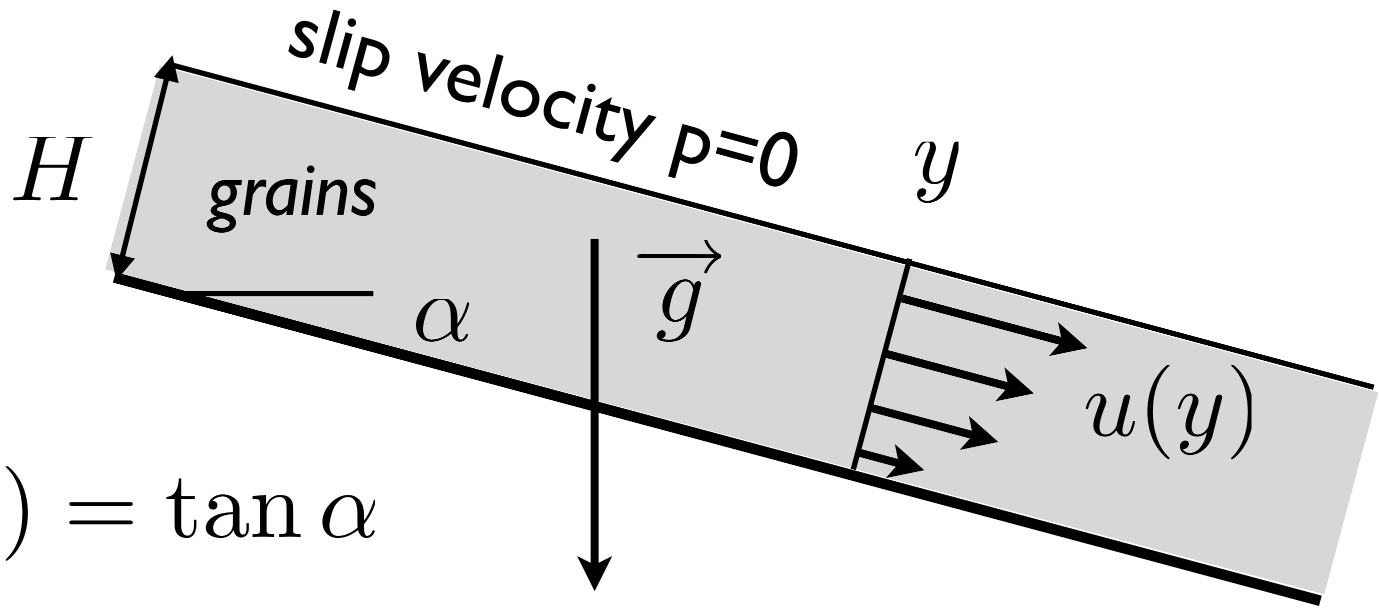


$$\mu(I) = \tan\alpha$$

$$u = \frac{2}{3} I_\alpha \sqrt{gd\cos\alpha \frac{H^3}{d^3}} \left(1 - \left(1 - \frac{y}{H}\right)^{3/2}\right),$$

$$v = 0, \quad p = \rho g H \left(1 - \frac{y}{H}\right)\cos\alpha.$$

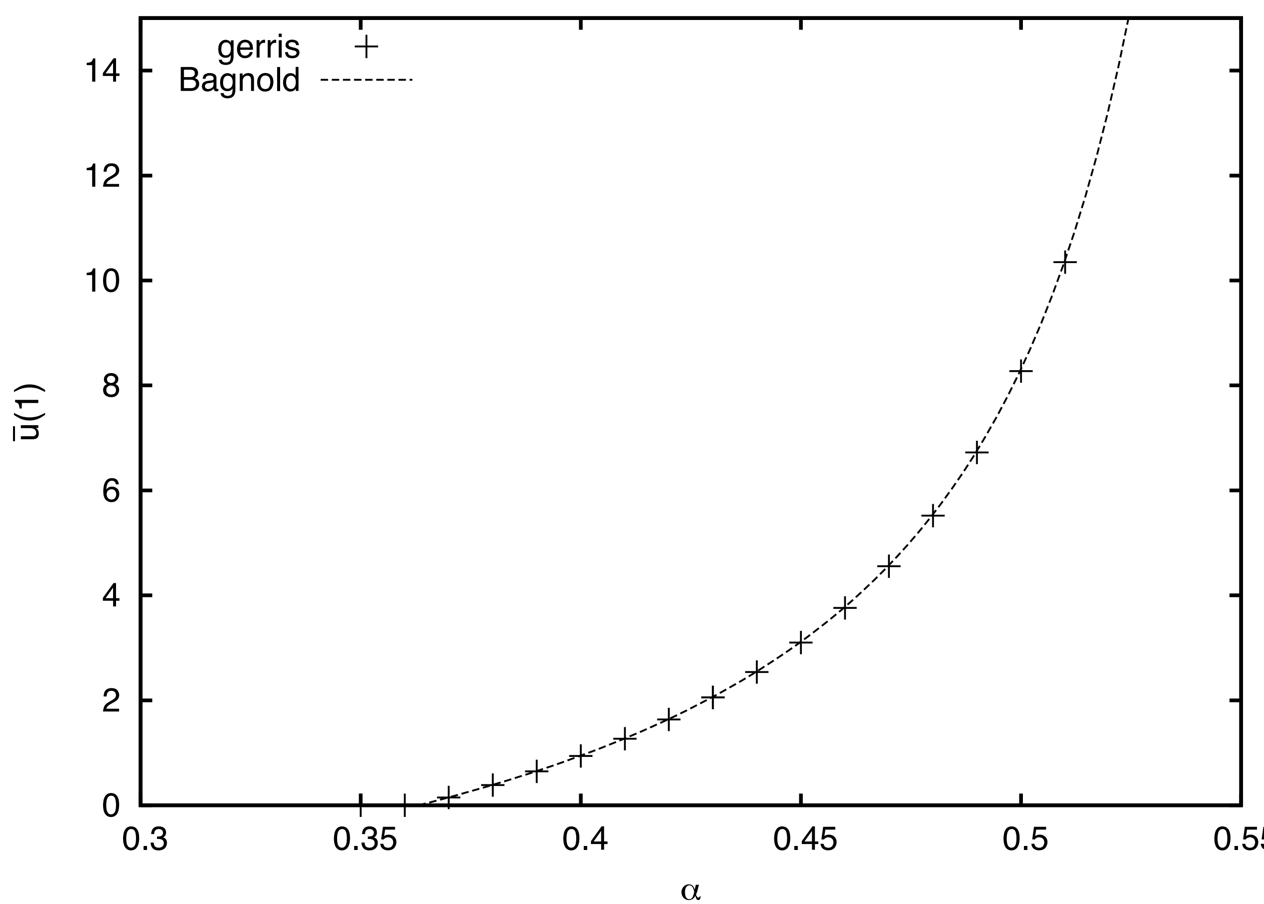

# Test of the code: «Bagnold» avalanche

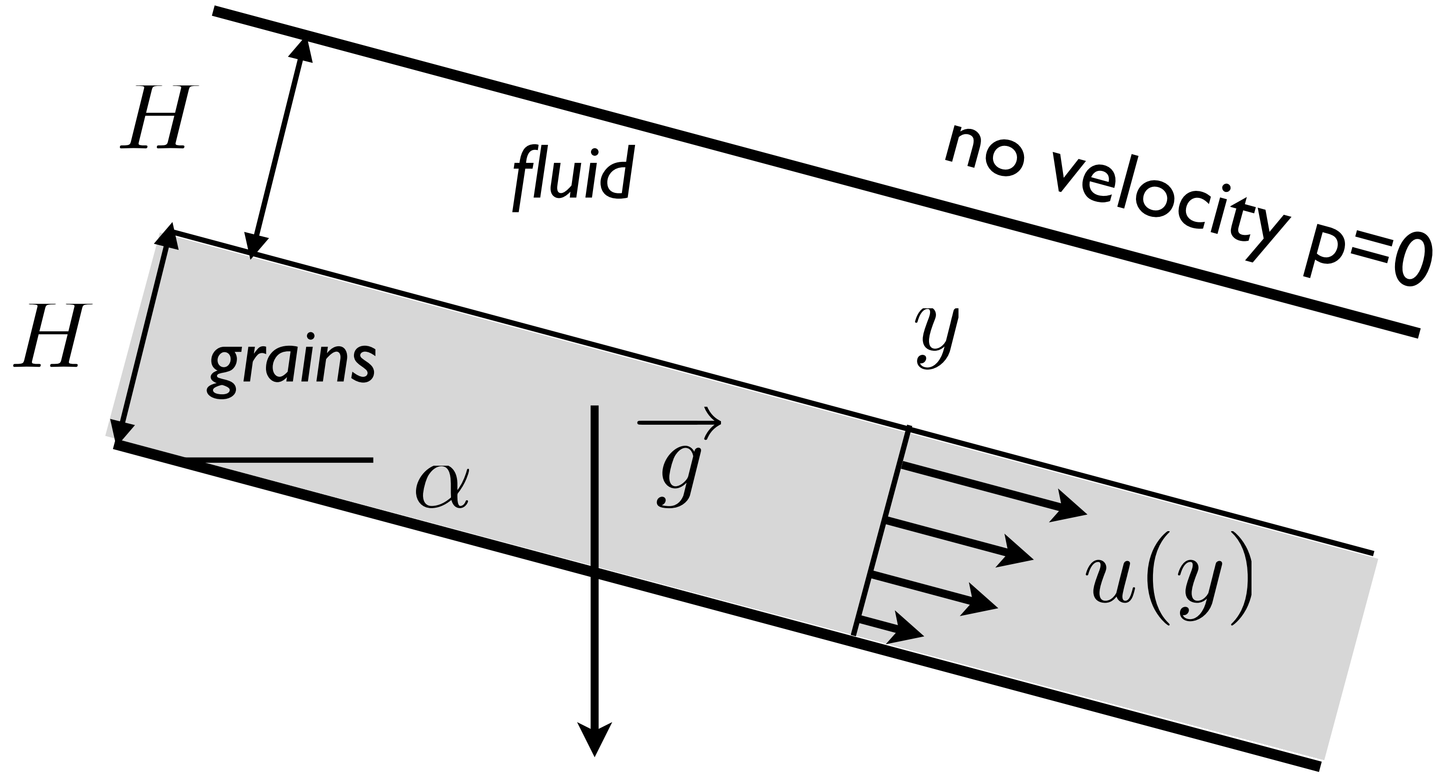


$$u(y) = \frac{(2H - y)\,(\rho_f g y \sin\alpha - 2\tau_0)}{2\mu_f}$$

$$d\frac{\partial u}{\partial y} = \max\left[\sqrt{p_0/\rho + gH\left(1 - \frac{y}{H}\right)\cos\alpha} \times \mu^{-1}\left(\frac{\tau_0 + \rho g H\left(1 - \frac{y}{H}\right)\sin\alpha}{p_0 + \rho g H\left(1 - \frac{y}{H}\right)\cos\alpha}\right), 0\right].$$

$$u(H^-) - u(H^+) = 0$$

# Test of the code: «Bagnold» avalanche

change of density of the fluid

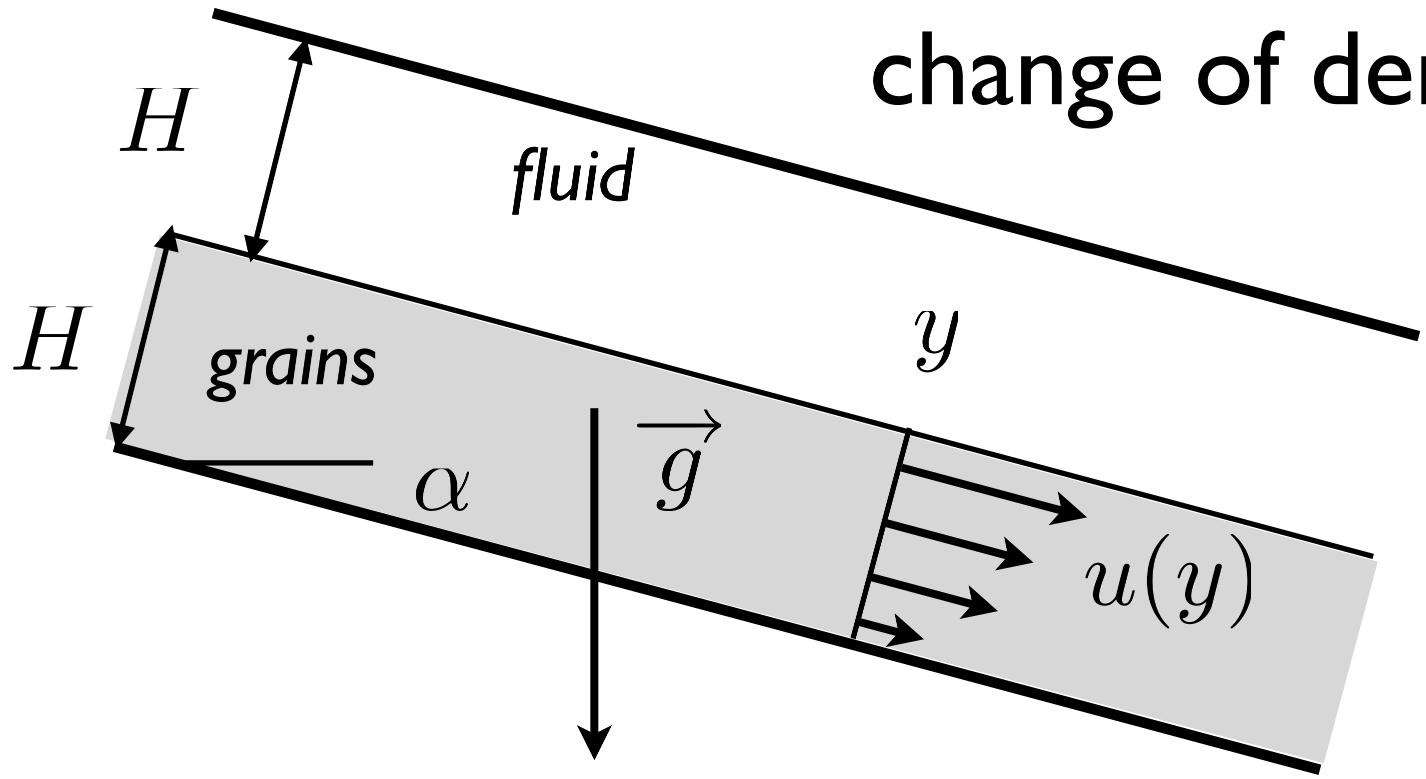


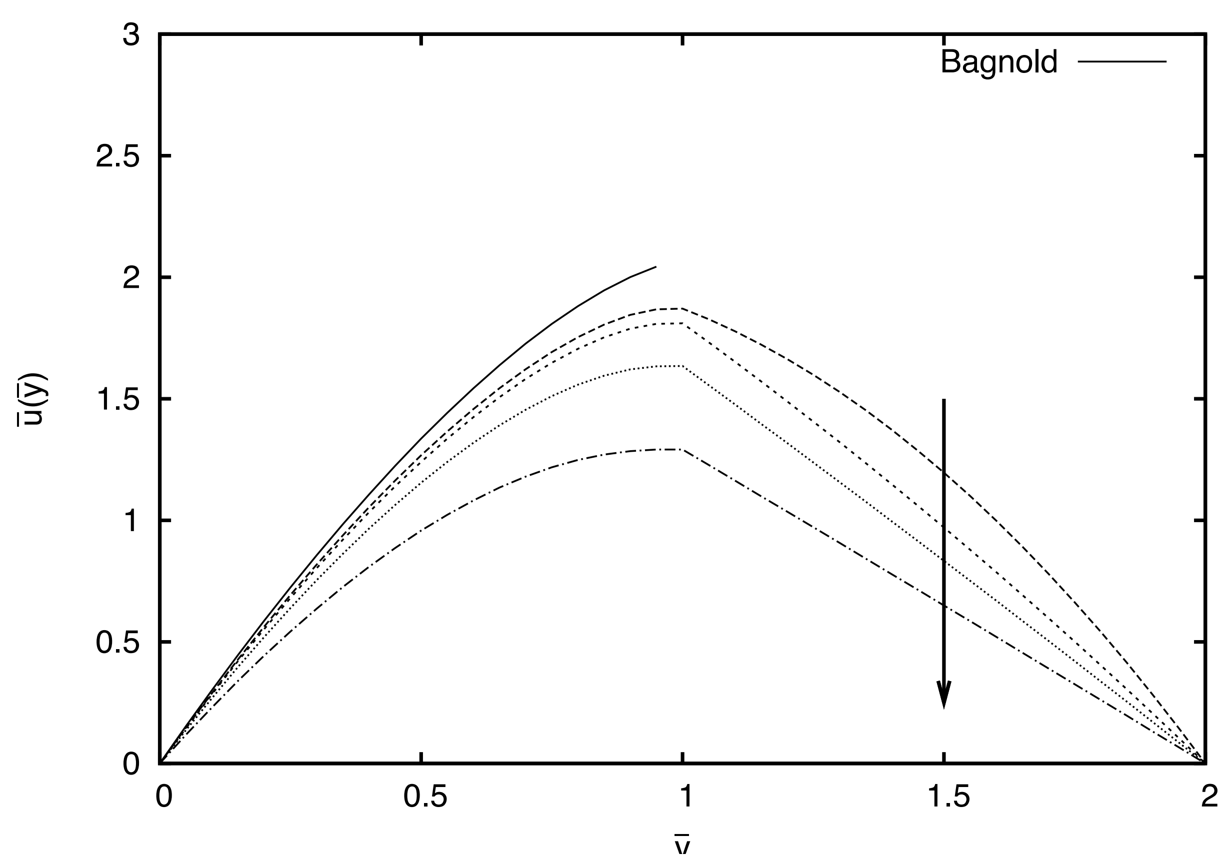

# Test of the code: «Bagnold» avalanche

## change of viscosity of the fluid

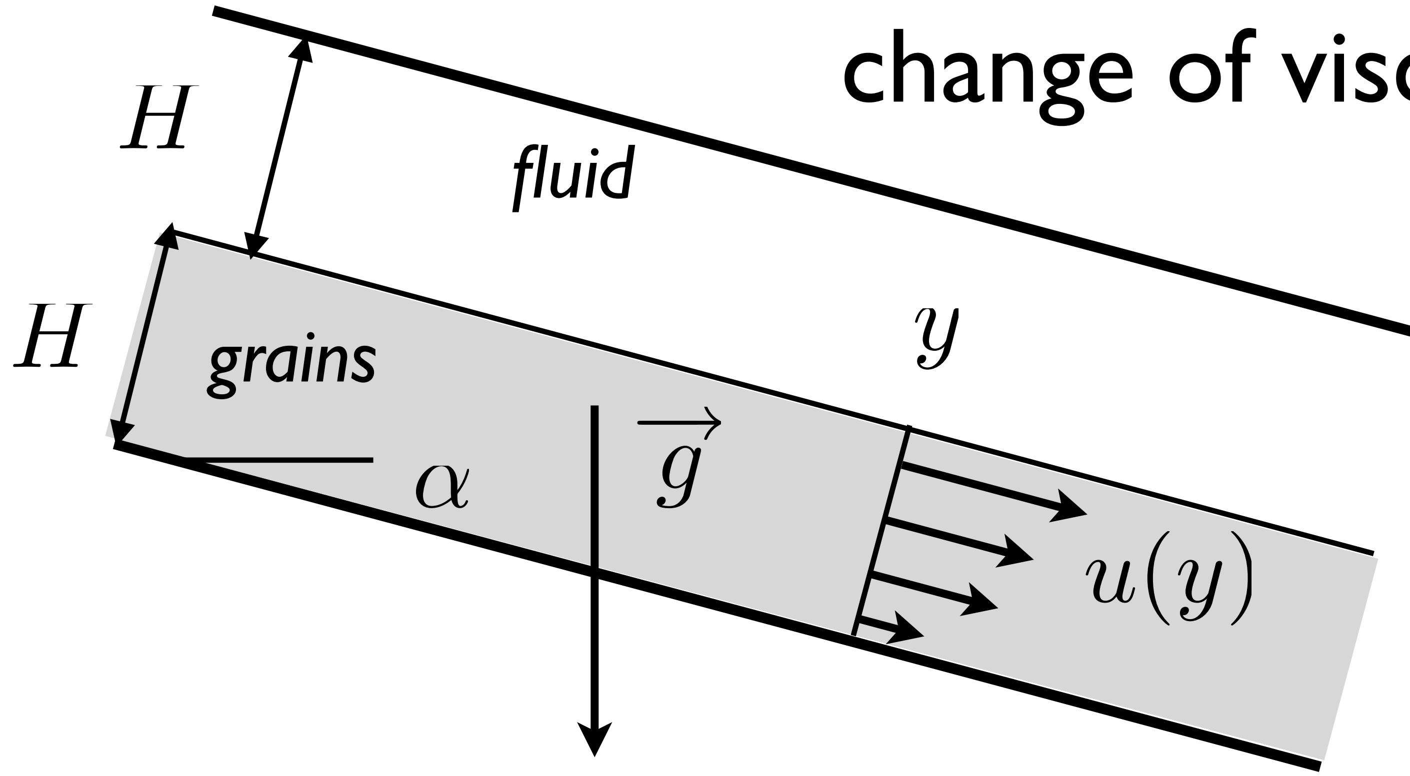


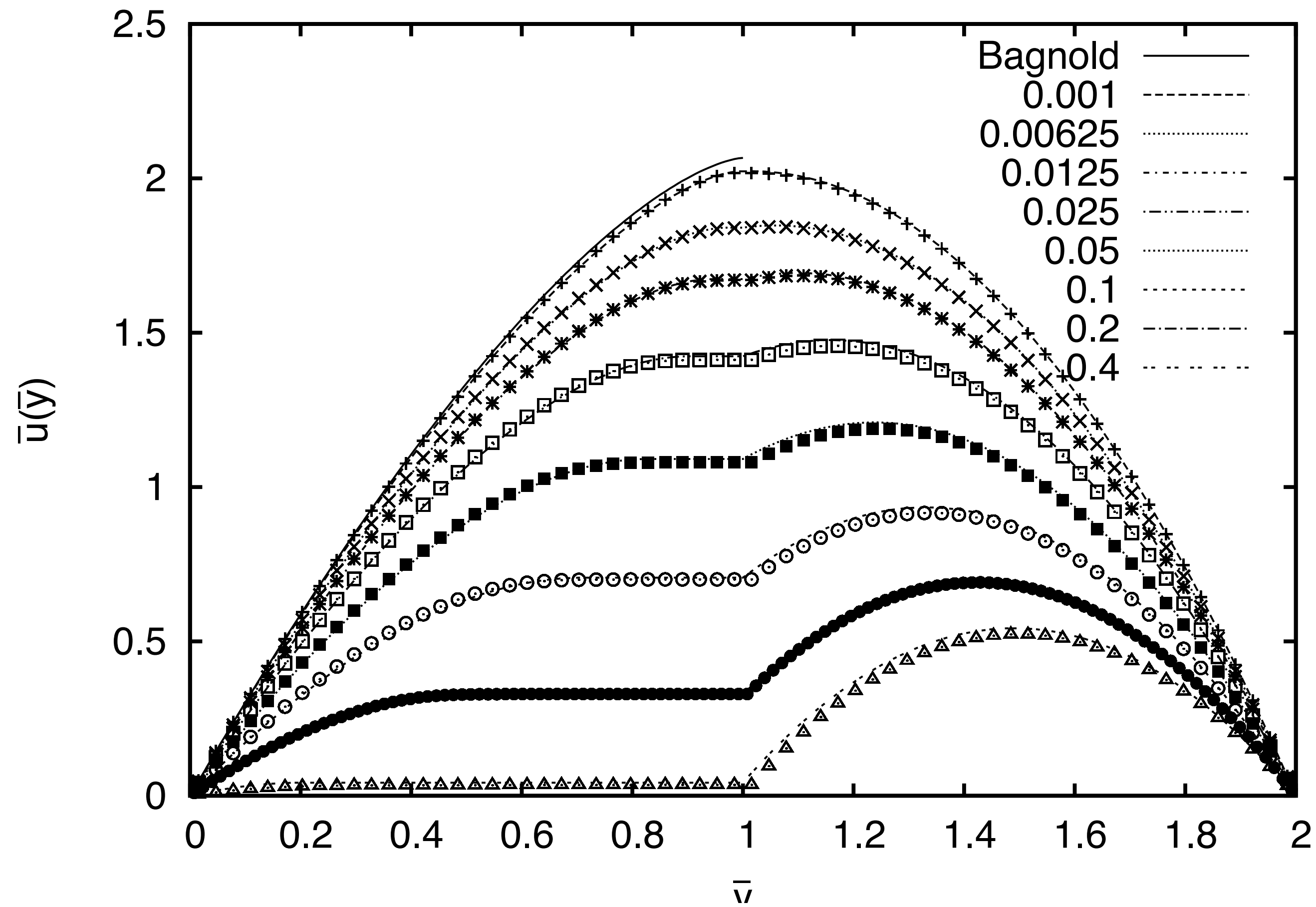

# • Bagnold 3D

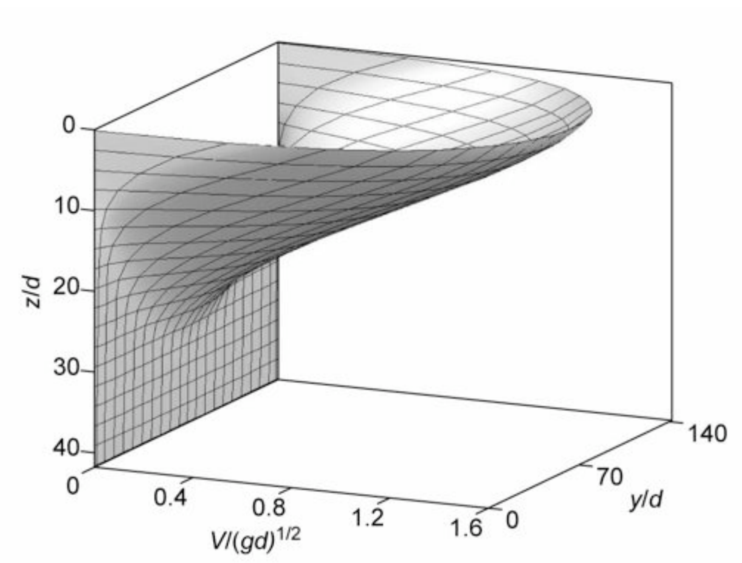


**Figure 3: Typical 3D velocity profile predicted by the rheology ($W$=142$d$, $\theta$ =22.6°, Q/$d^{3/2}g^{1/2}$=15.2).** For clarity only one quarter of the lines of the 71x80 computational grid is plotted.

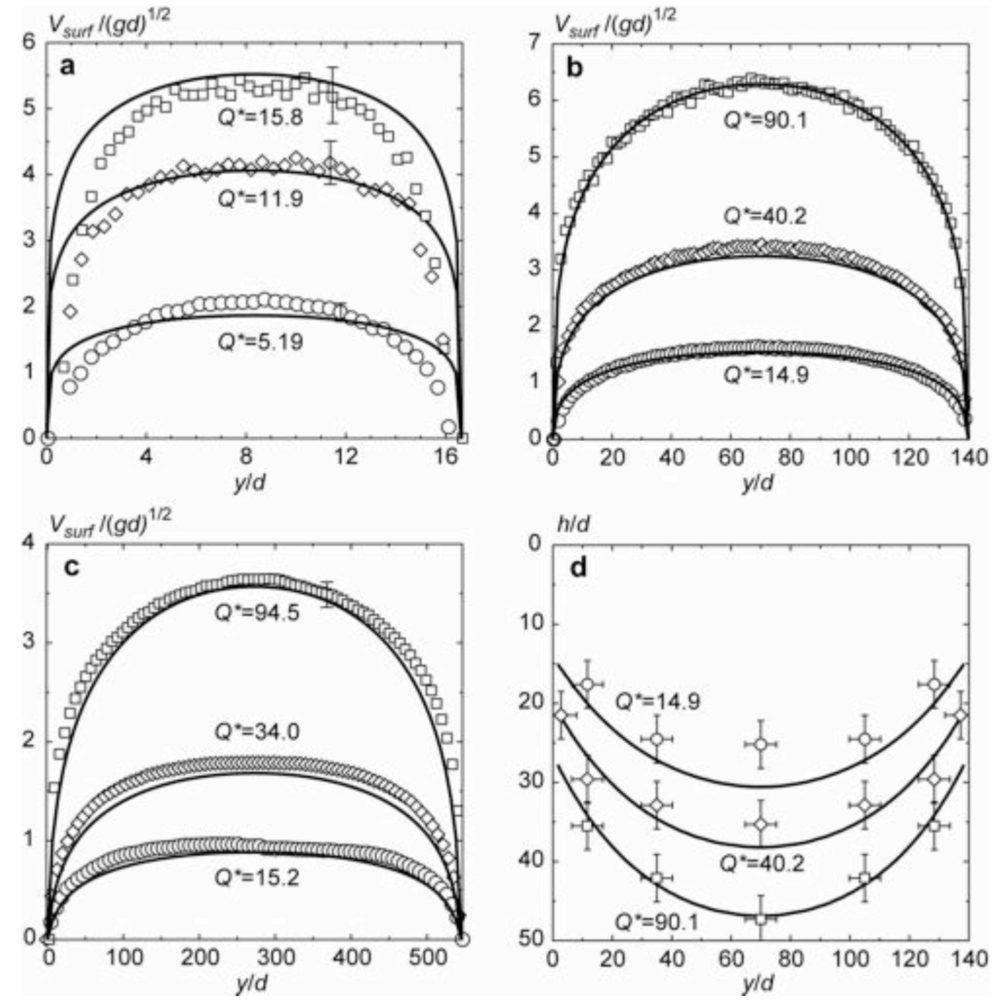


**Figure 4: Comparison of 3D simulations (lines) and experimental results (symbol different flow rates ($Q^*=Q/d^{3/2}g^{1/2}$). a, b, c,** Free-surface velocity profiles for channel $W$=16.5$d$ (**a**), $W$=140$d$ (**b**) and $W$=546$d$ (**c**). **d**, Depths of the flowing layer across the chan $W$=140$d$. The experimental and computational flow rates are equal within 2.5%. The erro represent the dispersion of the measurements for different experiments.

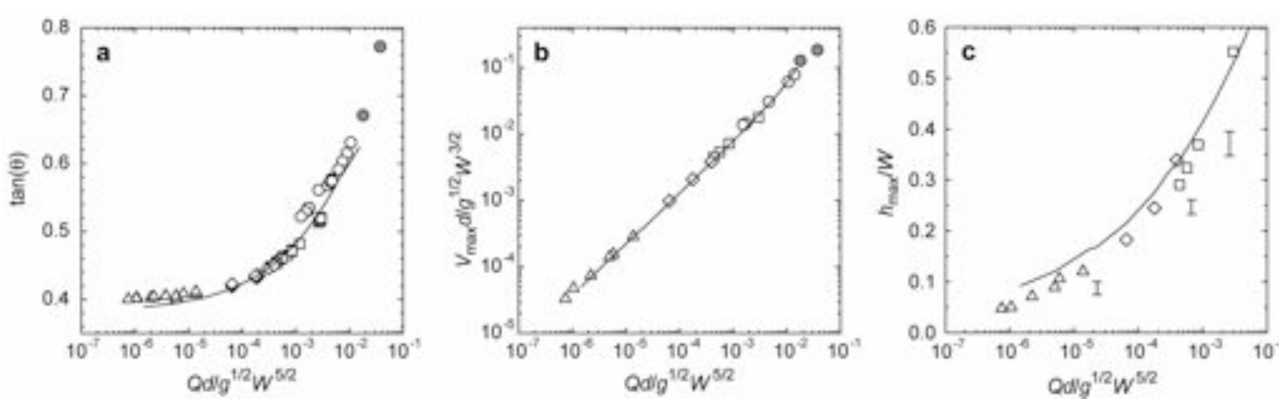


A constitutive law for dense granular flows
Pierre Jop1, Yoël Forterre1 & Olivier Pouliquen
nature 06

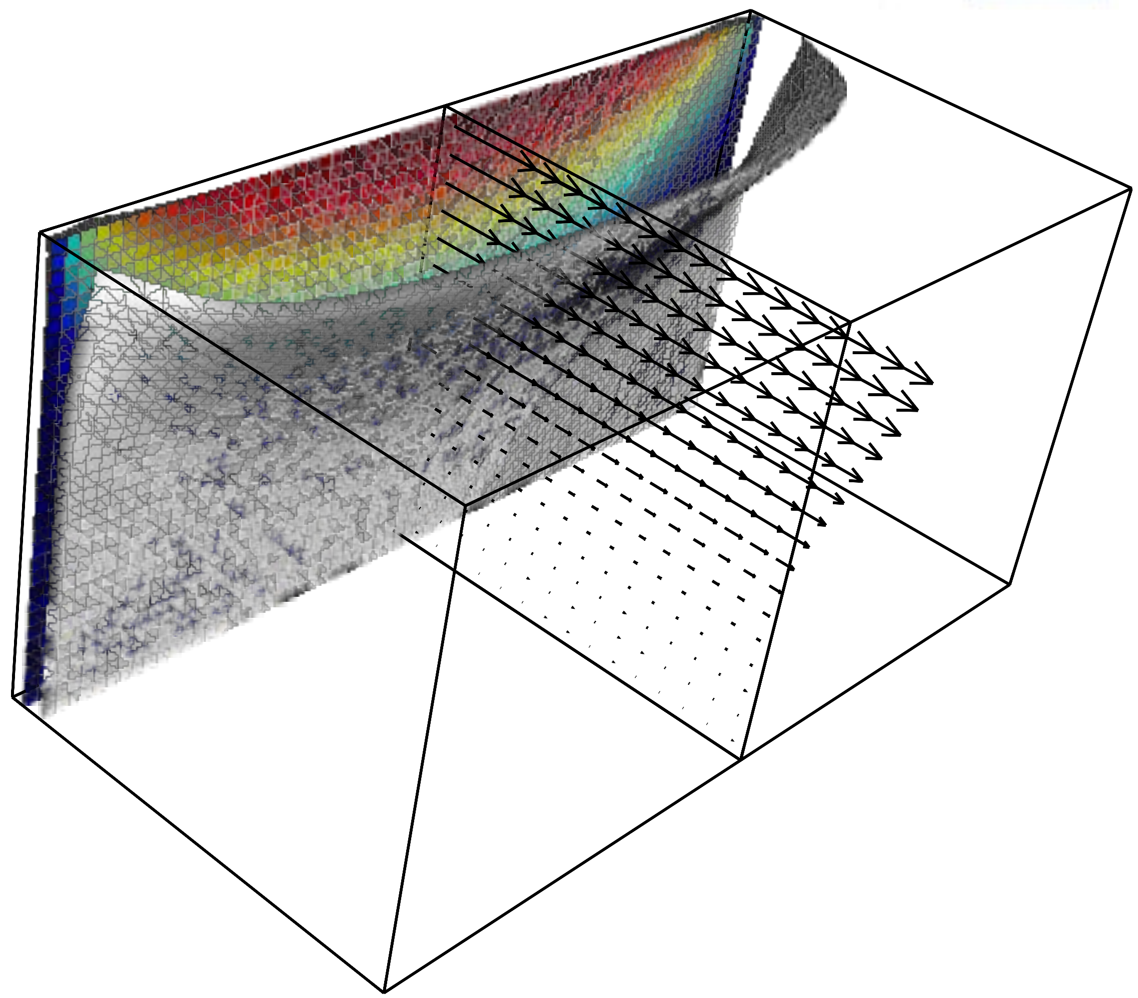

NS $\mu(I)$

influence de la largeur sur l’écoulement: on passe de Bagnold à un écoulement en surface

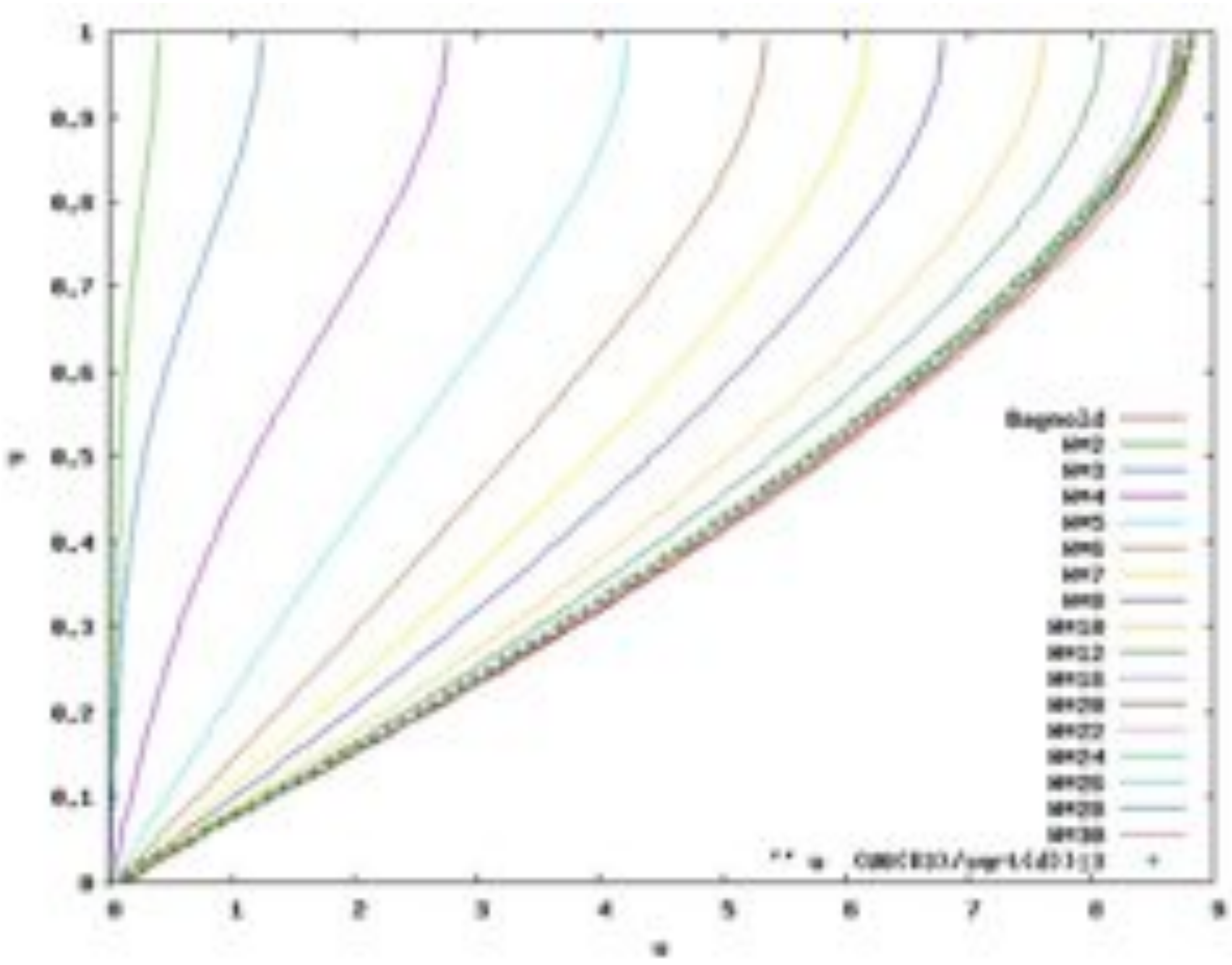


profils au centre en profondeur

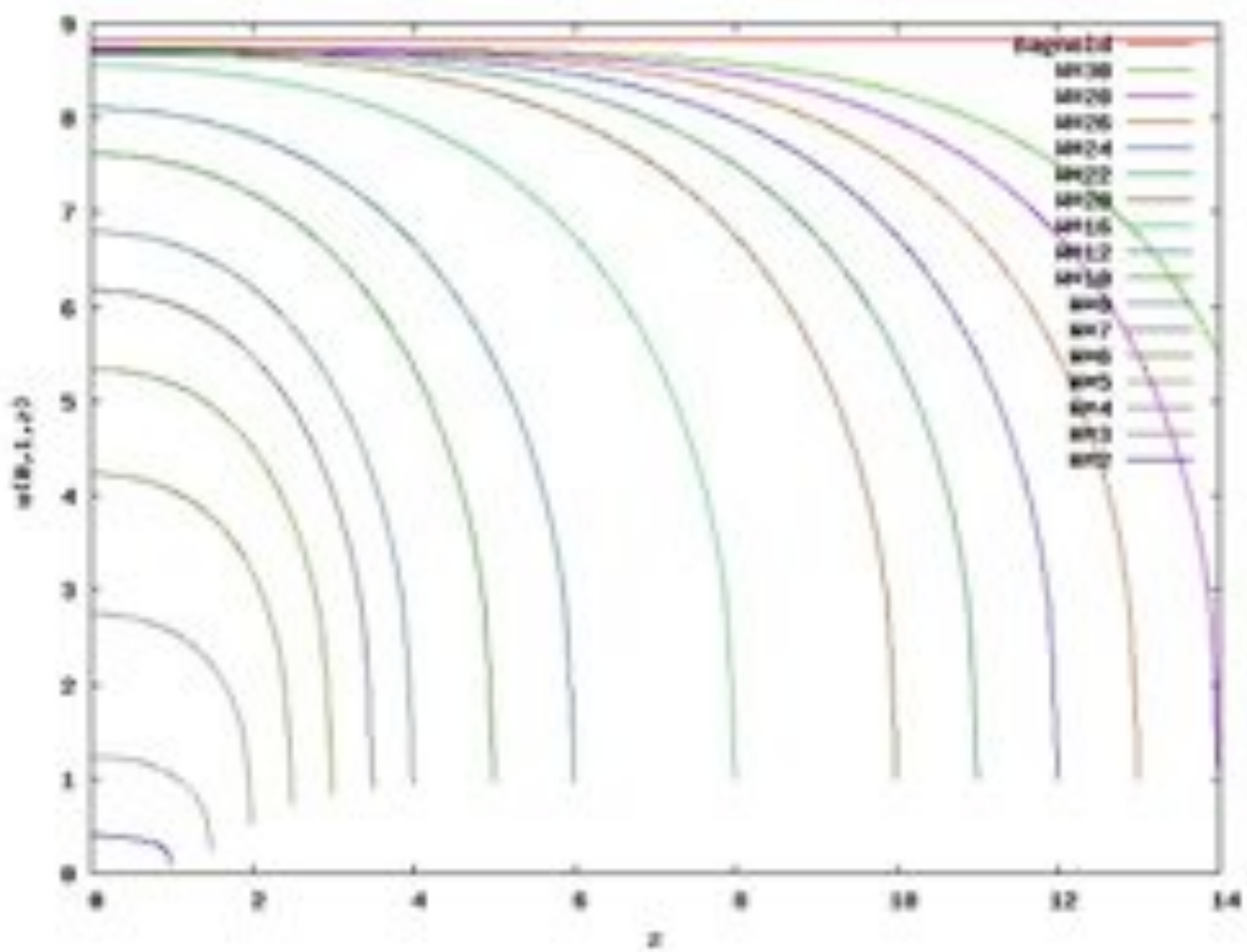


profils en surface vus de dessus

The sand pit problem: quickly remove the bucket of sand

http://www.mylot.com/w/photokeywords/pail.asp

# Granular Column Collapse

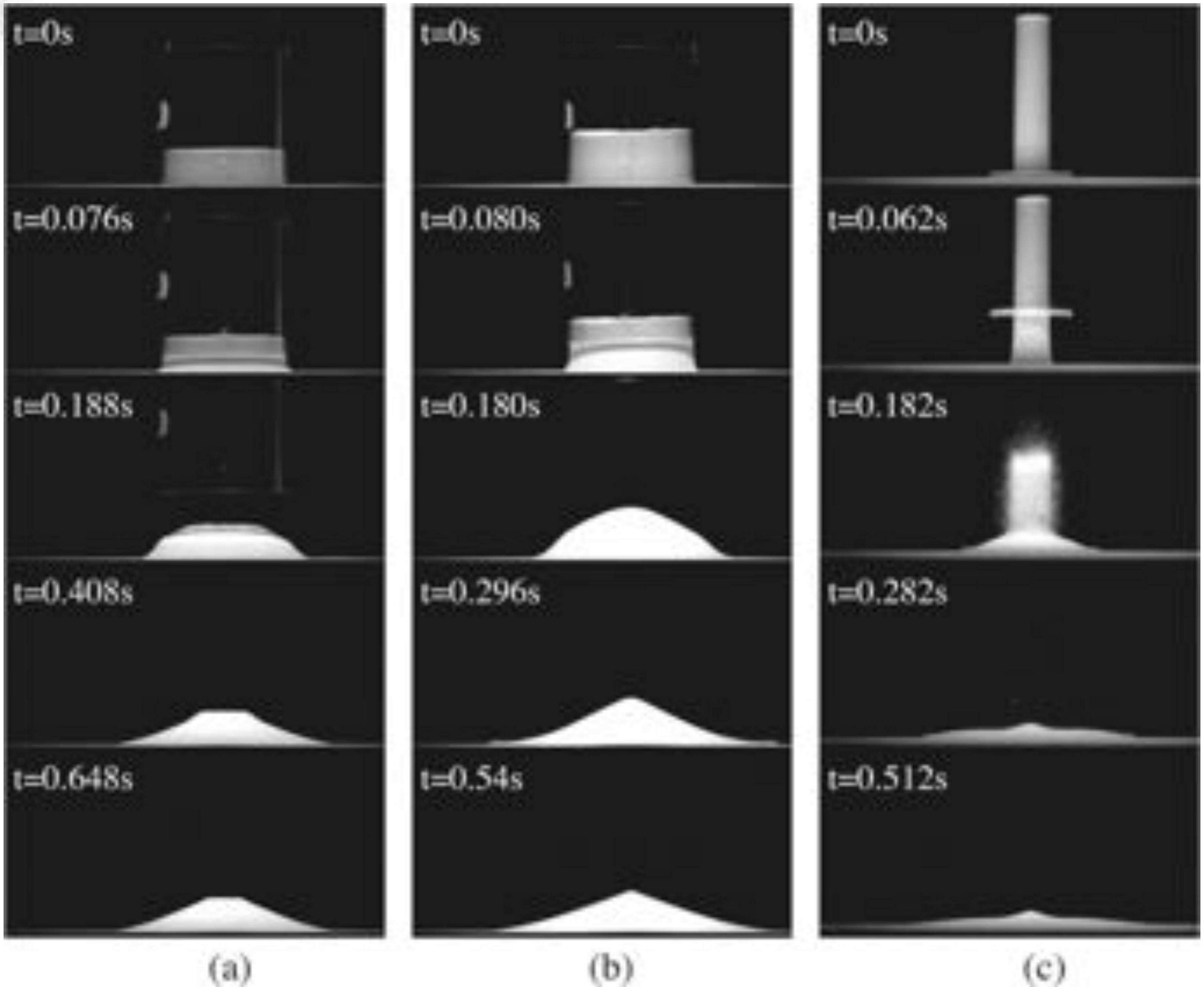


The sand pit problem: quickly remove the bucket of sand

http://www.mylot.com/w/photokeywords/pail.asp

# Collapse of columns

a=0.37

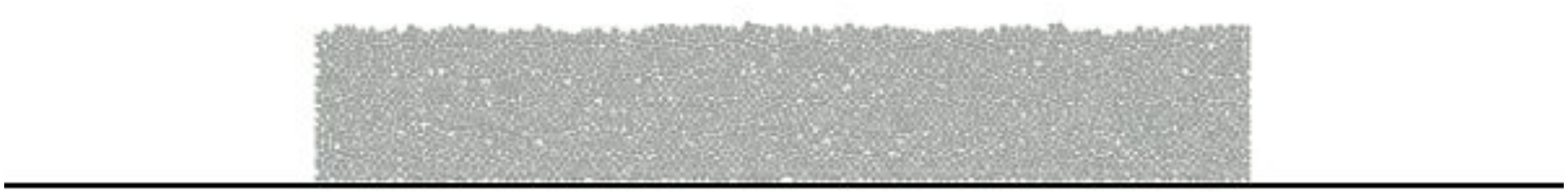

Contact Dynamic simulation Lydie Staron

# Collapse of columns

a=0.90

Contact Dynamic
simulation Lydie Staron

# Collapse of columns simulation *Gerris* $\mu(I)$

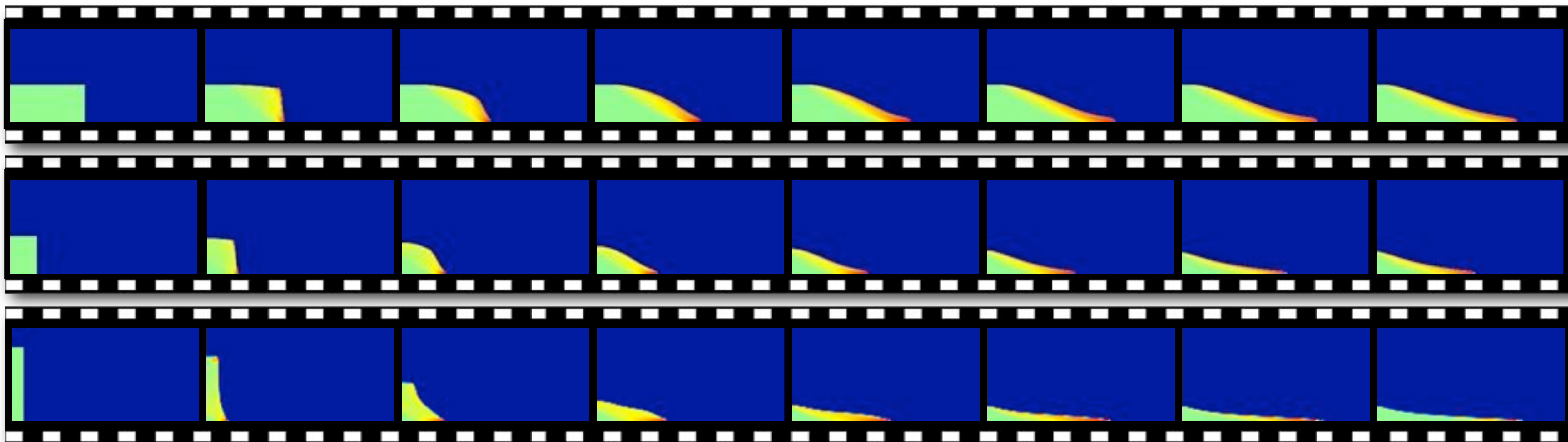

Snapshots of collapse of three columns of aspect ration 0.5 1.42 and 6.26 (top to bottom)

# Collapse of columns simulation *Gerris μ(I)*

Collapse of columns of aspect ratio 0.5 comparison of Discrete Simulation Contact Method and Navier Stokes gerris, shape at time 0, 1, 2, 3, 4 and position of the front of the avalanche as function of time (time measured with $\sqrt{H_0/g}$ and space with $aH_0$ )

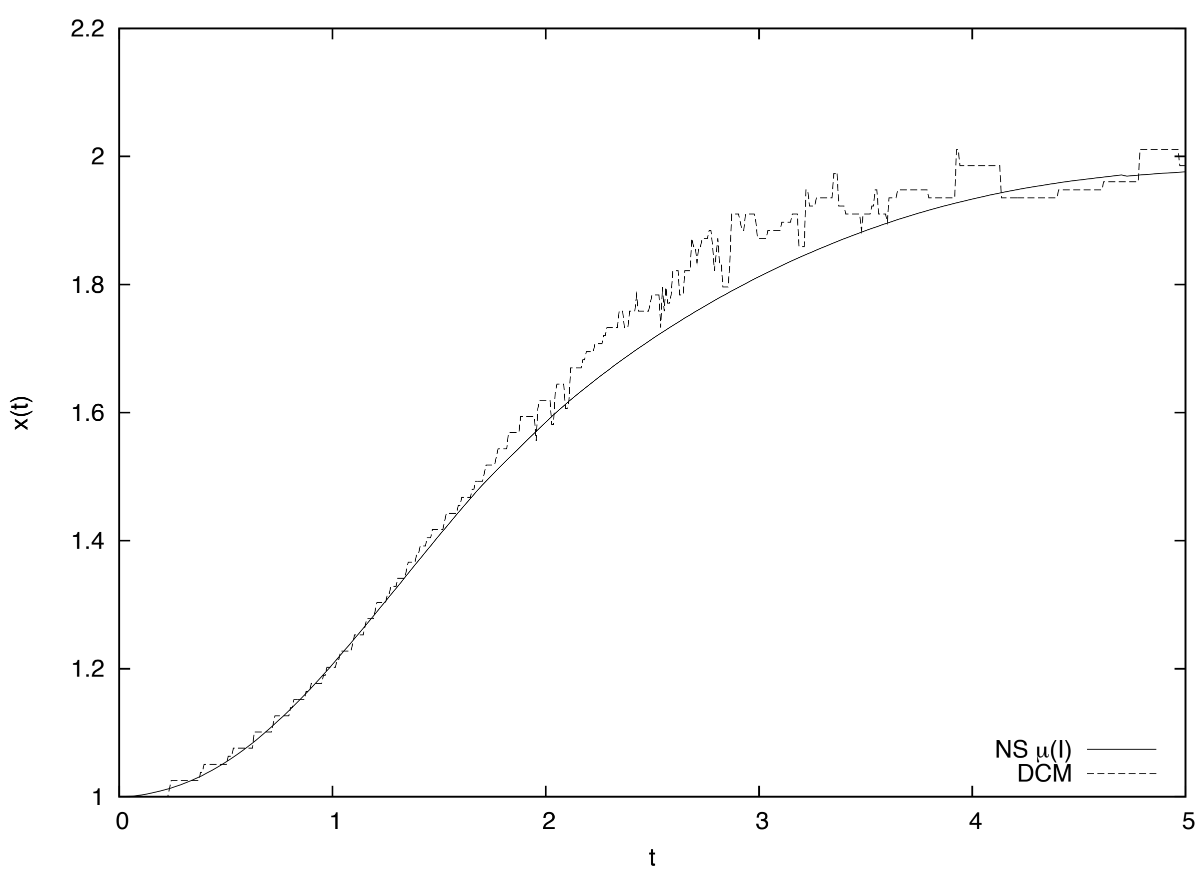


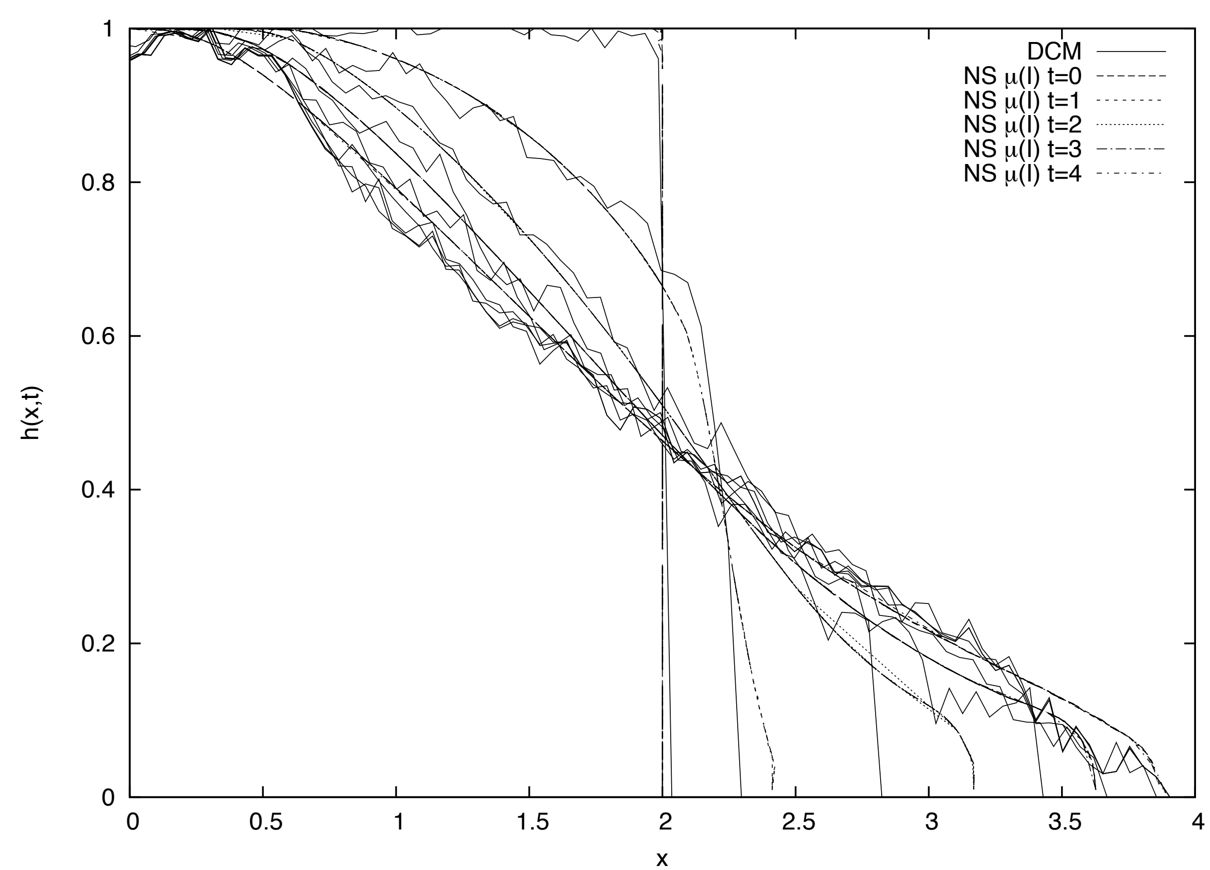

# Collapse of columns simulation *Gerris* $\mu(I)$

Collapse of columns of aspect ratio 1.42 comparison of Discrete Simulation Contact Method and Navier Stokes gerris, shape at time 0, 1, 2, 3, 4 and position of the front of the avalanche as function of time (time measured with $\sqrt{H_0/g}$ and space with $aH_0$ )

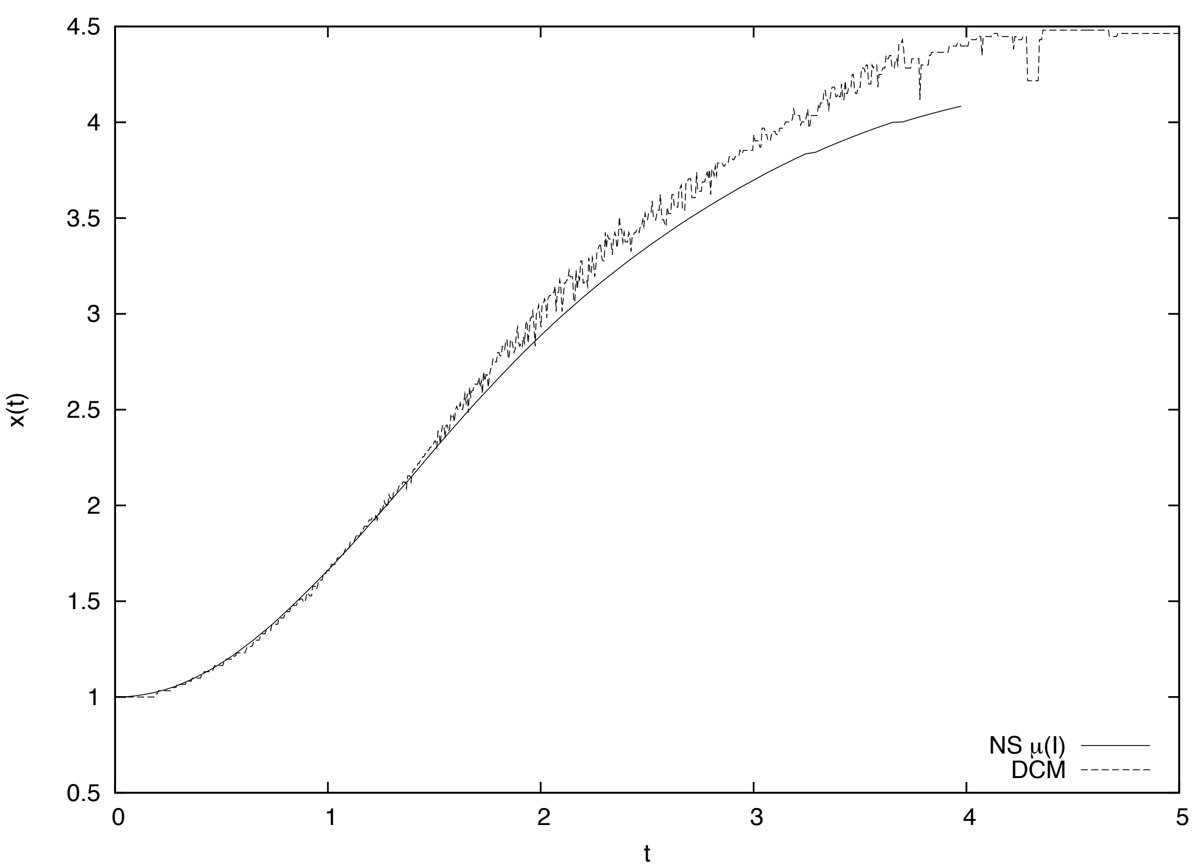


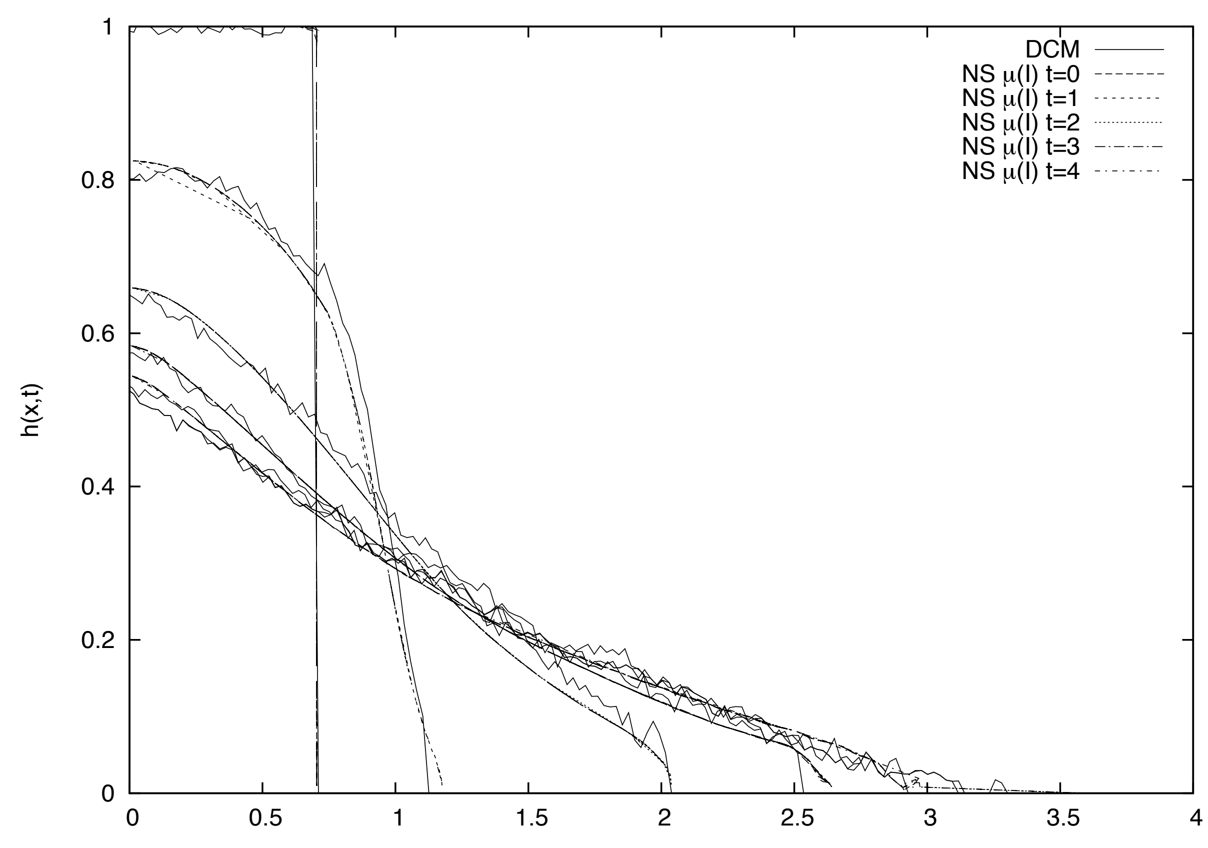

# Collapse of columns  simulation *Gerris μ(I)*

Collapse of columns of aspect ratio 6.26 comparison of Discrete Simulation Contact Method and Navier Stokes gerris, shape at time 0, 1, 2, 3, 4 and position of the front of the avalanche as function of time (time measured with $\sqrt{H_0/g}$ and space with $aH_0$ )

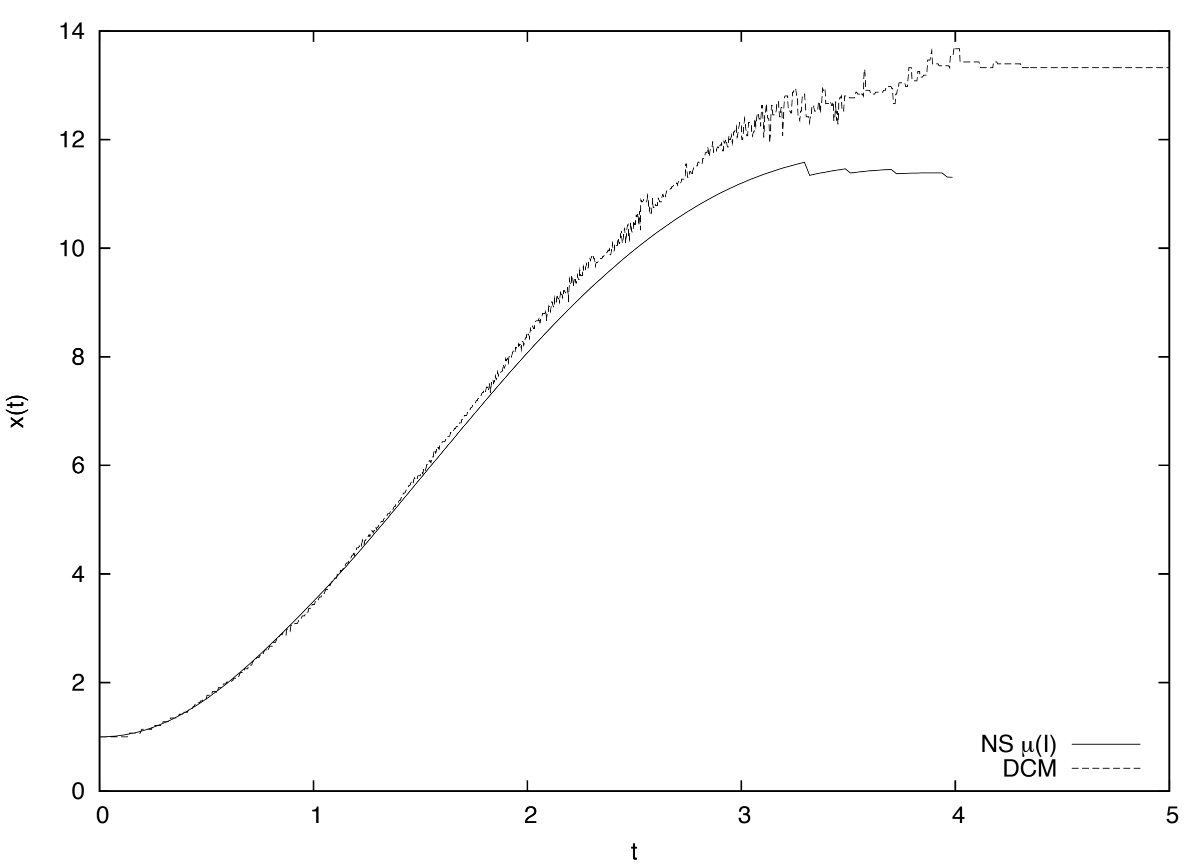


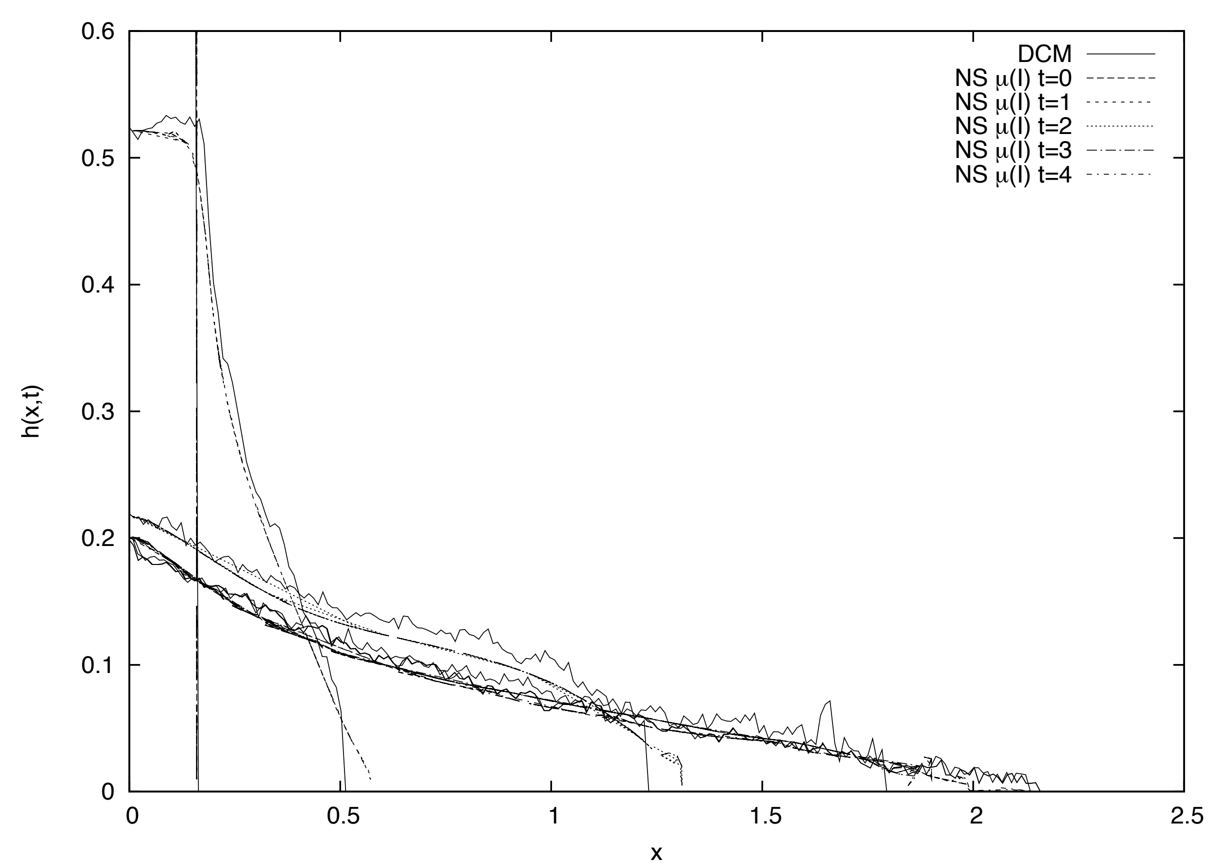

# Collapse of columns simulation *Gerris μ(I)*

## optimisation

$$\mu(I) = \mu_s + \frac{\Delta\mu}{\frac{I_0}{I} + 1}$$

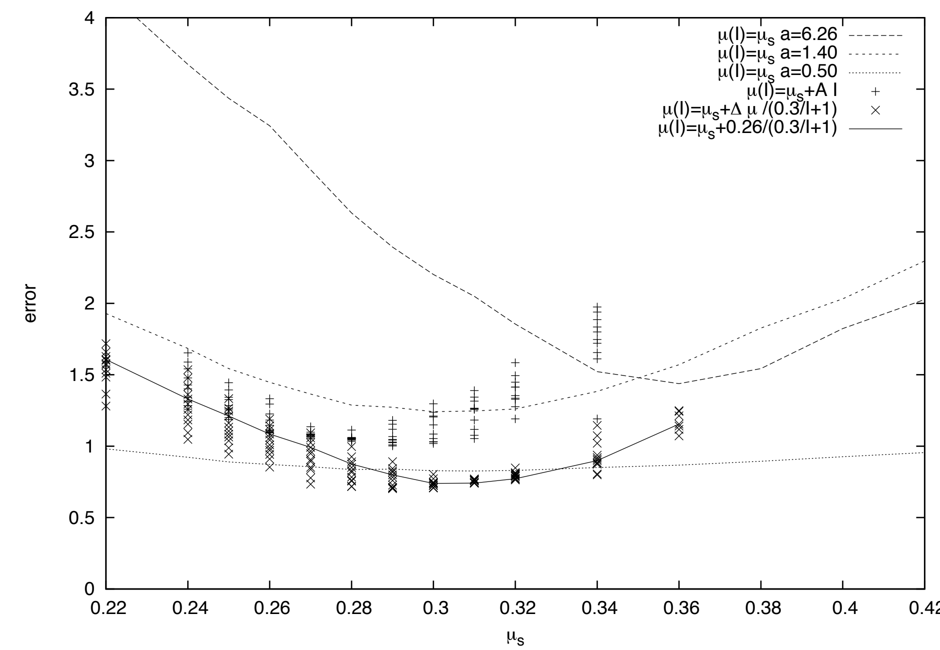


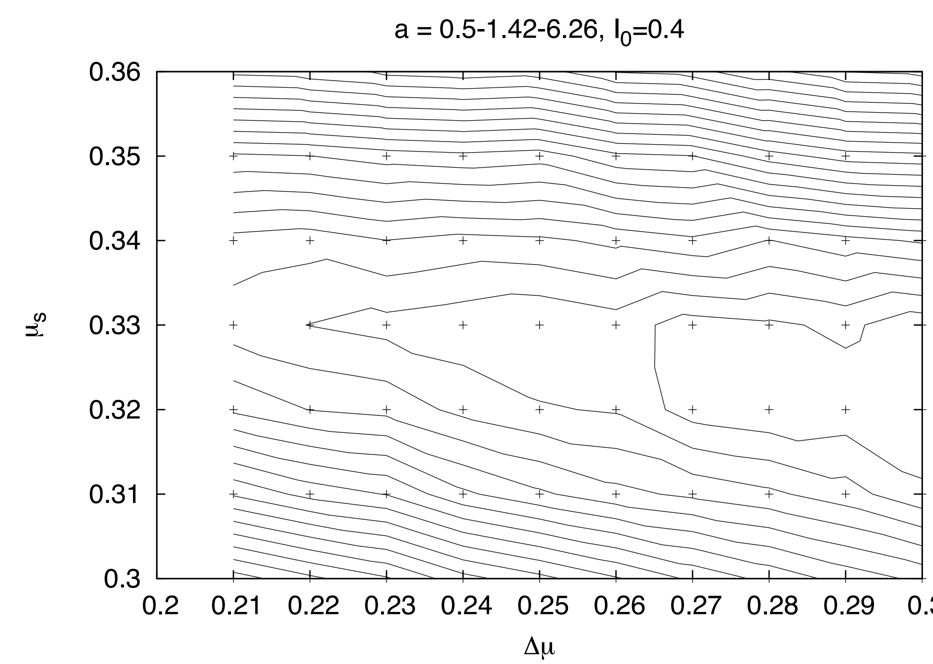


## final values

$$\mu_s = 0.32 \ \Delta\mu = 0.28 \ I_0 = 0.4$$

# Collapse of columns simulation *Gerris* $\mu(I)$

$a = 0.5$ DCM vs *Gerris* $\mu(I)$

# Collapse of columns simulation *Gerris* $\mu(I)$

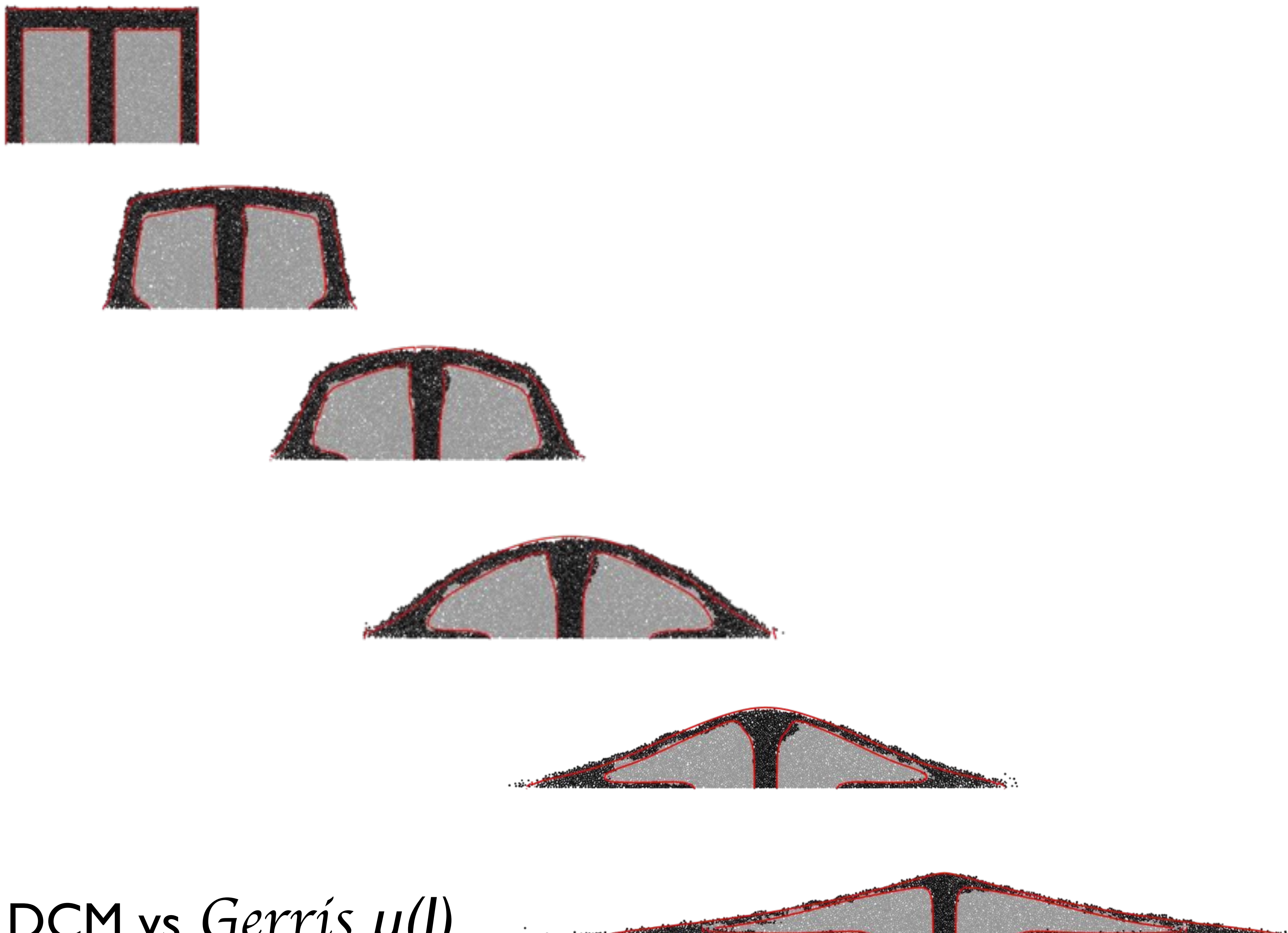

$a = 1.42$ DCM vs *Gerris* $\mu(I)$

# Collapse of columns simulation *Gerris* $\mu(I)$

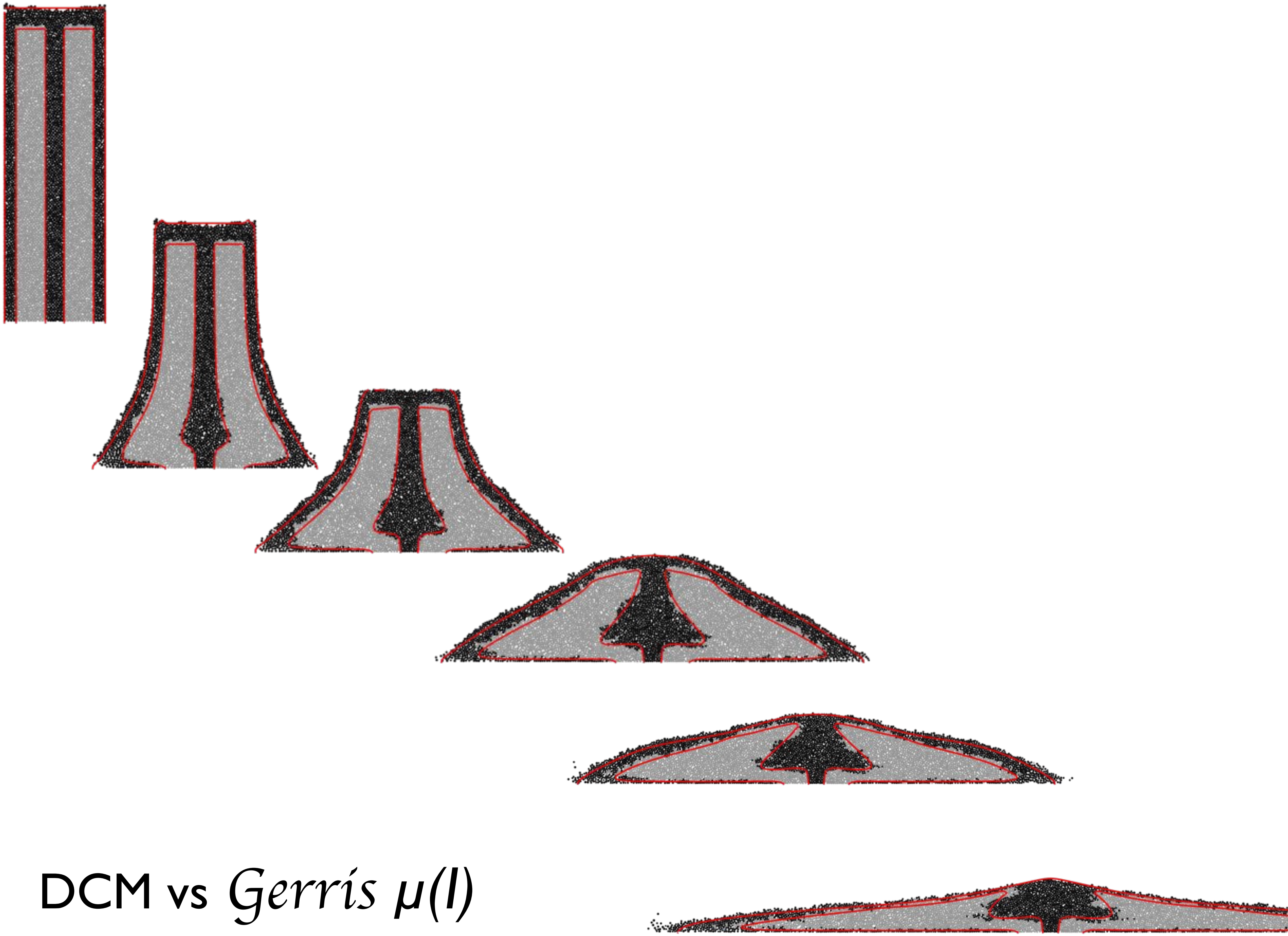

$a = 6.6$ DCM vs *Gerris* $\mu(I)$

# Collapse of columns  simulation *Gerris* $\mu(I)$

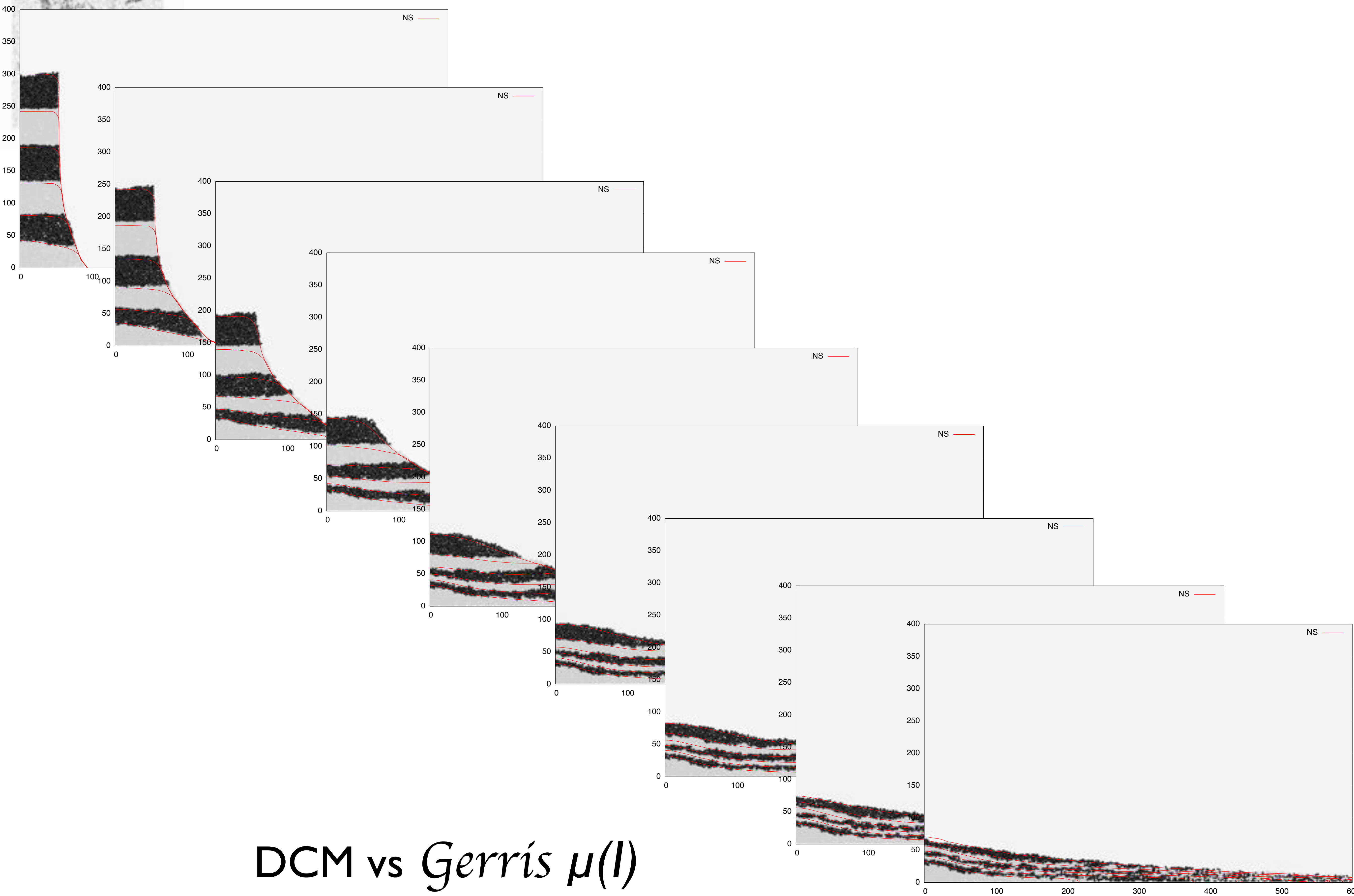


DCM vs *Gerris* $\mu(I)$

# Collapse of columns simulation *Gerris μ(I)*

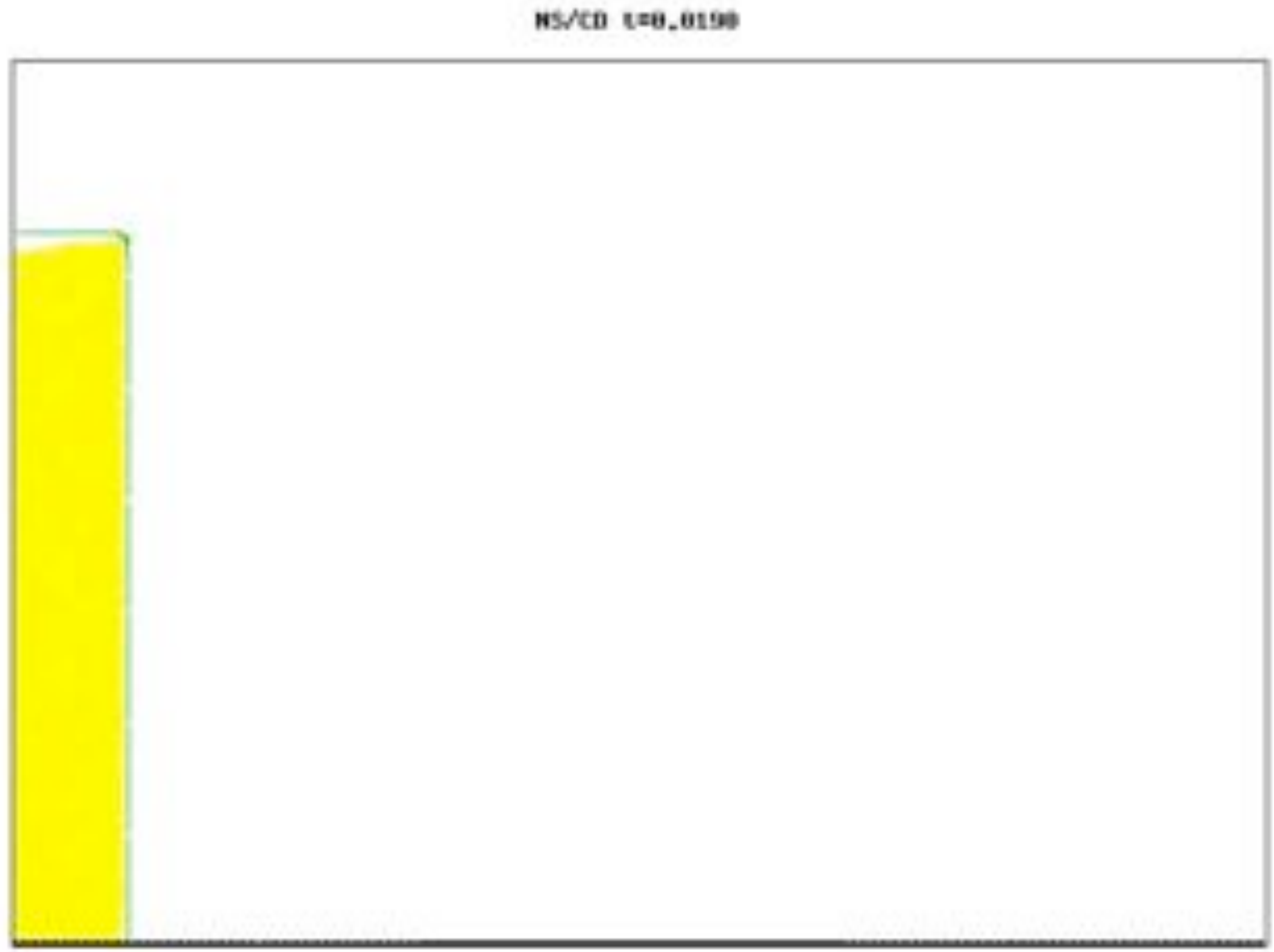


DCM vs *Gerris μ(I)*

# Collapse of columns simulation *Gerris μ(I)*


DCM vs *Gerris μ(I)*

# Collapse of columns   simulation *Gerris* $\mu(I)$

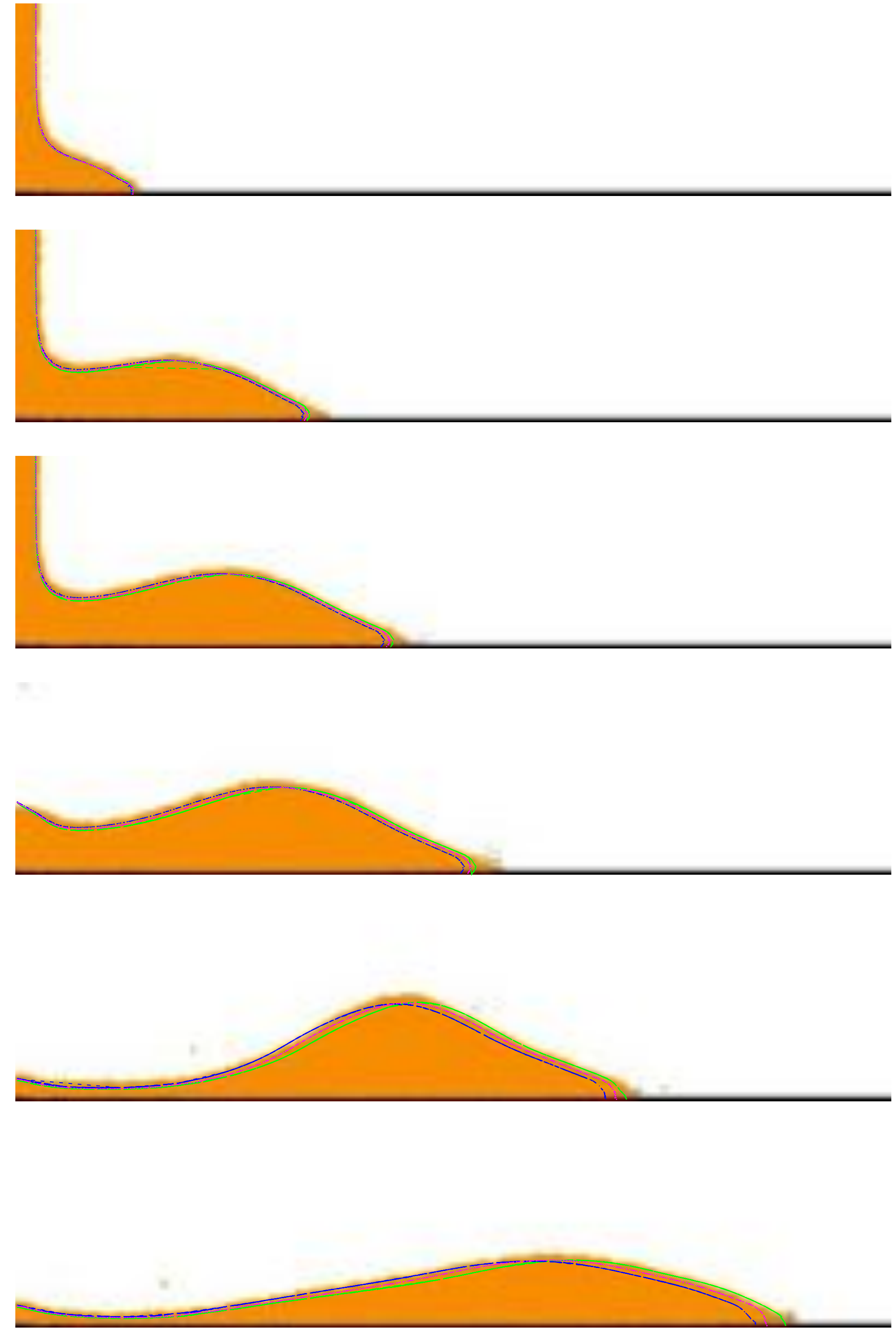

Figure 10: Strip representing a series of snapshots ($t = 0.5, 1.0, 1.2, 1.4, 1.7,$ and $2.0$) of a column collapse with aspect ratio $a = 68$. The most advanced curve (in green) corresponds to $\mu_s = 0.3$ $\Delta mu = 0.26$ and $I_0 = 0.30$. the less advanced (in blue) $\mu_s = 0.32$ $\Delta mu = 0.28$ and $I_0 = 0.30$ fits better the end of the heap. The curve in between (in cyan) corresponds to $\mu_s = 0.32$ $\Delta mu = 0.28$ and $I_0 = 0.40$ and fits better the top of the surge.

DCM vs *Gerris* $\mu(I)$

- comparaison of velocity profiles

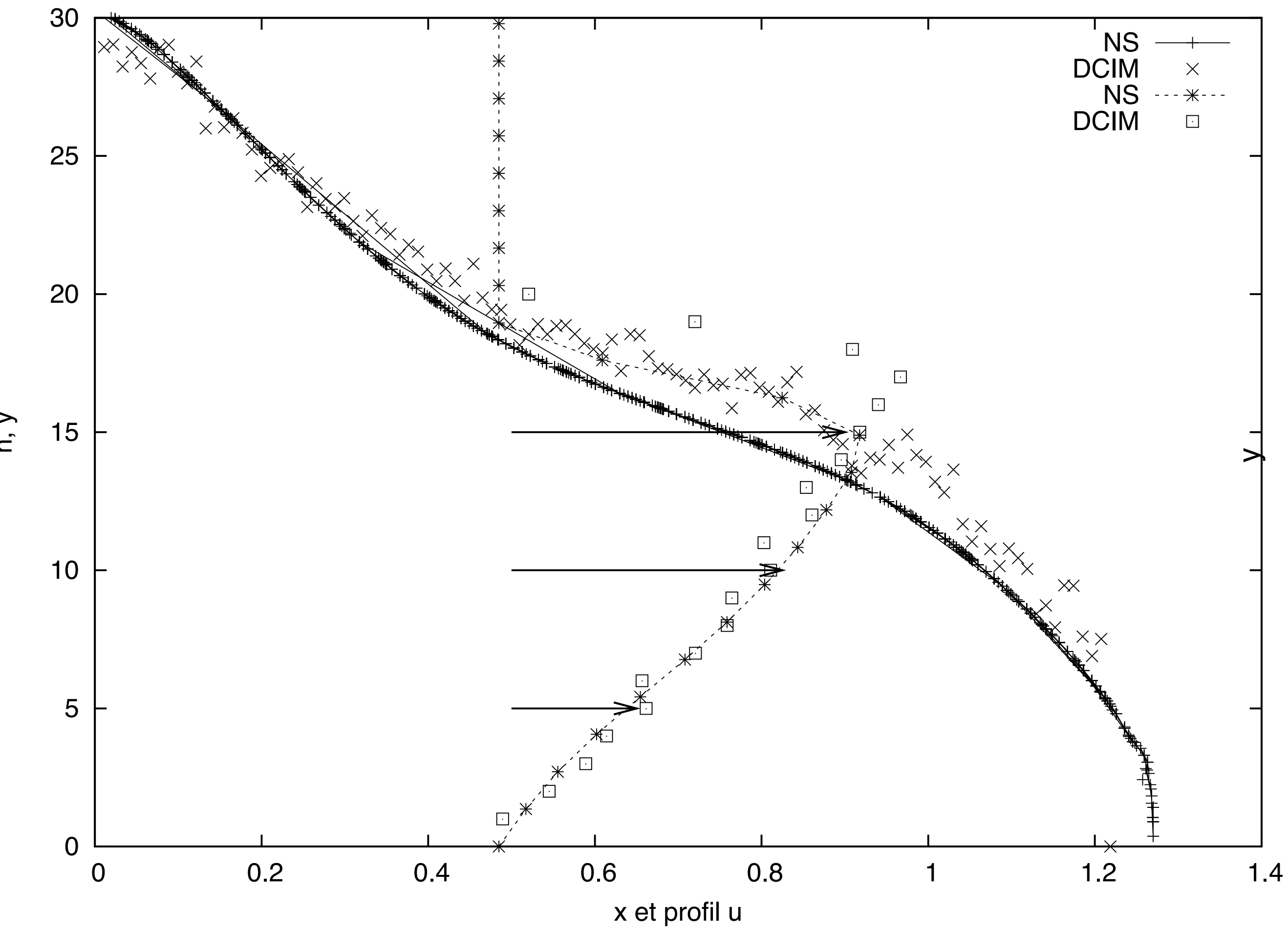


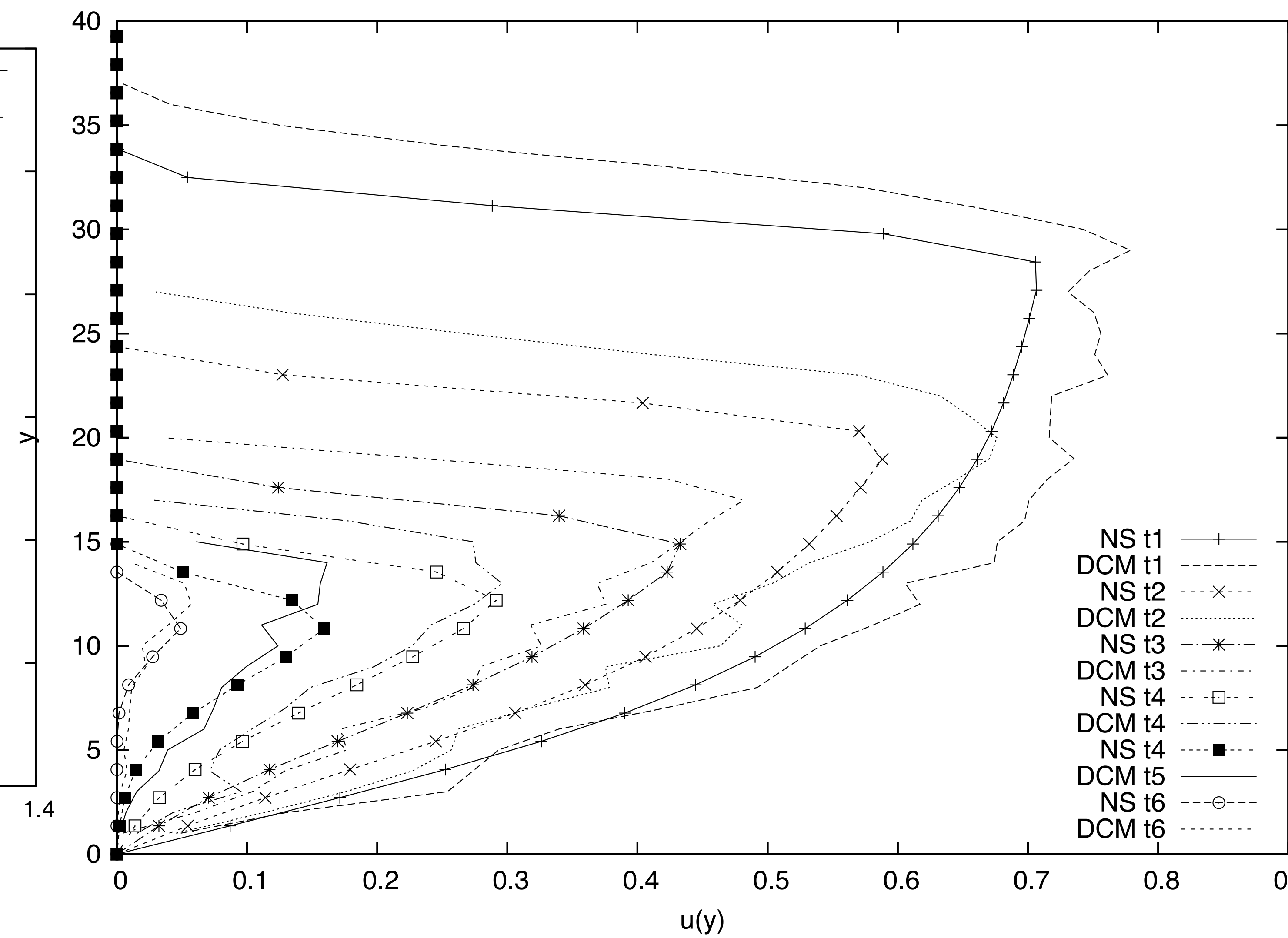


DCM vs *Gerris μ(I)*

- comparaison of velocity profiles

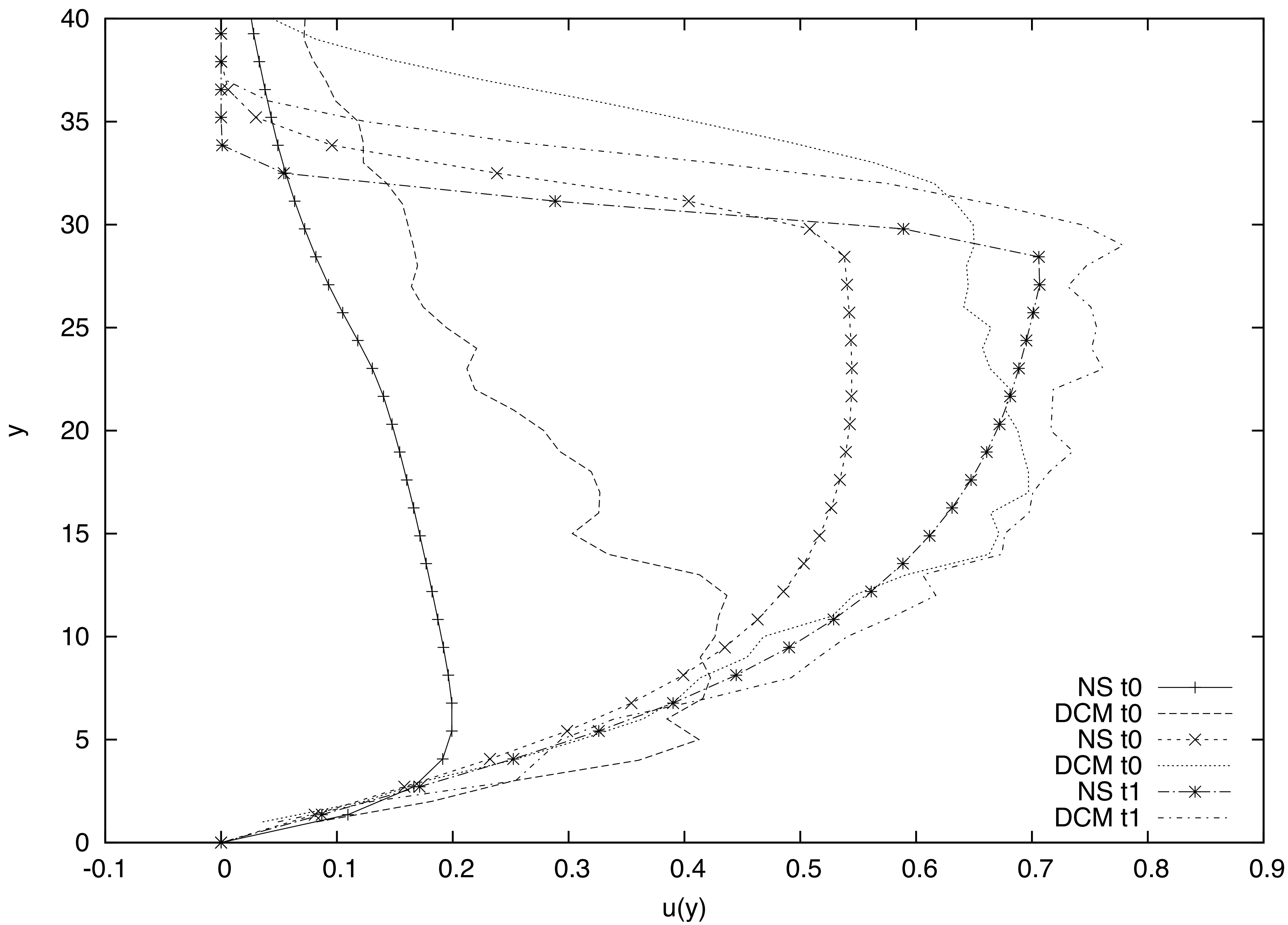


DCM vs *Gerris μ(I)*

- comparaison of velocity profiles

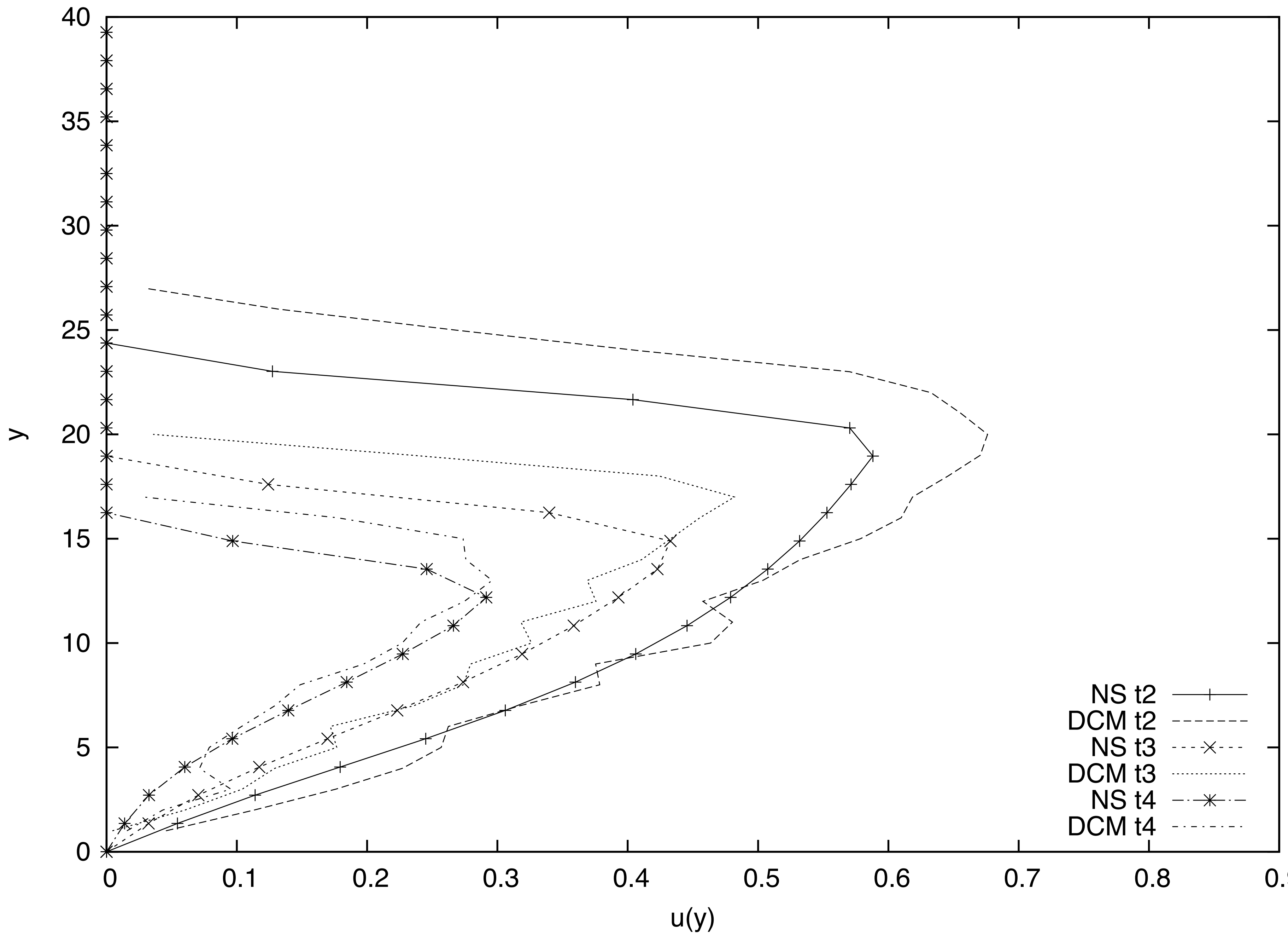


DCM vs *Gerris μ(I)*

- comparaison of velocity profiles

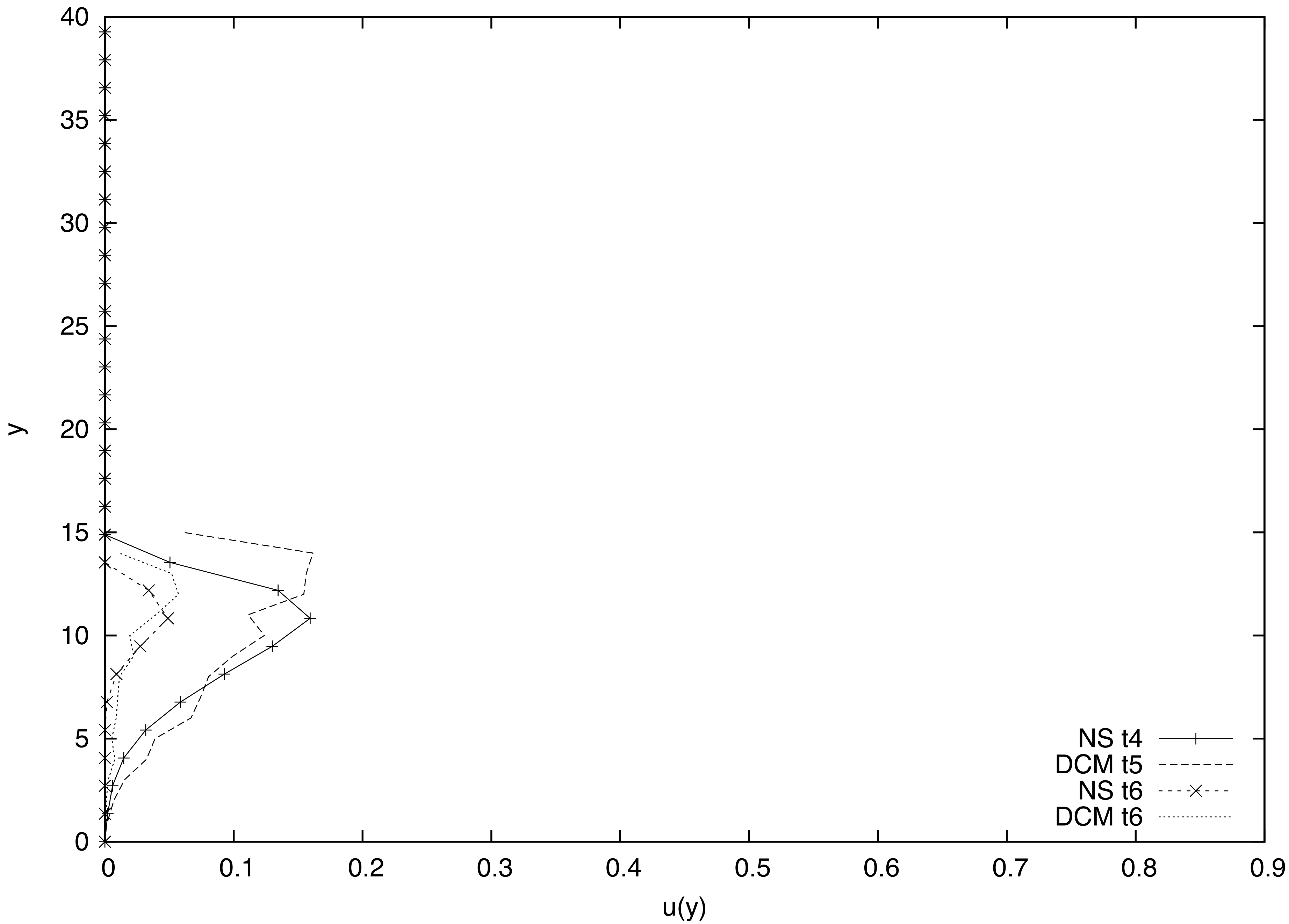


DCM vs *Gerris μ(I)*

# Collapse of columns   simulation *Gerris μ(I)*

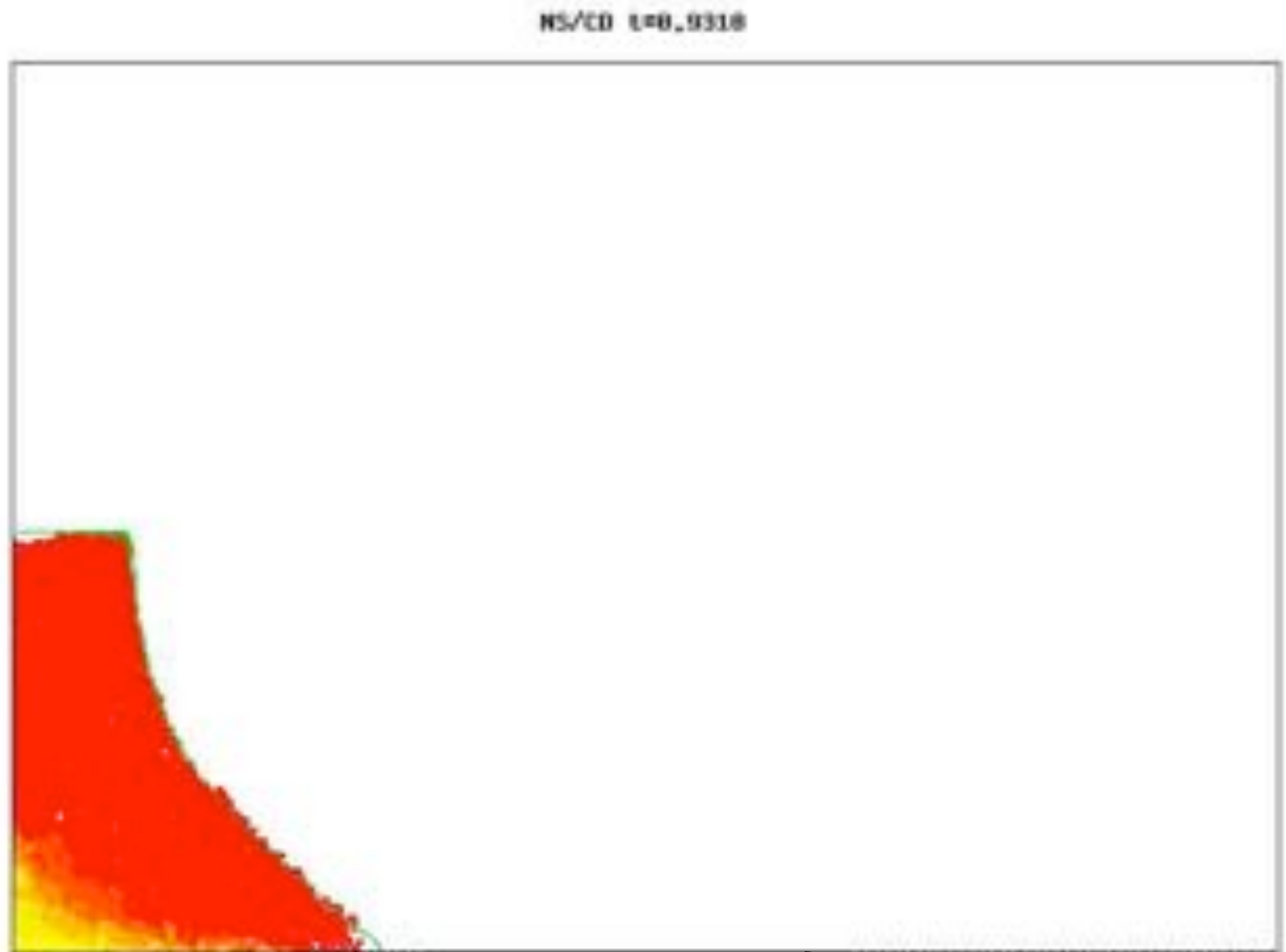


at the tip, a=6.6 t=1.33 2 2.66

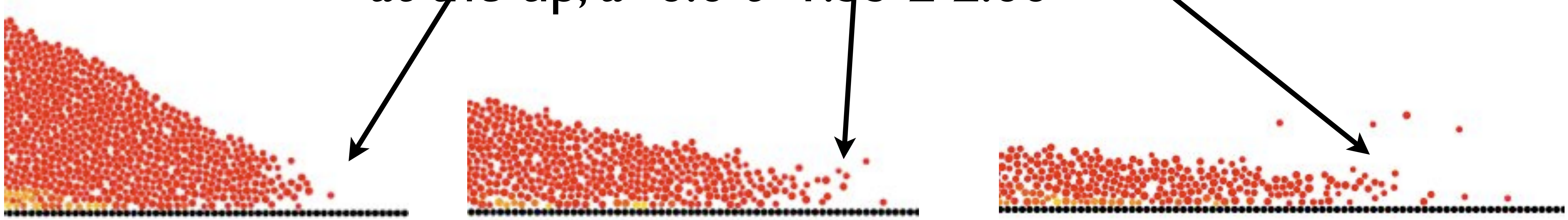

DCM vs *Gerris μ(I)*

# Collapse of columns simulation *Gerris* $\mu(I)$

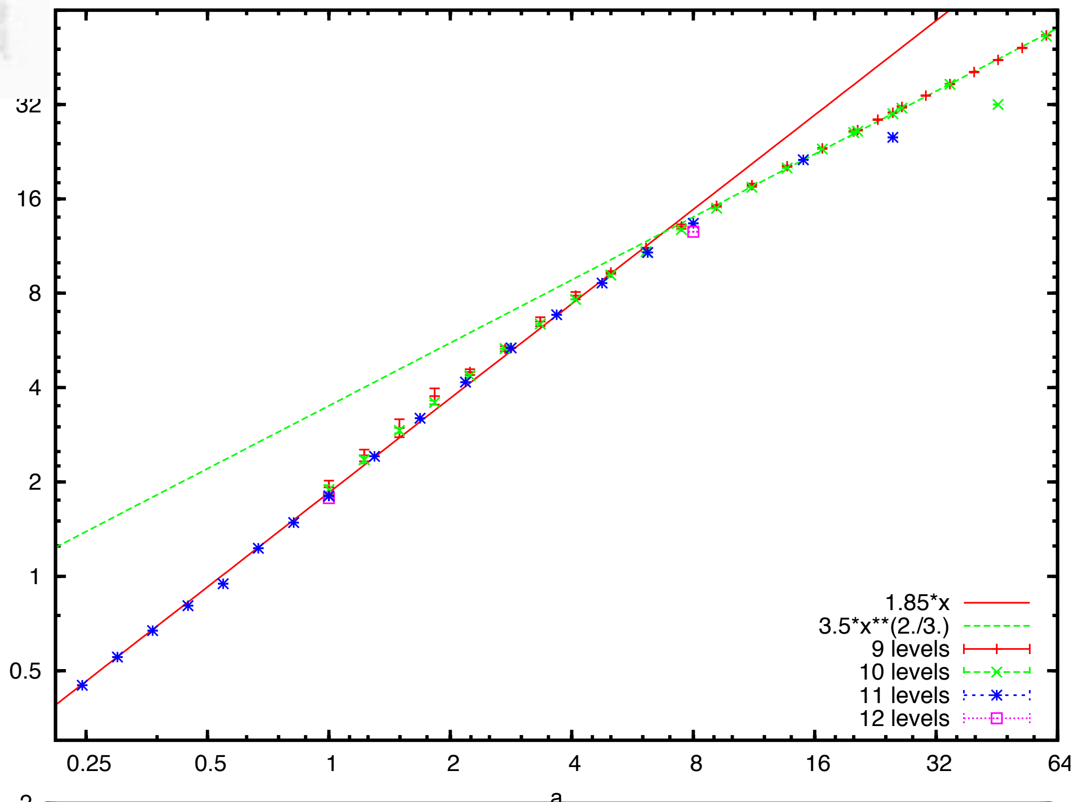


Normalised final deposit extent as a function of aspect ratio *a*.
Well-defined power law dependencies with exponents of 1 and 2/3 respectively.

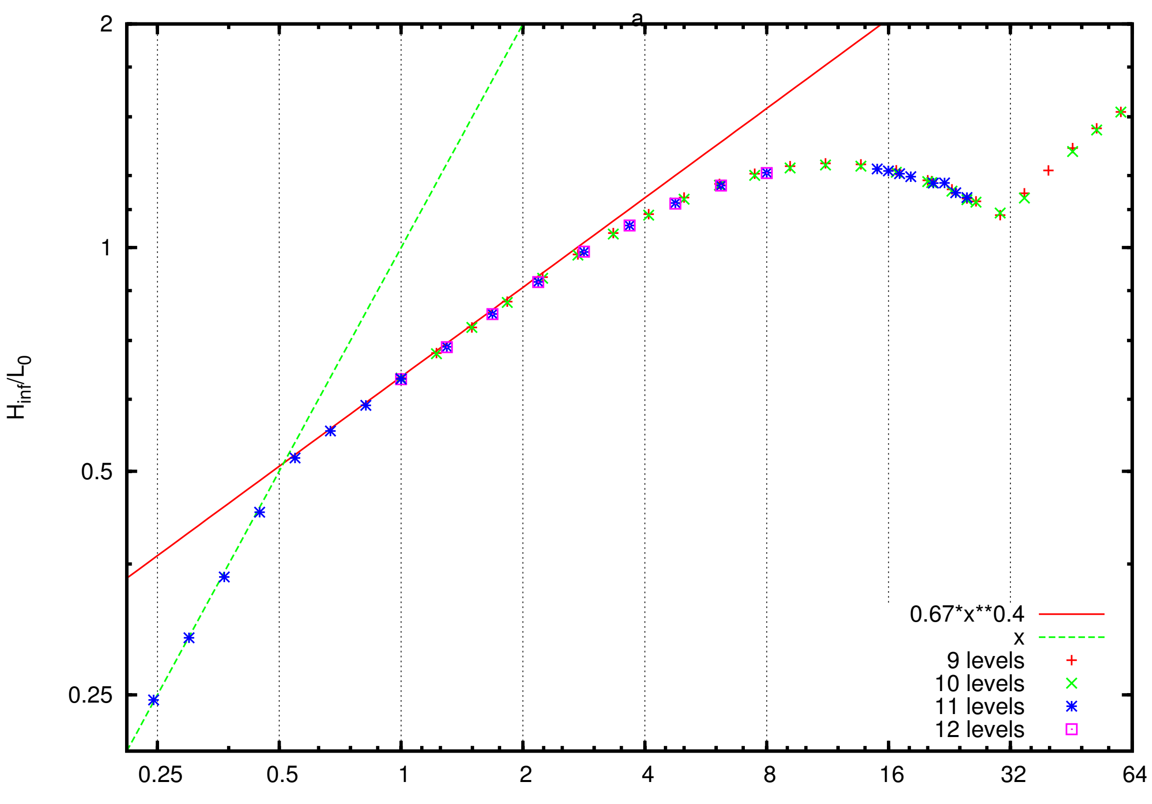


We recover the experimental scaling [Lajeunesse et al. 04] and [Staron et al. 05]. Differences between the values of the prefactors are due to the difficulties to obtain the run out length: friction in the Navier Stokes code tends to underestimate it, whereas direct simulation shows that the tip is very gazeous, it can no longer explained by a continuum mechanic description.

# conclusion

- μ(I) obtained from experimental flows of dry granular flows [Jop et al. 06], implemented it in *Gerris*
- test case: analytical solution of steady avalanche (Bagnold solution)
- collapse of granular columns (shape as function of time compared to Discrete Simulations).
-The experimental trends of the scaling of the run out are reobtained
- Saint Venant Savage Hutter to be compared with.
- complete spectra: discrete grains/ Saint Venant/ Navier Stokes

This opens the door to systematic studies of granular flows using this continuum approach.

# références:


P. Jop, Y. Forterre, O. Pouliquen, (2006) "A rheology for dense granular flows", Nature 441, pp. 727-730 (2006)

P.-Y. Lagrée, L. Staron and S. Popinet (to appear J.F.M.) "The granular column collapse as a continuum: validity of a two–dimensional Navier–Stokes model with a μ(I)-rheology"

E. Lajeunesse, A. Mangeney-Castelnau, and J.-P. Vilotte, (2004) "Spreading of a granular mass on an horizontal plane», Phys. Fluids, 16(7), 2371-2381.

L. Staron & E. J. Hinch (2005) "Study of the collapse of granular columns using two-dimensional discrete-grain simulation", J. Fluid Mech. (2005), vol. 545, pp. 1–27.